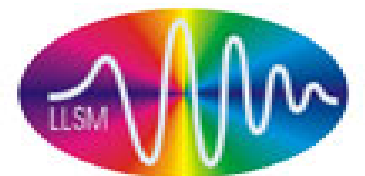


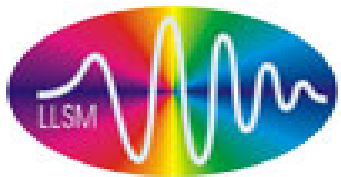
DECODING CANCER METABOLISM BY THE MULTIMODE ONCOLOGICAL OPTICAL PLATFORM

Halina Abramczyk

**Lodz University of Technology, Laboratory of Laser Molecular Spectroscopy
Poland**

<http://mitr.p.lodz.pl/raman/>





mitr.p.lodz.pl/raman

**LODZ UNIVERSITY OF TECHNOLOGY,
FACULTY OF CHEMISTRY ,
LABORATORY OF LASER MOLECULAR
SPECTROSCOPY, LODZ, POLAND**



prof. dr hab. Halina Abramczyk
head of Laboratory of Laser
Molecular Spectroscopy

abramczy@mitr.p.lodz.pl

pok. 233

[website](#)



dr hab. inż. Beata Brożek-Pluska

brozek@mitr.p.lodz.pl

pok. 303

[website](#)



dr inż. Jakub Surmacki

jsurmacki@mitr.p.lodz.pl

pok. 303

[website](#)



dr inż. Arkadiusz Jarota

ajarota@mitr.p.lodz.pl

pok. 309

[website](#)

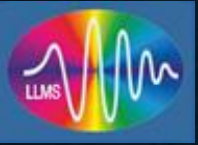


dr inż. Monika Kopeć

mkopec@mitr.p.lodz.pl

pok. 303

[website](#)



COOPERATION WITH MEDICAL CENTERS AND HOSPITALS

Uniwersytet Medyczny w Łodzi

Katedra Onkologii

Prof. dr hab. n med. Radziław Kordek

Dr n med. Jacek Musiał

WSS i M. Kopernika w Łodzi

Prof. dr hab. n med. J. Morawiec

Lekarz med. Marek Tazbir

Dr Beata Romanowska -Pietrasiak

Instytut Centrum Zdrowia Matki Polki w Łodzi

Prof. dr hab. n. med. Lech Polis

Dr n. med. Bartosz Polis

Uniwersytecki Szpital Kliniczny im. Wojskowej Akademii

Medycznej w Łodzi – Centralny Szpital Weteranów Klinika

Neurochirurgii, Chirurgii Kręgosłupa i Nerwów Obwodowych

Prof. dr n. med. Maciej Radek

dr n. med. Maciej Błaszczyk

Uniwersytecki Szpital Kliniczny im. WAM –

Centralny Szpital Weteranów

Prof. dr hab. n. med. Adam Dziki

Uniwersytet Medyczny w Łodzi

Klinika Chirurgii Nowotworów Głowy i Szyi

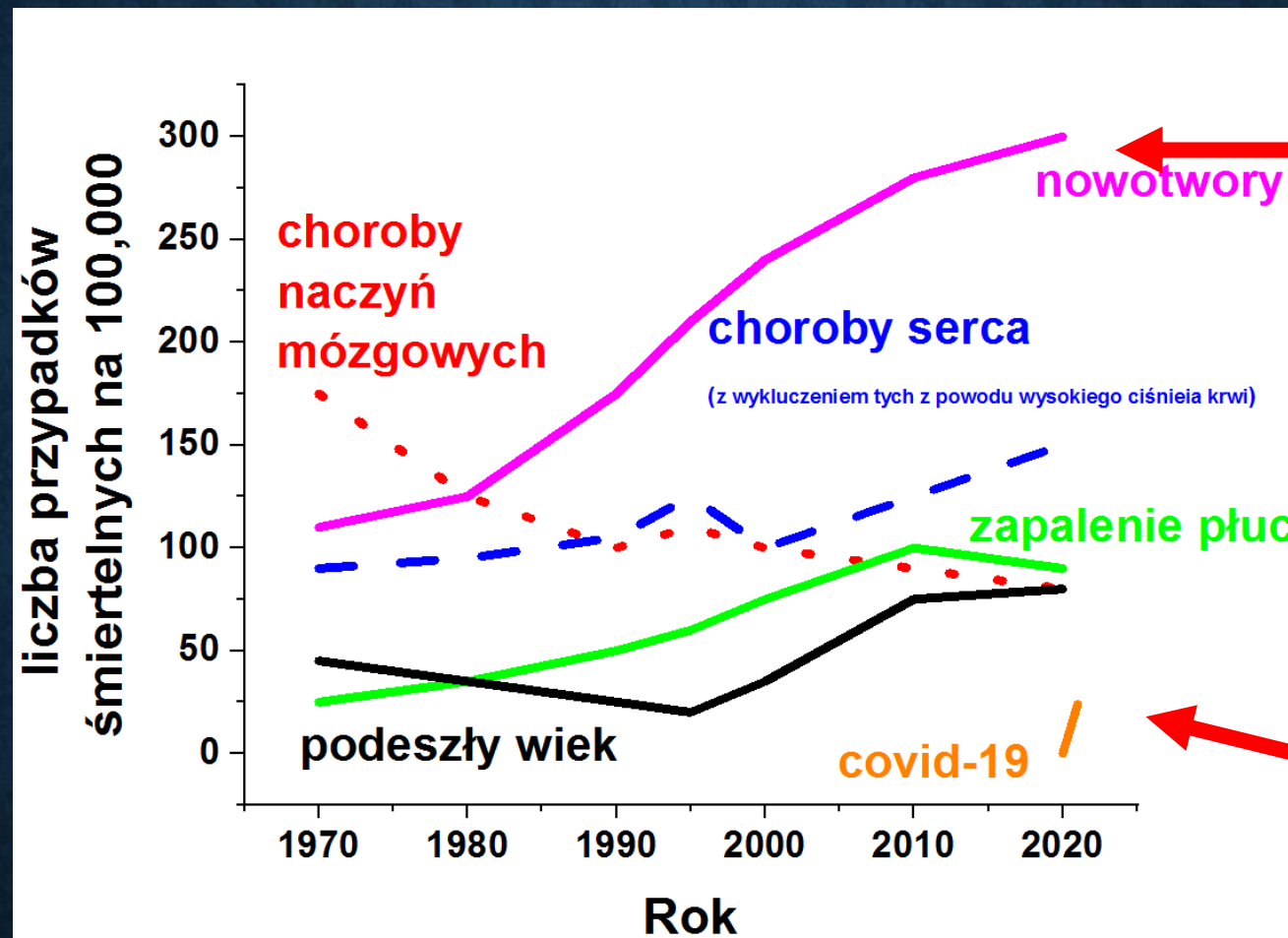
Oddział Laryngologii Onkologicznej –

Regionalny Ośrodek Onkologiczny

Wojewódzkiego Szpitala Specjalistycznego i

m. Kopernika Prof. dr hab. n med. Alina Morawiec-Sztandera

Dr n med. Izabela Niedźwiecka



CANCERS

COVID-19

Cancer is one of the most common and serious diseases in the European and world population and one of the main causes of morbidity and mortality, the conducted research provides innovative tools for improved (precise, objective and quick) diagnostics.

LABORATORY OF LASER MOLECULAR SPECTROSCOPY

www.mitr.p.lodz.pl/raman



Laboratory of Raman spectroscopy

Ramanor U 1000 (Jobin Yvon), 488-514nm



Laboratory of Raman imaging

Microscope Raman/AFM/SNOM/TERS, Witec

Raman confocal microscope (Renishaw)



Laboratory of femtosecond spectroscopy

Millennia, Tsunami, Empower30, Spitfire Ace, Topas (Spectra Physics)

LABORATORY OF LASER MOLECULAR SPECTROSCOPY

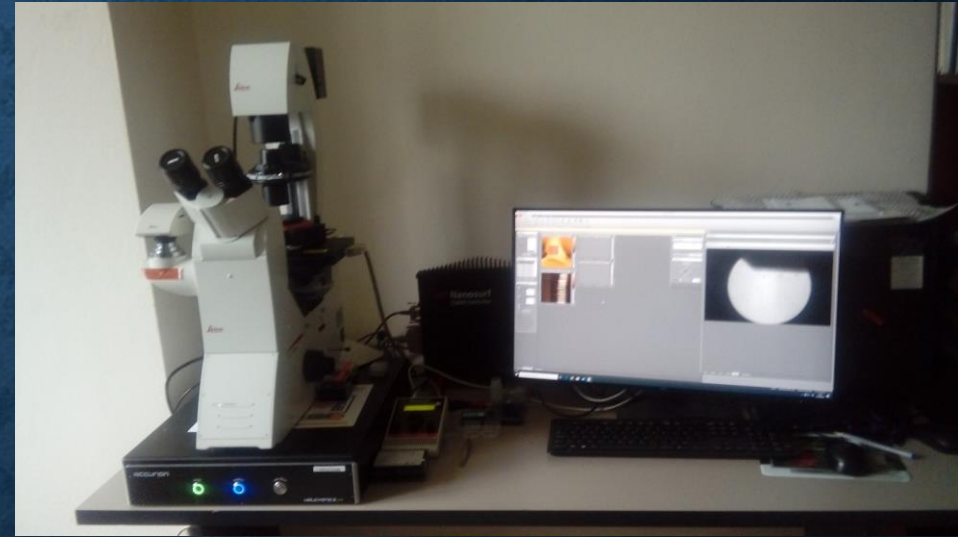
www.mitr.p.lodz.pl/raman

Laboratory of IR imaging



FTIR microscope (Agilent Technologies
Cary 600 Series)

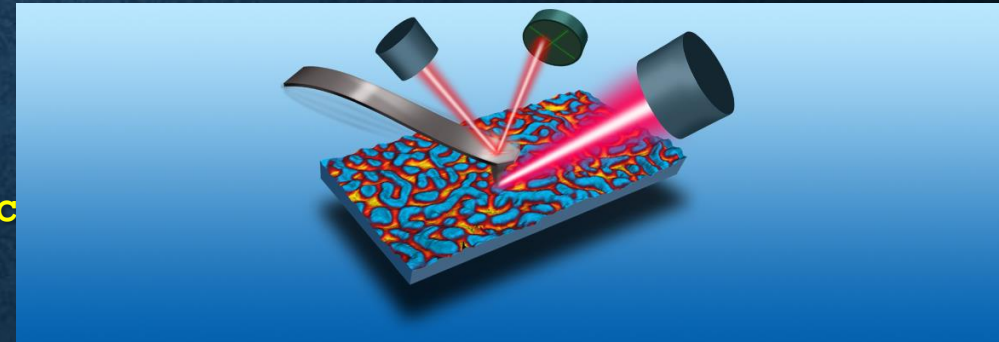
Laboratory of AFM imaging



-atomic force microscope with a controller and scanning range of $100 \times 100 \mu\text{m}$ in the X and Y axes and $15 \mu\text{m}$ in the Z axis with a positioning resolution in the XY axis of 6 pm and in the Z axis of 0.9 pm , equipped with an inverted microscope, enabling measurements in air and liquid, in contact and tapping modes, equipped with software to generate maps of mechanical properties, including: topography, stiffness,

NANOSCALE IR-AFM CHEMICAL IMAGING SOLUTION

- A system that uses the effect of photothermally induced expansion (thermal expansion) that allows the simultaneous measurement of infrared radiation absorption, sample topography and nanomechanical properties of the sample by recording changes in the amplitude and oscillation frequency of the AFM probe.
- **10nm resolution** and monolayer sensitivity IR chemical imaging
- High-speed chemical imaging - 10x faster
- Direct FTIR correlation enabling nanoscale FTIR
- The highest nanoIR performance with Tapping AFM-IR and FASTspectra



BIOLABORATORY



LABORATORY OF MOLECULAR AND CELL BIOLOGY

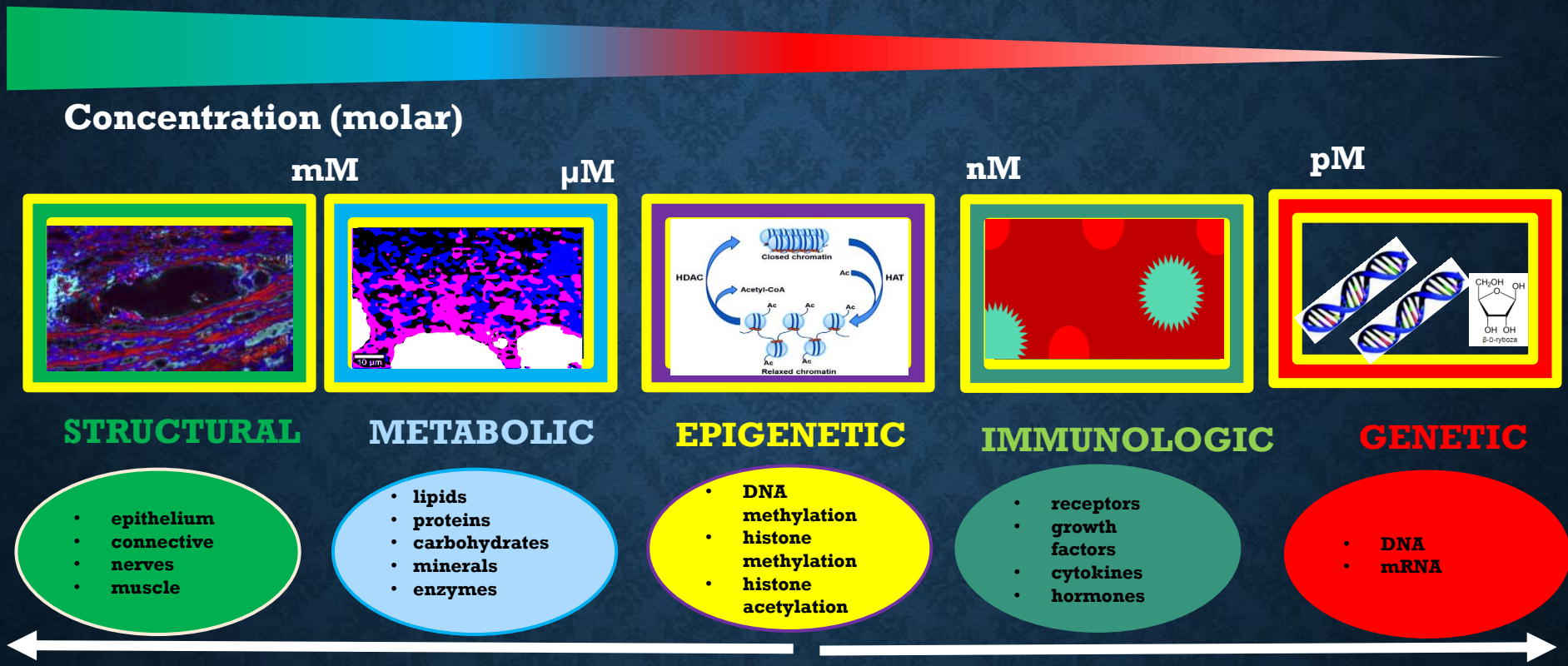


Set for cell viability analysis based on absorbance and fluorescence measurements, equipped with an automatic, inverted fluorescence microscope, for cellular bright field imaging, fluorescence and optical phase contrast imaging, equipped with a multi-detection of microplate reader - enabling the detection of fluorescence intensity, fluorescence polarization, luminescence and absorbance. Detection with 96 or 384-well plate; a set that meets the requirement of full control of imaging conditions - temperature, humidity and atmosphere composition (CO₂ / O₂) enabling measurements in cell culture conditions. Equipped with a fully insulated imaging chamber that can be heated to a minimum of 60°C, the system is equipped with an external peristaltic pump module that allows dosing of various reagents directly into the set well of the microplate

LABORATORY OF MOLECULAR AND CELL BIOLOGY

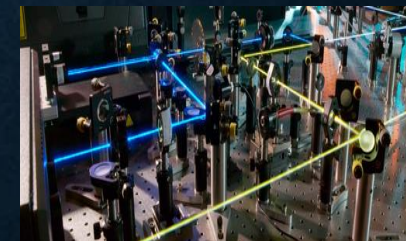
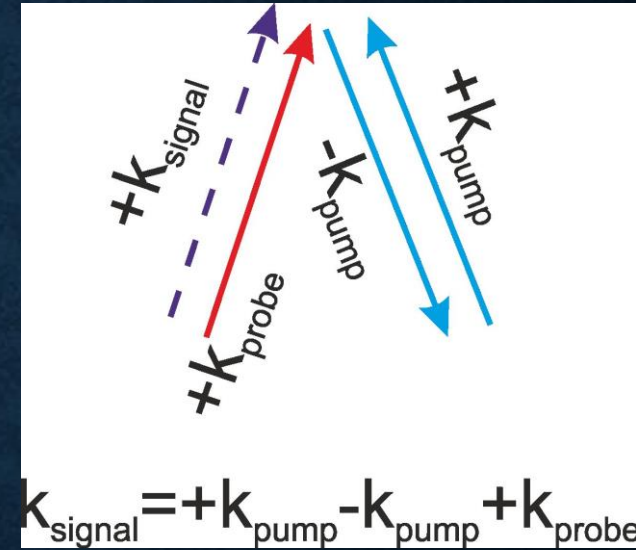
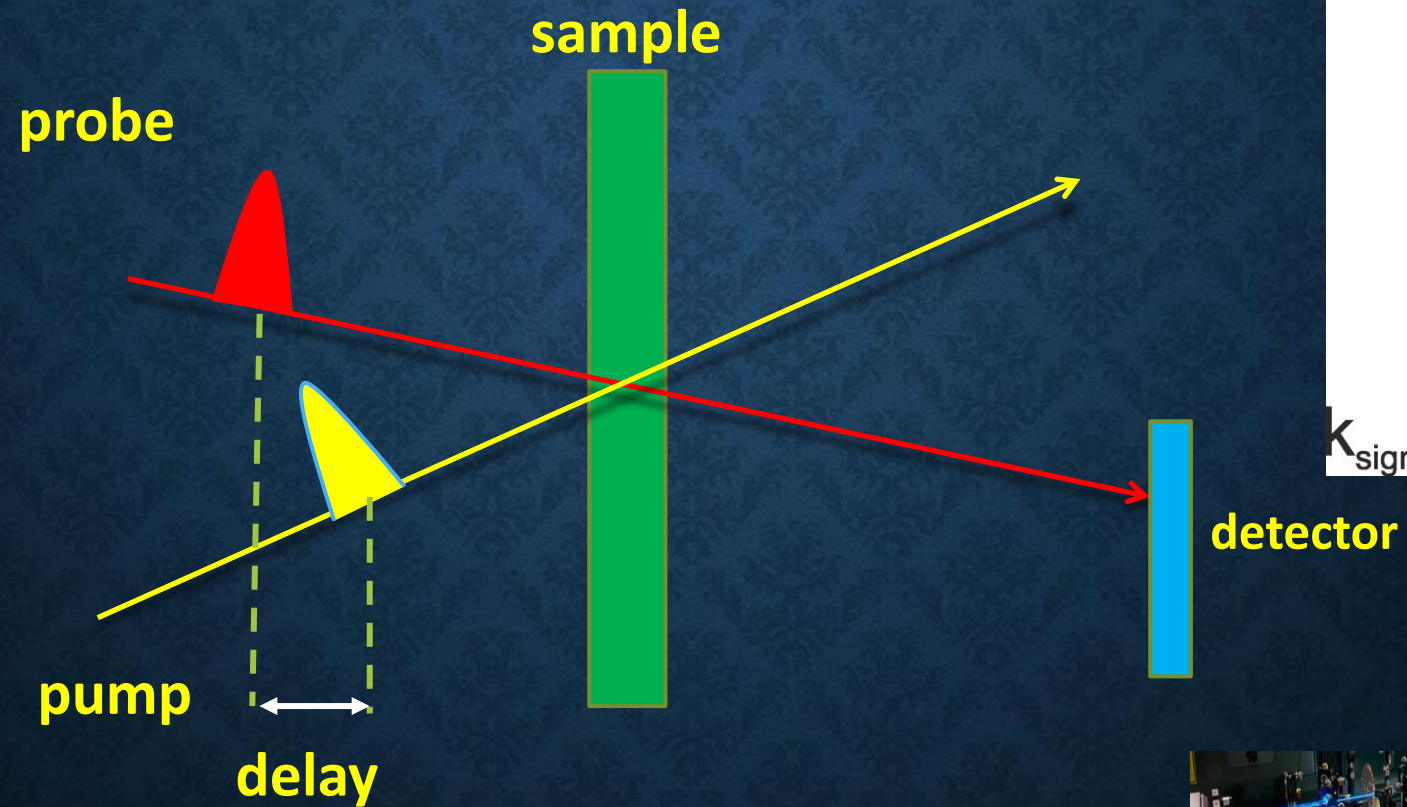
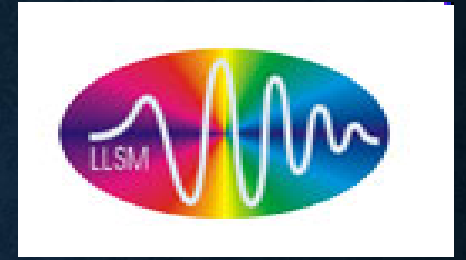


- Set for the analysis of fluorescence and chemiluminescence of biological systems enabling the visualization of proteins and antibodies, equipped with kits enabling the isolation of proteins and their staining, based on the western blot analysis, which includes the preparation of samples with the analyzed protein mixture, electrophoresis, transfer of separated proteins from the gel to the membrane, incubation with appropriate antibodies and the detection of the desired protein, by using visible and infrared light.

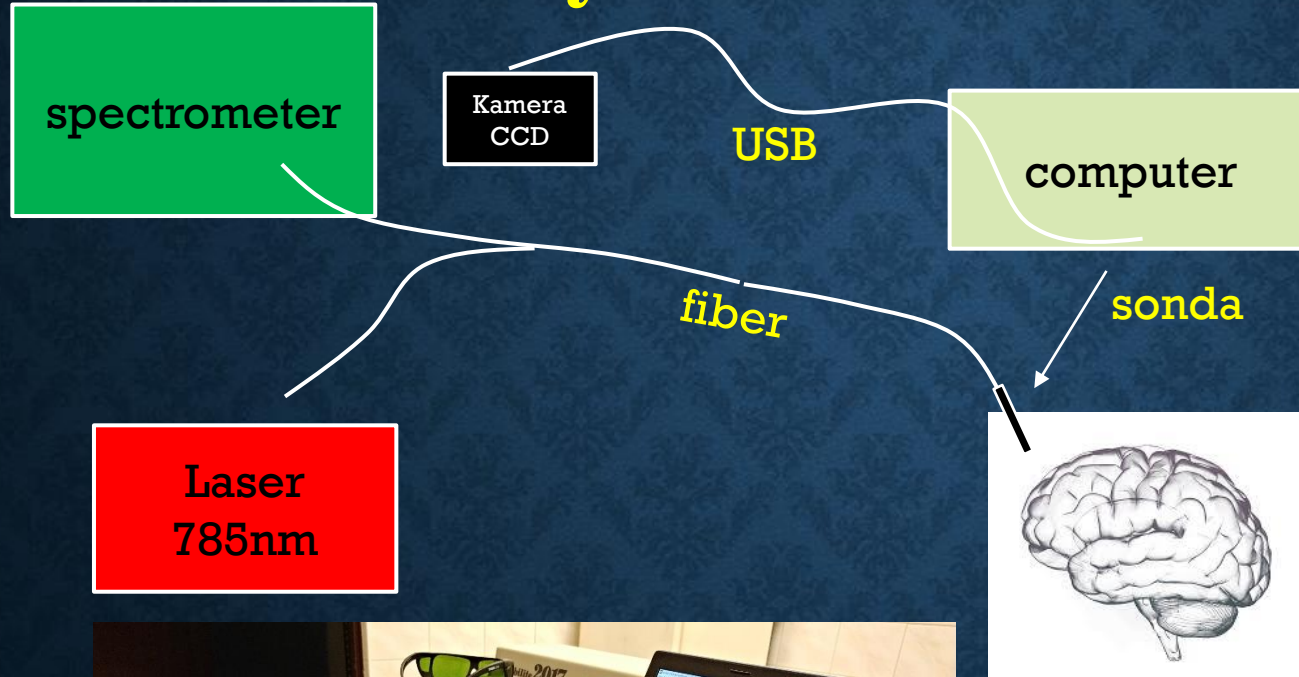
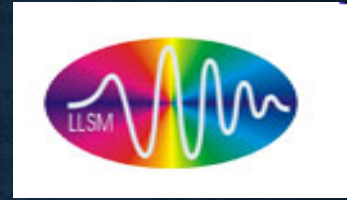


Detectable molecular features in tissue can be divided into five physiological categories: structural, metabolic, epigenetic, immunologic and genetic. The key factor limiting most imaging methods is signal-to-noise related to the concentration of the feature to be imaged. Fig.1 shows detectable molecular features in tissue (specificity) vs. concentration (sensitivity). Metabolic markers and immunologic markers (growth factors, cytokines or hormones) can be secreted at concentrations several times higher than surface receptors, which make them easier to detect.

PUMP - PROBE TRANSIENT ABSORPTION SPECTROSCOPY



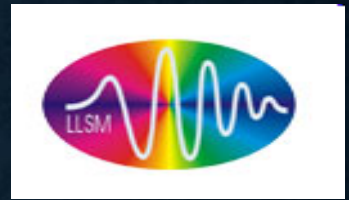
The real-time *in vivo* neurosurgical Raman system in our laboratory



RAMAN SPECTROSCOPY GUIDES IN VIVO BRAIN OPTICAL BIOPSIES



BIOMEDICAL APPLICATIONS



- **High spatial resolution RAMAN IMAGING**
- **SNOM microscopy (far below the diffraction limit, SNOM)**
- **Strong signal enhancement enabling monitoring the genetic and immunological responses in biological systems (SERS COMBINED WITH NANOPARTICLES)**
- **Specificity of interactions (BIOCONJUGATES)**
- **AFM topography, stiffness, adhesion, Young modulus (AFM)**
- **High temporal resolution (FEMTOSECOND PUMP-PROBE SPECTROSCOPY)**

WHAT?



Human normal and cancerous breast tissue, brain, neck and head , intestine tissues

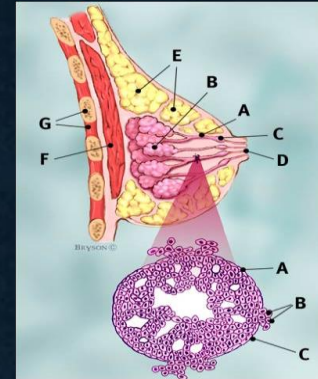
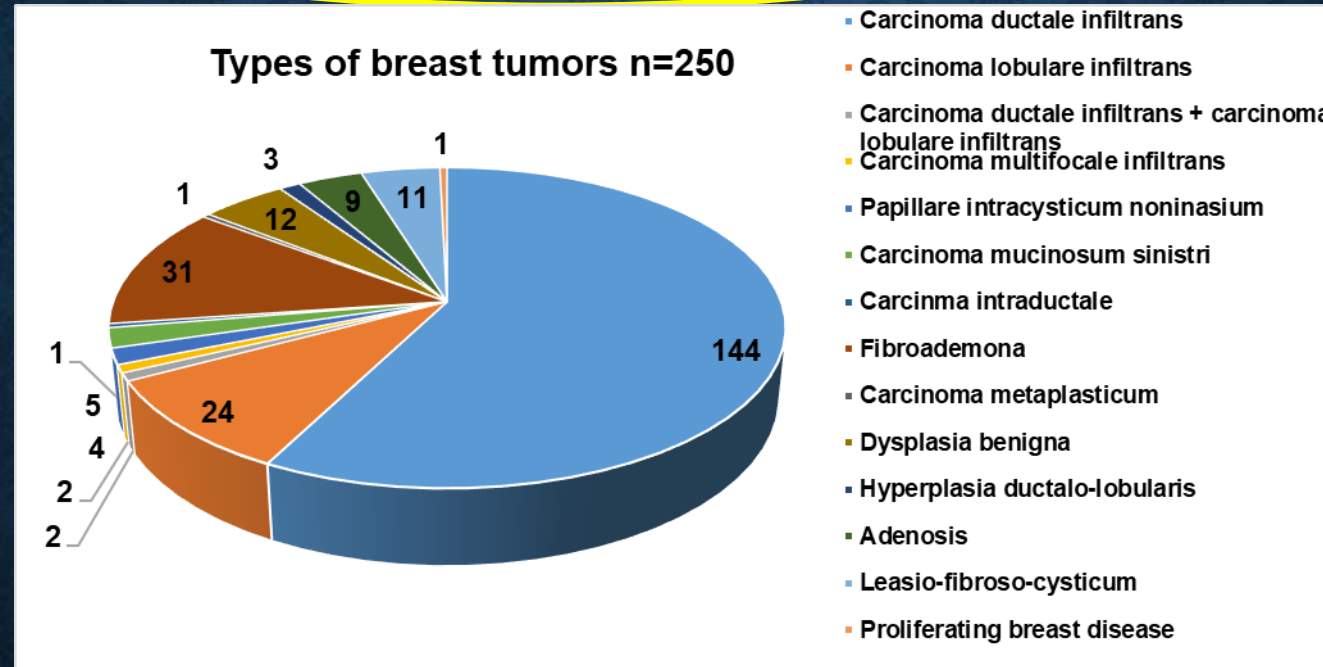
Cell human Lines: breast normal (MCF-10A,) and cancerous epithelial : (MCF-7, MDA-MB-231) and brain glial cells: NHA Astrocytes CC2565), astrocytoma (CCF-STTG1 (ATCC CLR1718) and glioblastoma (U87MG) (ATCC[®] HTB-14), lung normal and lung carcinoma epithelial cells (A549)

In vivo animal models (brain)

Drugs (temodal,erlotinib, trastuzumab, mRNA vaccines, amantadine, thalidomid)

Patients Statistics- breast

❖ 250 patients

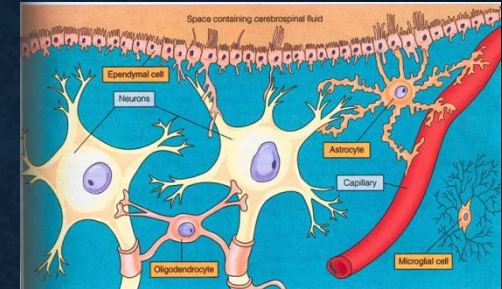
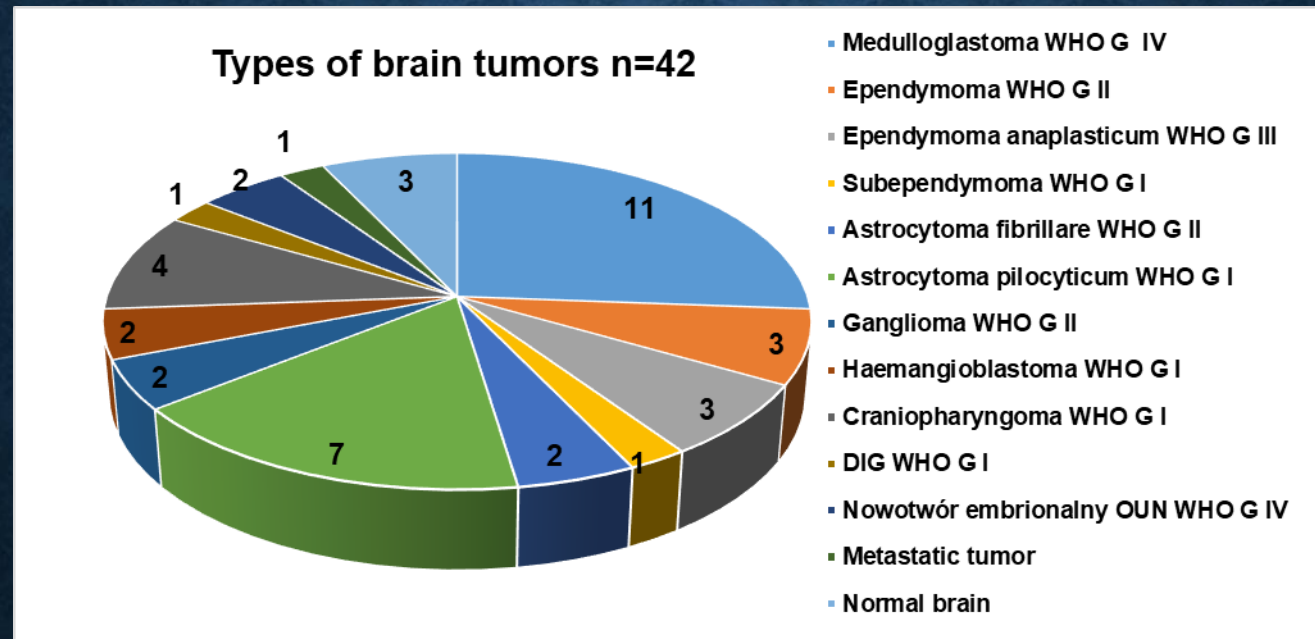


The pathology reports indicated that 70% of the cancer samples were ductal carcinomas; the remaining samples were lobular or untyped mammary carcinomas, metastases were found in 60% of patients

We will deal with epithelial cancer types. Most cancers have epithelial origin and they represent approximately 80-85% of all cancers.³⁸

PATIENTS STATISTICS-BRAIN

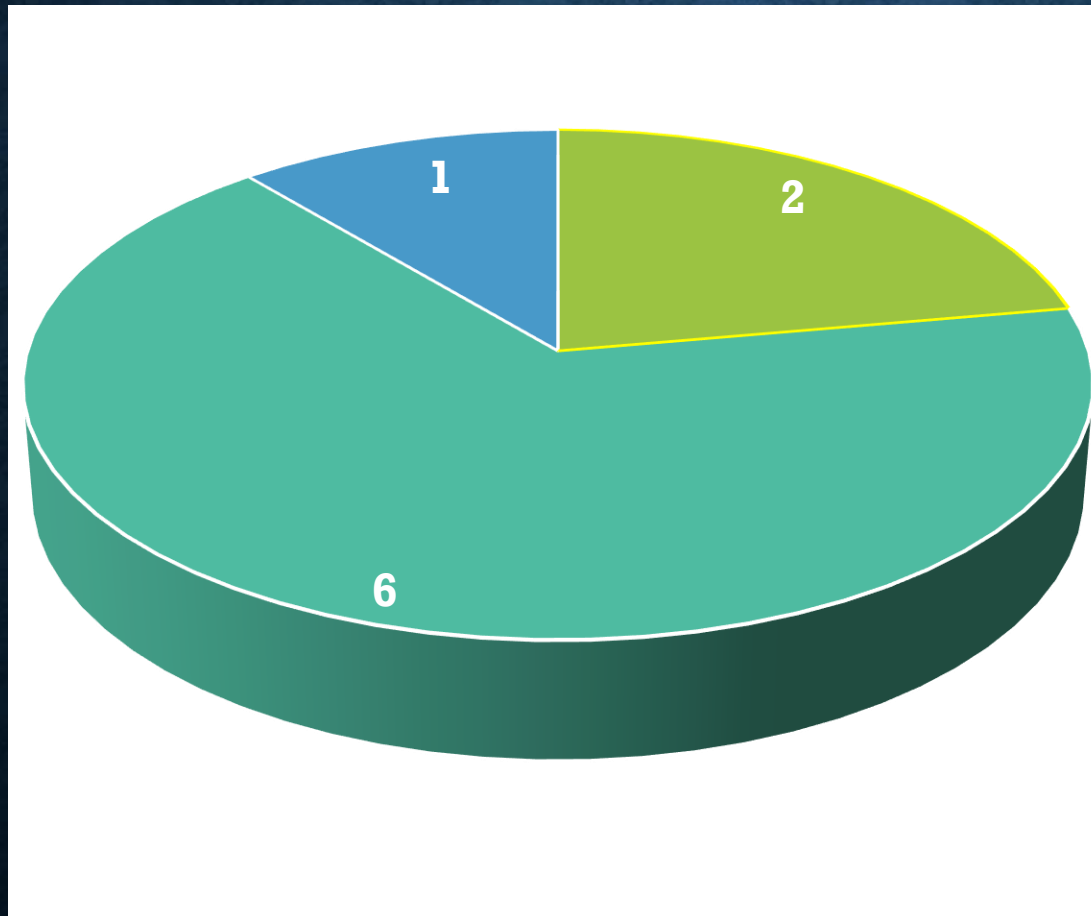
42 patients



The epithelium cells cover the body and lines in the majority of organs, such as the milk ducts in the breast gland or the digestive tract and are involved in the absorption of food, although it is just only one of the many features of epithelia.³⁷ The cells lining the brain called ependymocytes, are a type of glial cells, covering the walls of the ventricular system of the brain: the brain ventricles and the central tube of the spinal cord. They are involved in the exchange of material between the cerebrospinal fluid and nervous tissue and, unlike epithelial cells, have no basal membrane. Despite these differences, for simplicity both groups will be called

PATIENTS STATISTICS- INTESTINE

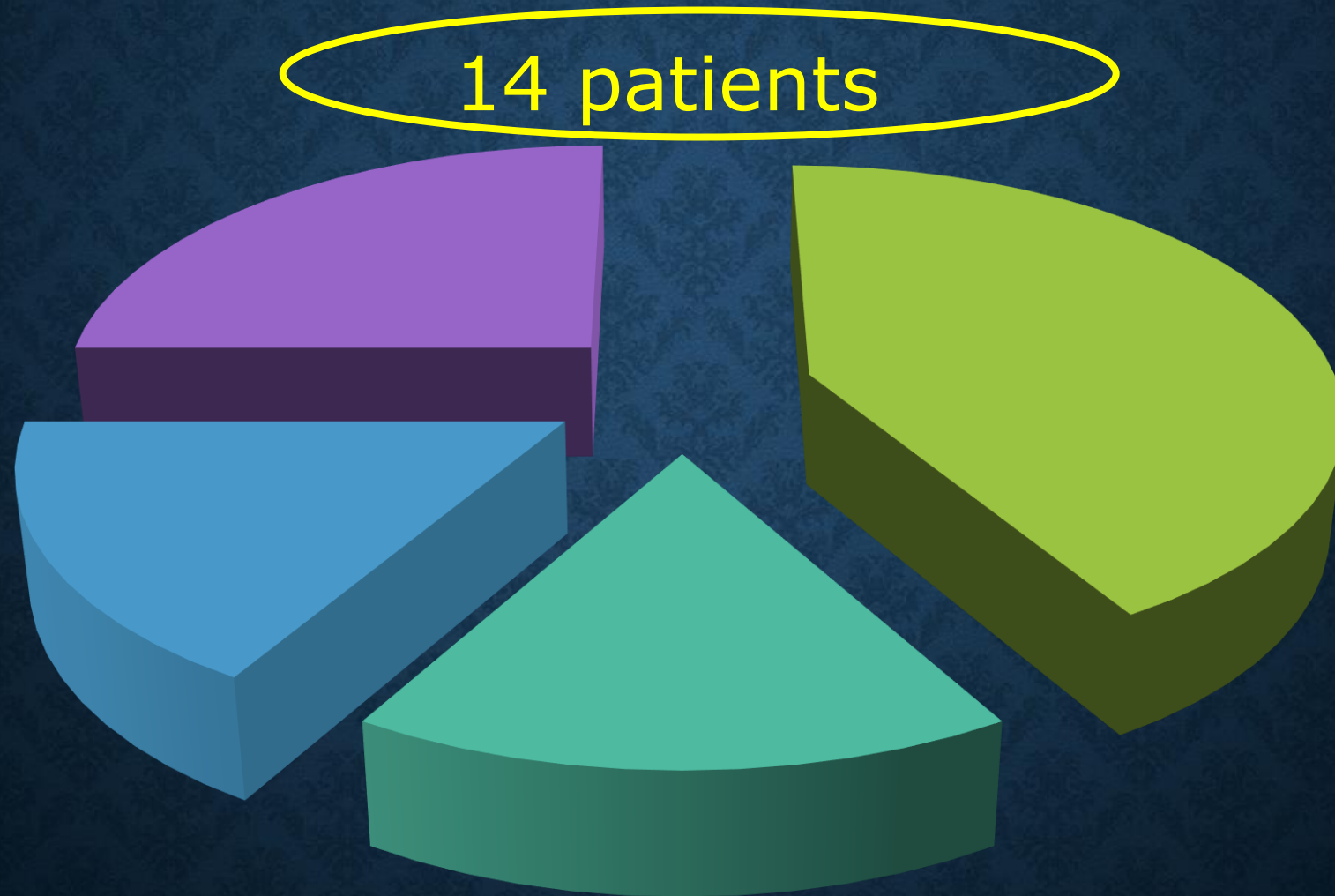
40 patients



■ rectal tumor

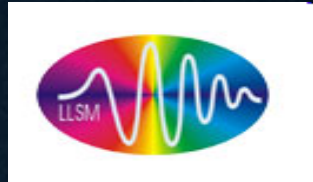
■ large intestine

PATIENTS STATISTICS-HEAD AND NECK



The epithelium cells cover the body and lines in the majority of organs, such as the milk ducts in the breast gland or the digestive tract and are involved in the absorption of food, although it is just only one of the many features of epithelia.³⁷ The cells lining the brain called ependymocytes, are a type of glial cells, covering the walls of the ventricular system of the brain: the brain ventricles and the central tube of the spinal cord. They are involved in the exchange of material between the cerebrospinal fluid and nervous tissue and, unlike epithelial cells, have no basal membrane. Despite these differences, for simplicity both groups will be called

INNOVATIONS



- Raman biomarkers
- Raman optical biopsy
- Virtual Raman histopathology
- The real-time *in vivo* neurosurgical Raman method

HOW DOES RAMAN SPECTROSCOPY AND IMAGING BENEFIT CANCER RESEARCH?

•RAMAN OPTICAL BIOPSY



The completeness of the surgical resection is a key factor in the progress of patients with cancer. The safety margin can be positive which means that not all cancer cells have been removed in the surgery. Patients with a positive margin often require more surgery to make sure that all the cancer is removed. The advantage of the "Raman biopsy" is that it provides direct biochemical information (vibrational fingerprints) in real time, it is not prone to subjective interpretation, and it monitors biological tissue without any external agents, in contrast to histopathological assessment.

H. Abramczyk, B. Brozek-Plaska, J. Surmacki, J. Jablonska-Galewicz, R. Kordek, *PMBB* 108 (2012) 74-81

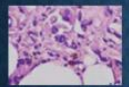
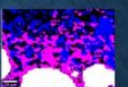
HOW DOES RAMAN SPECTROSCOPY AND IMAGING BENEFIT CANCER RESEARCH?

•RAMAN BIOMARKERS OF CANCER




Rumacki J, Brozek-Plaska B, Kordek R, Abramczyk H. The lipid-reactive oxygen species phenotype of breast cancers. Raman spectroscopy and mapping, PCA and PLADA for breast ductal carcinoma and invasive lobular carcinoma. Molecular tumor (epic) mechanisms beyond Warburg effect, *Analyst*, 2015, 140, 2122 - 2133, (21-23)

VIRTUAL RAMAN HISTOPATHOLOGY IMAGE

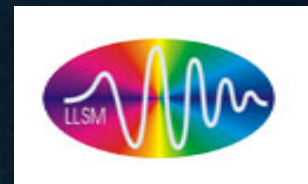



Abramczyk H et al., patent application

- Fast histopathological analysis for clinical practice
- Label-free histopathological analysis (without any staining procedures)
- Real time diagnostics to access the safety margin during operation by Raman-guided surgery
- High spatial resolution (small cancer changes can be easy identified)
- Objective diagnosis (without human interpretation, Raman spectra)
- Discrimination of grades with high specificity and sensitivity (c.a. 90%)
- Monitoring of tumor tissue heterogeneity

RAMAN SPECTROSCOPY GUIDES IN VIVO BRAIN OPTICAL BIOPSIES





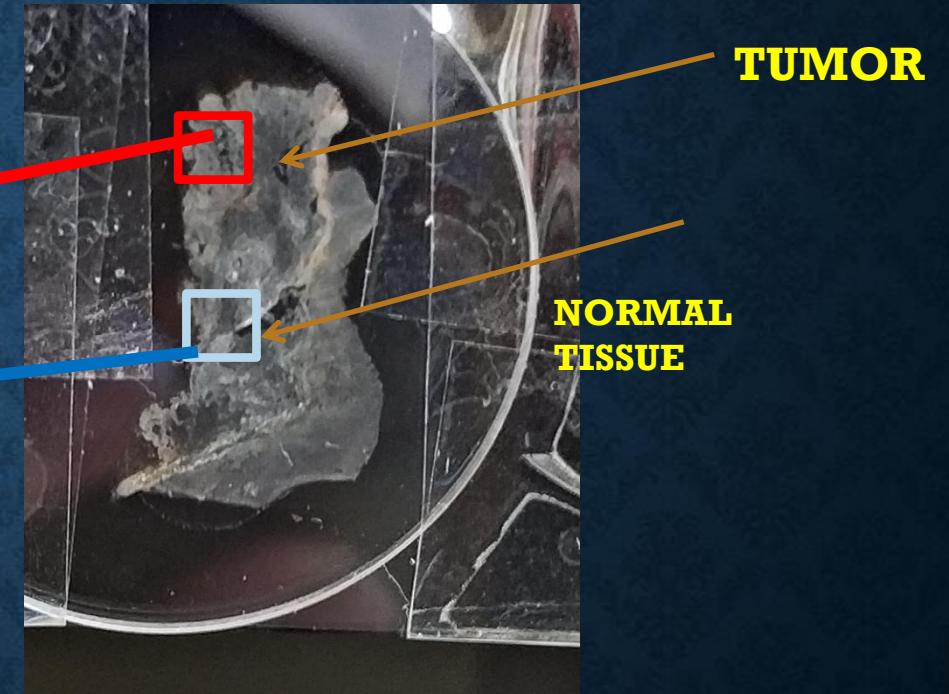
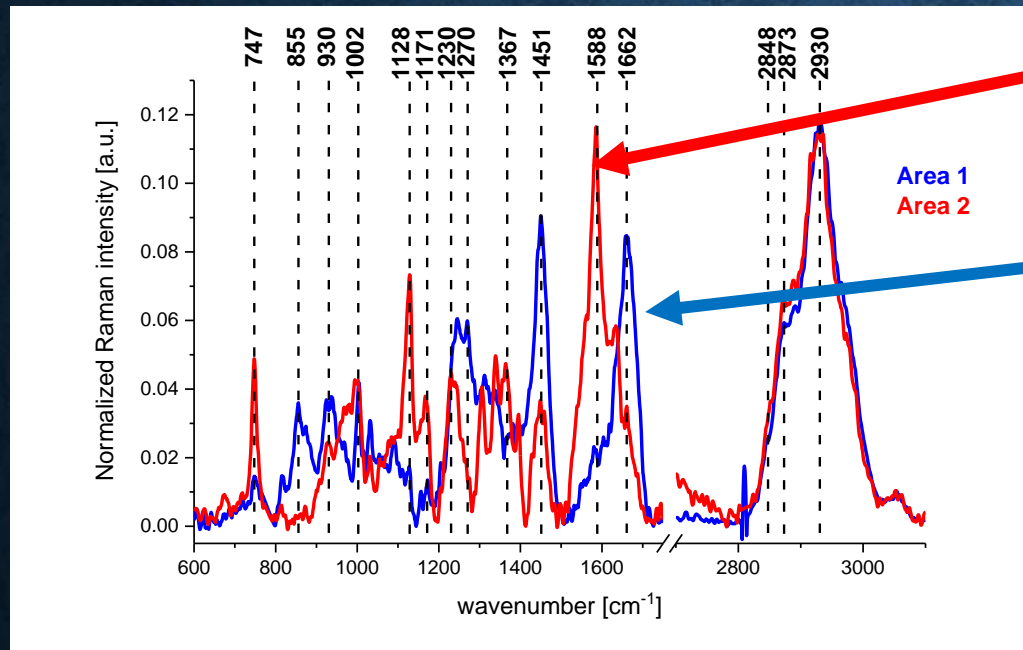
VISUALIZE CANCER IN REAL TIME AS DOCTORS OPERATE

- **For these reasons, a great need exists for practical tools that fit into the current surgical practice, and that enable surgeons to visualize cancer in real time as they operate.**

There is an urgent need to improve the conventional methods of cancer diagnostics. For example, it has in fact been found that 70–90% of mammographically detected lesions are found to be benign upon needle biopsy. Current imaging methods are often limited by inadequate sensitivity, specificity, spatial and spectral resolutions.

MRI- limited spatial resolution
FLUORESCENCE- limited spectral resolution

Raman spectroscopy has proven effective for detecting invasive brain cancer



Glioblastoma multiforme
Tissue brain section. Regrowth
after first removal

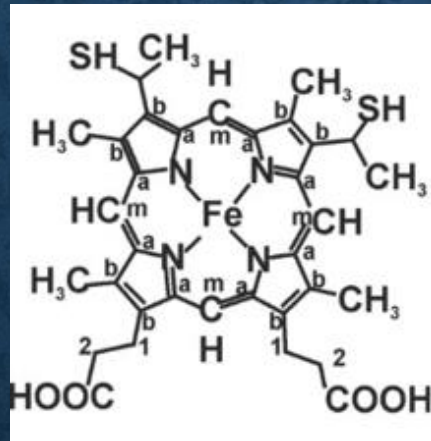
**DOUBLE FACE OF
CYTOCHROME C IN
CANCERS**

DOUBLE FACE OF CYTOCHROME C

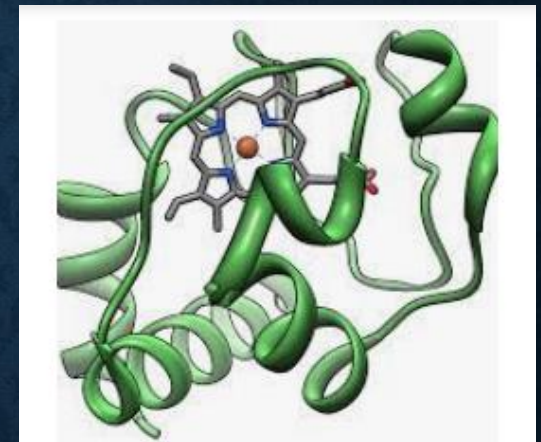
CYT C BELONGS TO FAMILY OF HEME CONTAINING METALLOPROTEINS



apocytochrome c



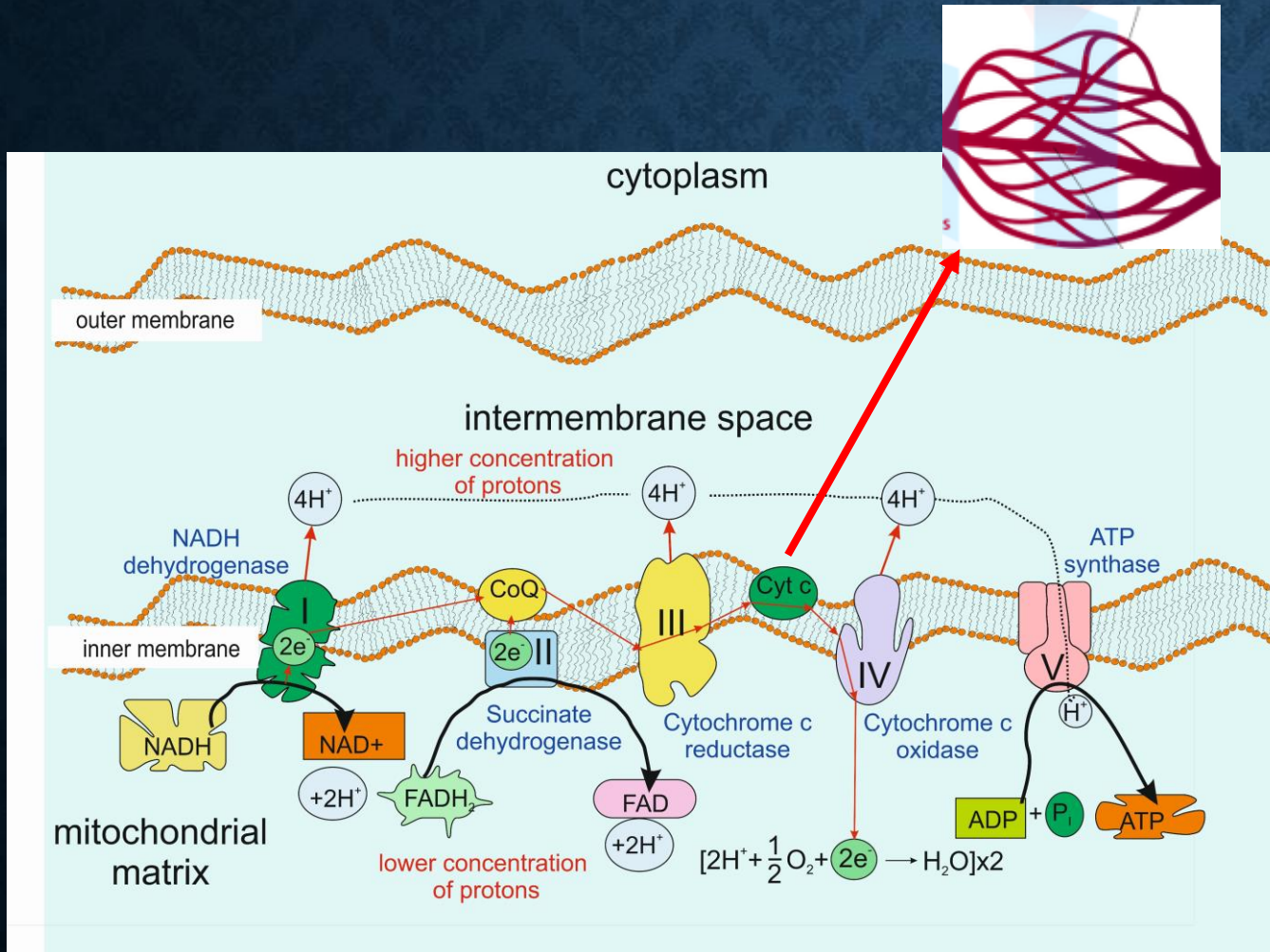
heme



cytochrome c

Cytochrome *c* is synthesized from two inactive precursor molecules: apocytochrome *c* (a protein that is encoded by a nuclear gene and imported into mitochondria) and heme (which is synthesized in mitochondria).

DOUBLE FACE OF CYTOCHROME C

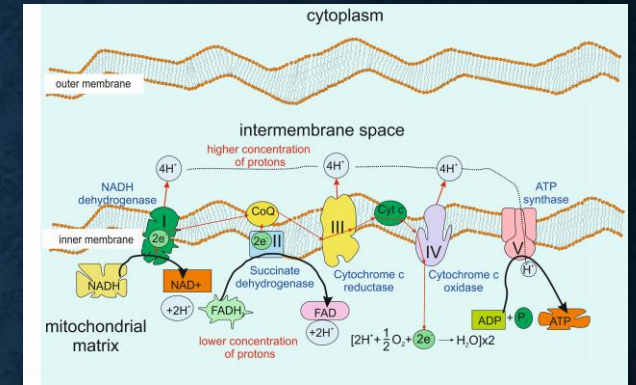


The native cytochrome *c* favors its most common function as an electron shuttle between complexes III and IV of mitochondria.

At normal conditions Cyt *c* is located in the intermembrane space of mitochondria. But it is released into bloodstream during pathological conditions.

Multiple functions of cyt *c*

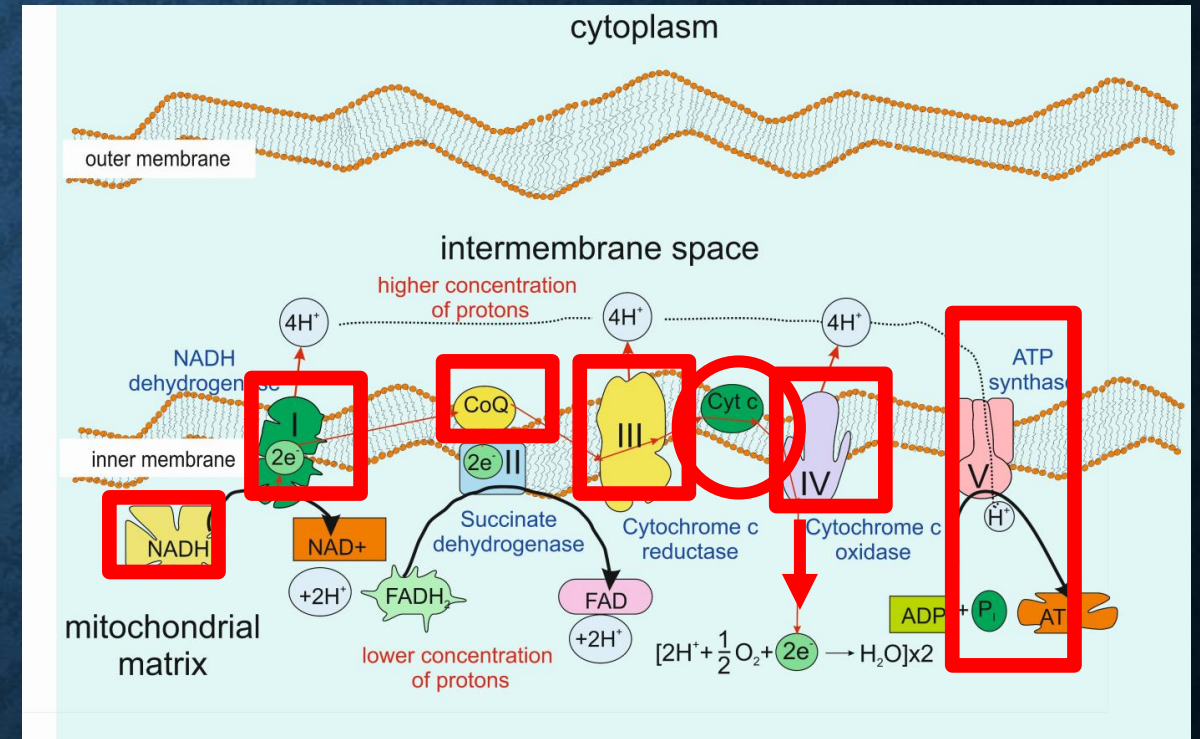
- in mitochondrial electron transport
- Apoptosis via interactions with Apaf-1 (Apoptotic protease activating factor 1) in the cytosol
- peroxidase oxidation of cardiolipine (CL)



raise a question about regulation and switching mechanisms involved in its diverse pathways

ELECTRON TRANSPORT CHAIN

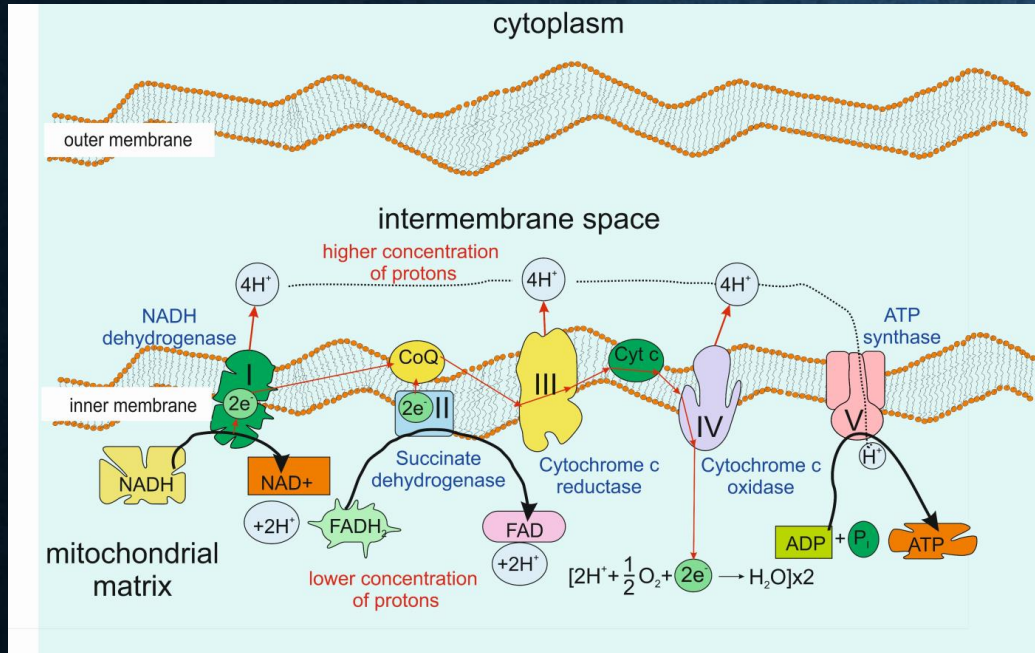
The electrons are transported from NADH to the oxygen atoms through the electron transport chain. NADH transfers electrons to NADH dehydrogenase, a large protein complex containing FMN and two types of iron-sulfur (Fe-S) centers embedded in iron-sulfur proteins. FMN takes electrons going into FMNH₂ and forwards them further to the Fe-S center, where the iron atom picks up and donates electrons oscillating between the Fe³⁺ state and the Fe²⁺ state. From NADH dehydrogenase, electrons are transferred to ubiquinone (coenzyme Q, CoQ), transformed into ubiquinol (i.e. CoQH₂) and passed on to cytochrome b₁ complex III. The latter includes cytochrome b and cytochrome c₁, as well as the Fe-S protein. Each cytochrome contains a heme group with an iron atom in the center, which, when receiving an electron, changes from Fe³⁺ to Fe²⁺. After donating the electron to the next carrier, the iron atom returns to the Fe³⁺ state. The cytochrome b₁ complex transfers electrons to cytochrome c, which in turn transfers them to cytochrome oxidase, complex IV containing two cytochromes (cytochrome a and cytochrome a₃) bound to two copper atoms (Cu A and Cu B, respectively). During electron transfer, the copper atoms oscillate between the Cu²⁺ state and the Cu⁺ state. Eventually, cytochrome oxidase transfers 4 electrons to molecular oxygen, forming two water molecules. The energy and hydrogen atoms released as a result of these processes participate in chemosmosis.



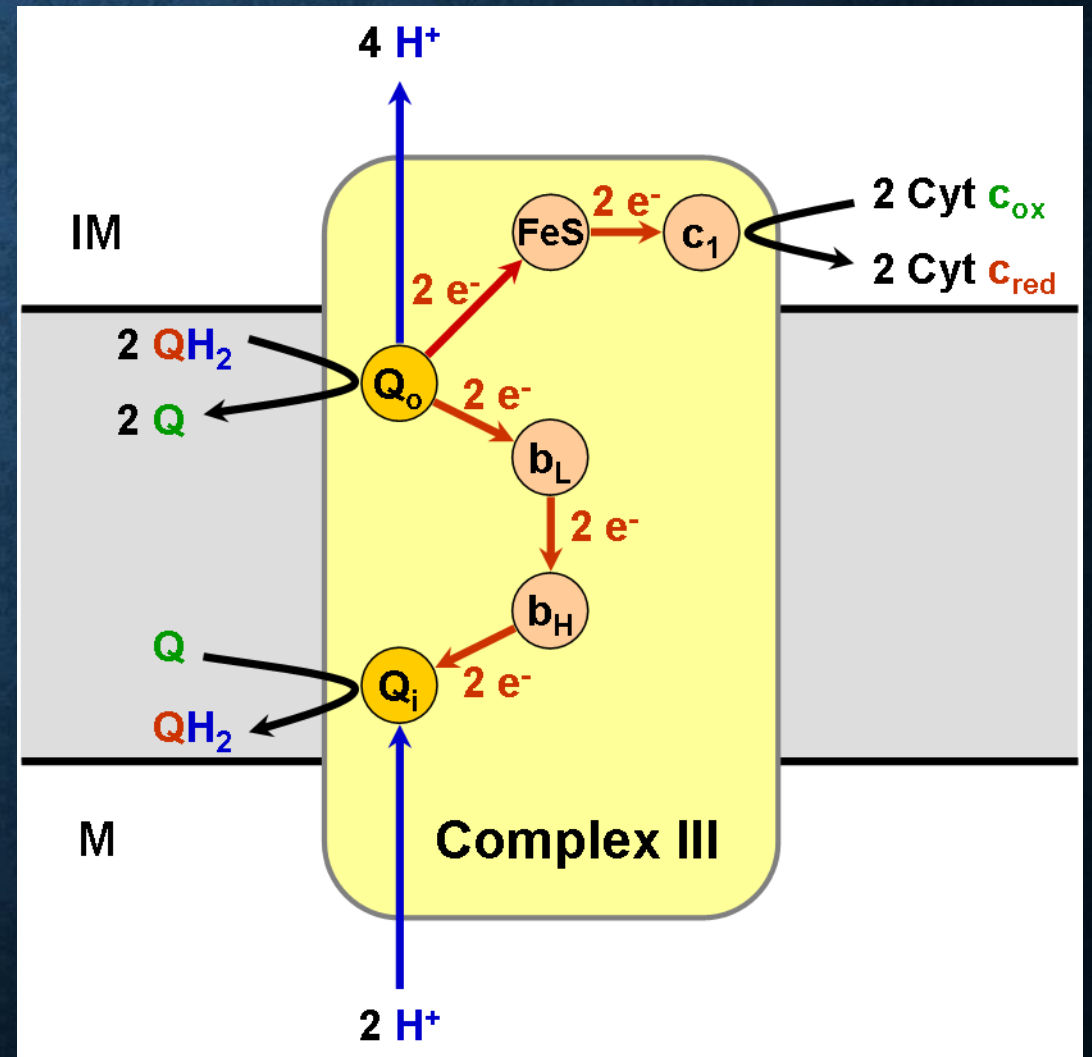
Cytochrome c (cyt c) is a globular redox protein that shuttles electrons between respiratory Complexes III and IV in mitochondria

Oxidases - enzymes that catalyze the transfer of hydrogen to oxygen to form water or hydrogen peroxide. Stands out: first-team oxidase - the product is water (e.g. cytochrome oxidase has a prosthetic group in the form of two heme groups)

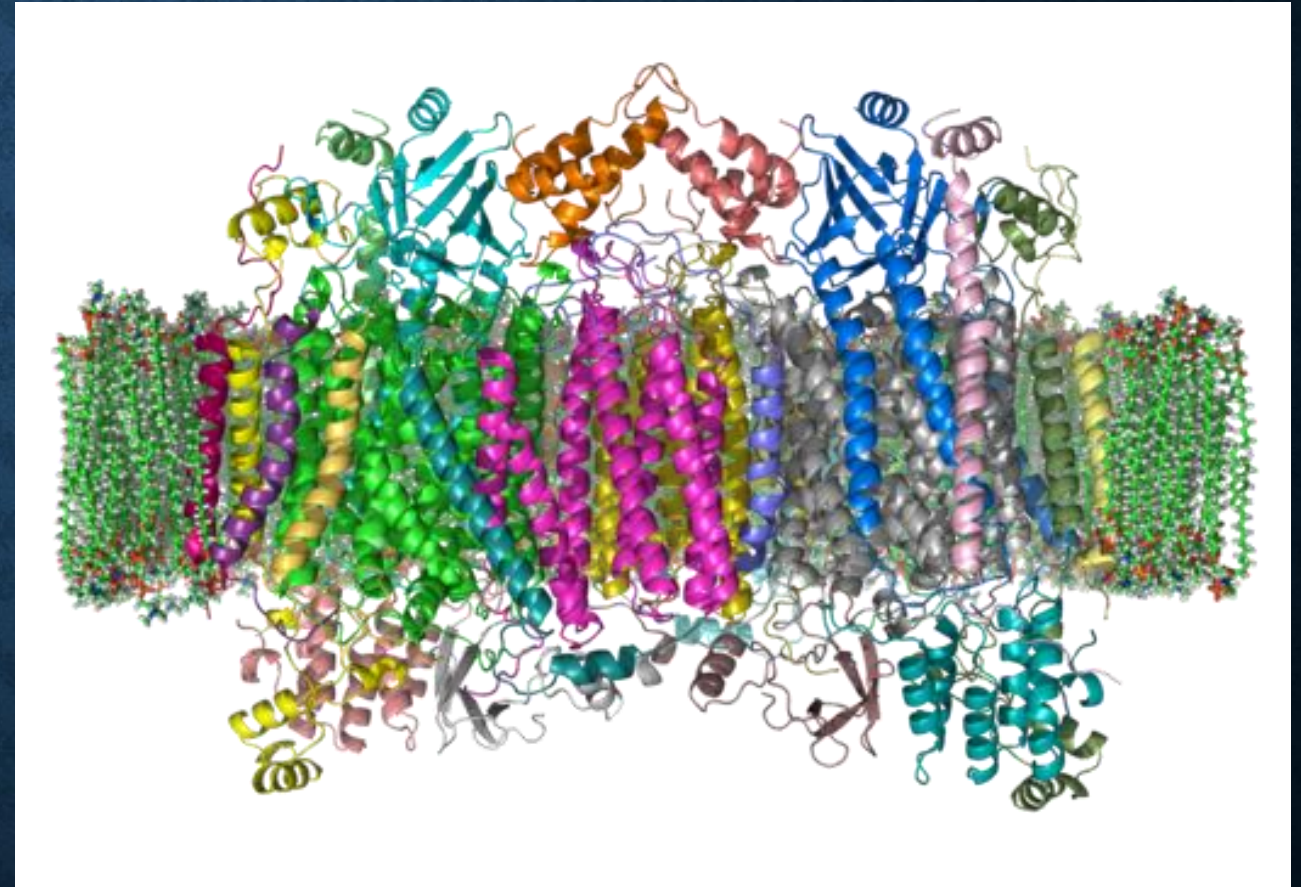
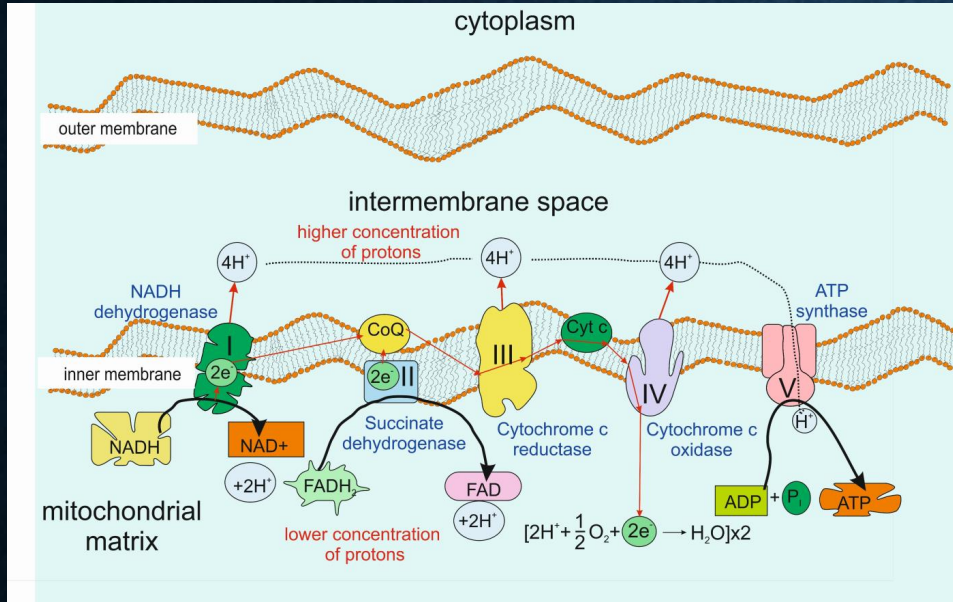
Cytochrome c reductase (complex III)



REDUCTASES - A GROUP OF ENZYMES THAT CATALYZE REDUCTION REACTIONS



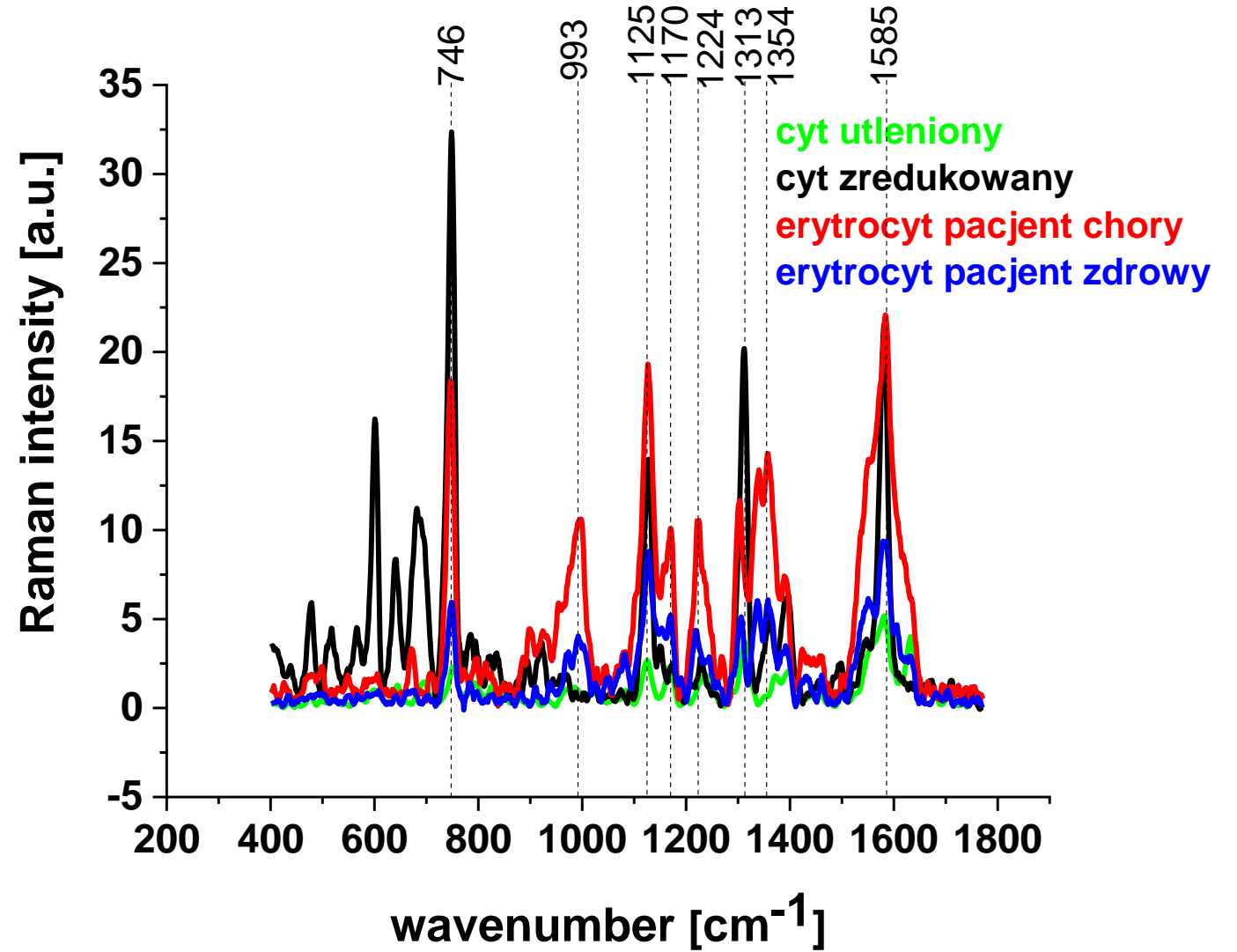
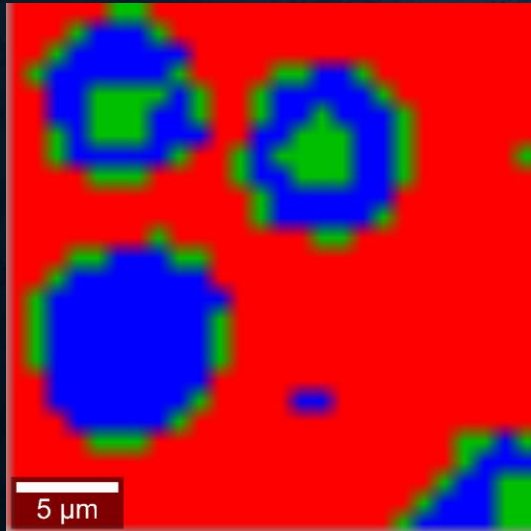
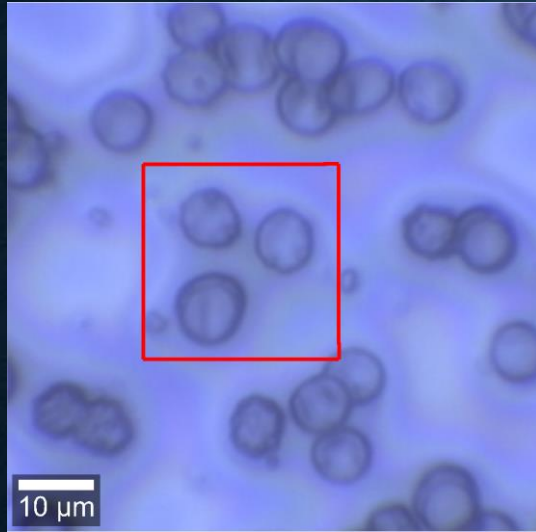
CYTOCHROME C OKSIDASE (COMPLEX IV)



Oxidases - enzymes that catalyze the transfer of hydrogen to oxygen to form water or hydrogen peroxide. Stands out: first-team oxidase - the product is water (e.g. cytochrome oxidase has a prosthetic group in the form of two heme groups)

Cytochrome c oxidase (also cytochrome oxidase, complex IV of the respiratory chain) - is a large transmembrane protein complex of the inner membrane of the mitochondria and bacteria. It is the last protein in the respiratory chain (IV). It receives electrons (oxidizes) from cytochromes c and transfers them to the oxygen molecule, reducing it, as a result of which, when H⁺ ions are attached, two water molecules are formed. During this process, it also transfers four H⁺ ions across the membrane, supporting the formation of the chemosmotic potential.

Cytochrome c vs hemoglobine in human blood erythrocytes



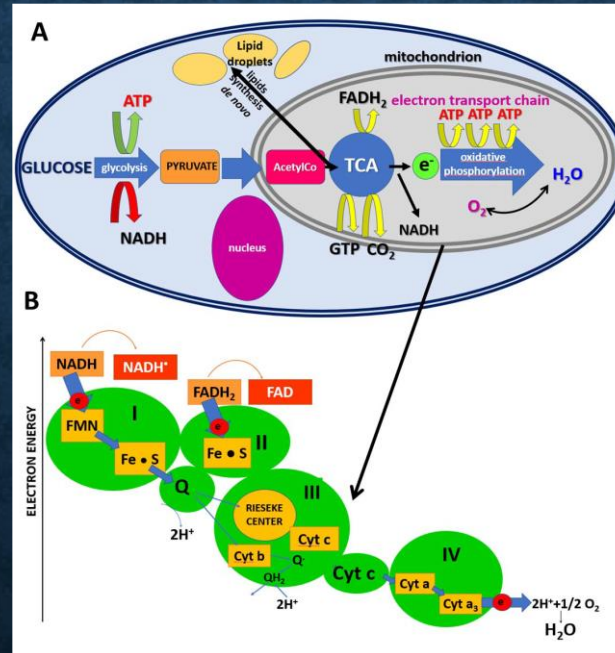
DOUBLE FACE OF CYTOCHROME C

respiration
Oxidative
phosphorylation

The dual-function of Cyt c comes from its capability to act as mitochondrial redox carrier that transfers electrons between the membrane-embedded complexes III and IV and to serve as a cytoplasmic apoptosis-triggering agent, activating the caspase cascade

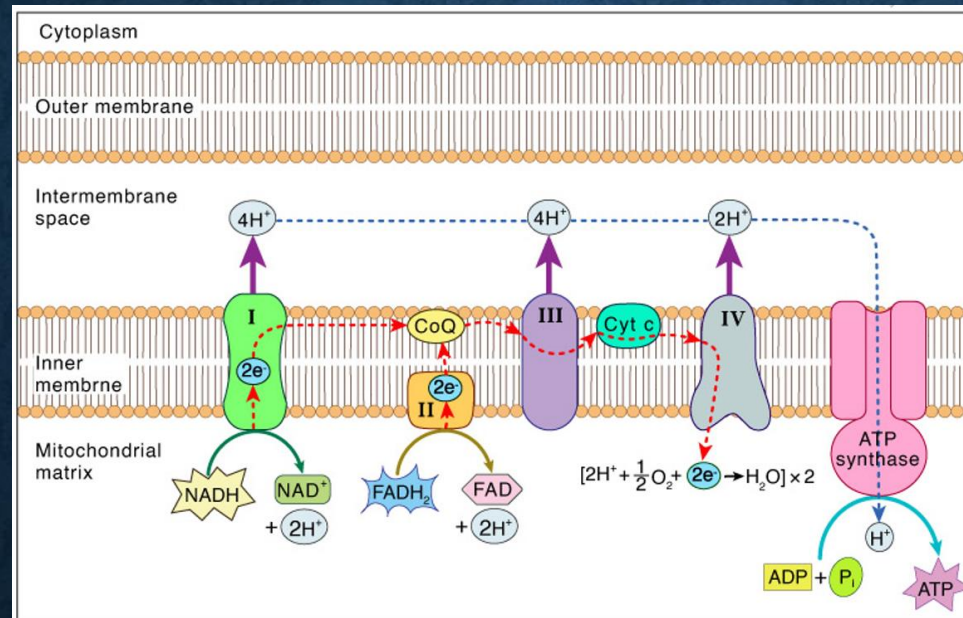
cell death
(apoptosis)

Glycolysis takes place in the cytoplasm. Within the mitochondrion, the citric acid cycle (TCA) occurs in the mitochondrial matrix, and oxidative metabolism and the electron transport chain occurs at the internal mitochondrial membranes.



CYTOCHROME C (CYT C) IS A KEY PROTEIN THAT IS NEEDED TO MAINTAIN LIFE (RESPIRATION) AND CELL DEATH (APOPTOSIS).

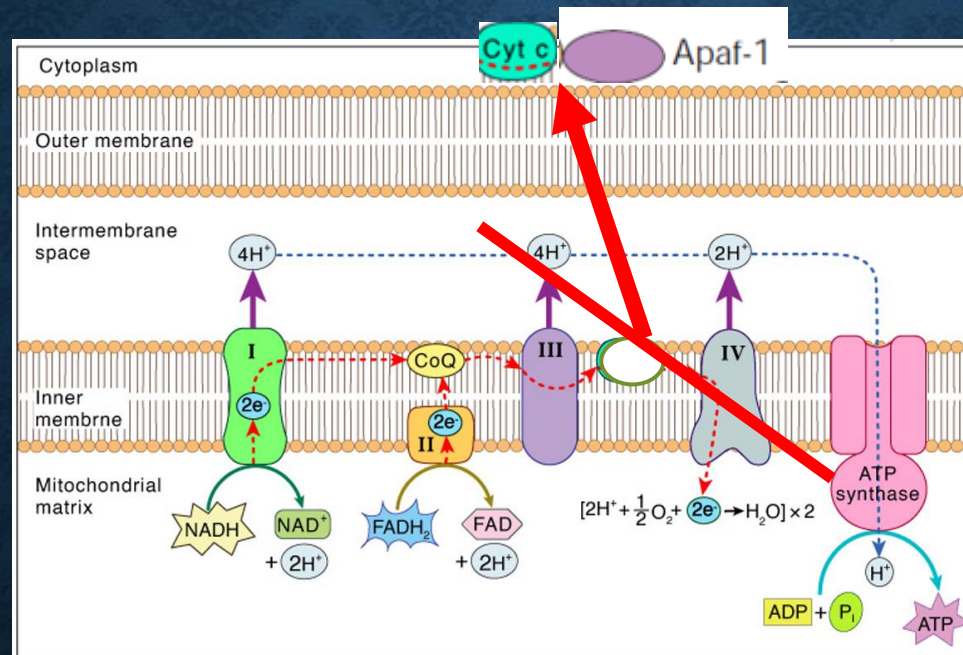
Respiration
Oxidative
phosphorylation



cell death
(apoptosis)

During apoptosis cytochrome c is released from the intermembrane space along with other soluble intermembrane proteins. This blocks the transfer of electrons between complexes III and IV of the respiratory chain, resulting in loss of ATP synthesis. Ectopic cytochrome c interacts with Apaf-1 to trigger the caspase cascade.

CYTOCHROME C (CYT C) IS A KEY PROTEIN THAT IS NEEDED TO MAINTAIN LIFE (RESPIRATION) AND CELL DEATH (APOPTOSIS)



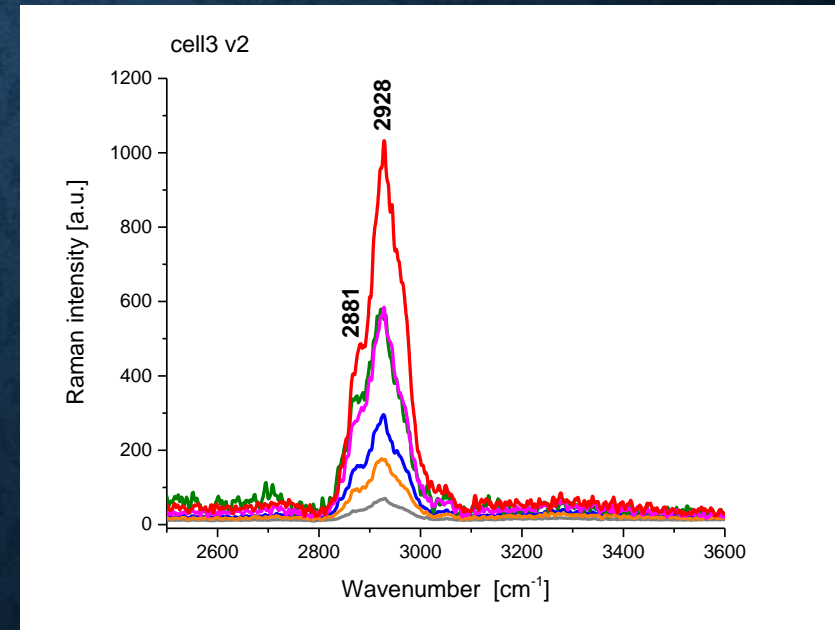
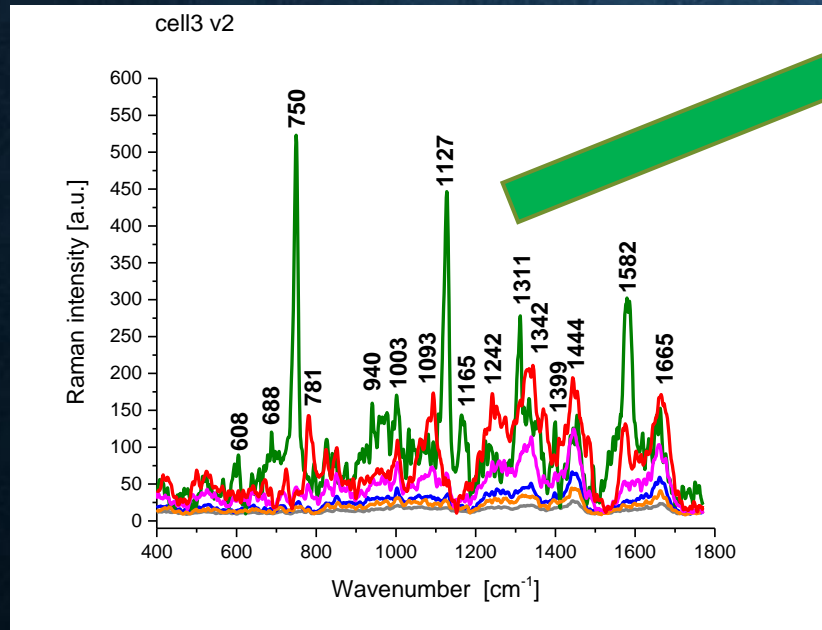
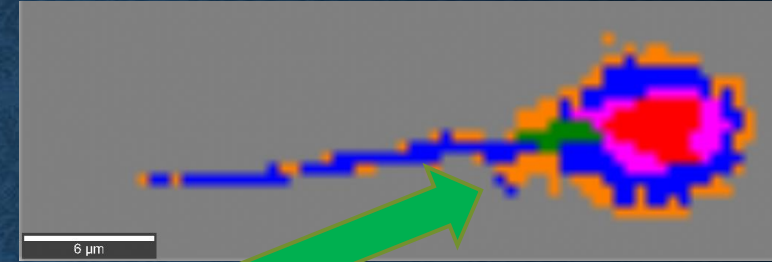
cell death
(apoptosis)

During apoptosis cytochrome c is released from the intermembrane space along with other soluble intermembrane proteins to cytosol. Cytochrome c, which is in an abnormal place or position in cytosol interacts with Apaf-1 to trigger the caspase cascade and apoptosis. This blocks the transfer of electrons between complexes III and IV of the respiratory chain, resulting in loss of ATP synthesis.

Life and death decisions are made by cytochrome *c*?

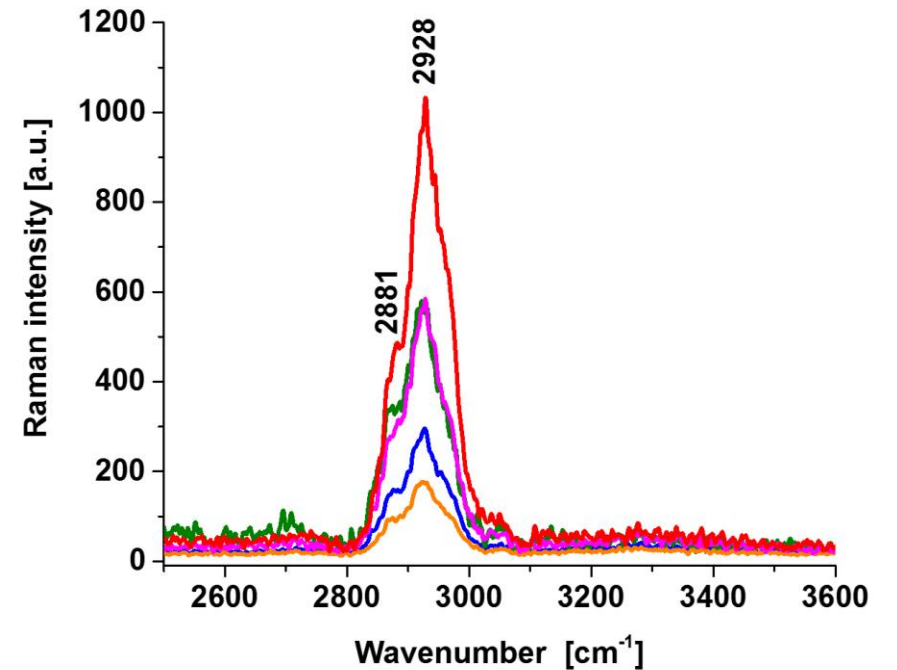
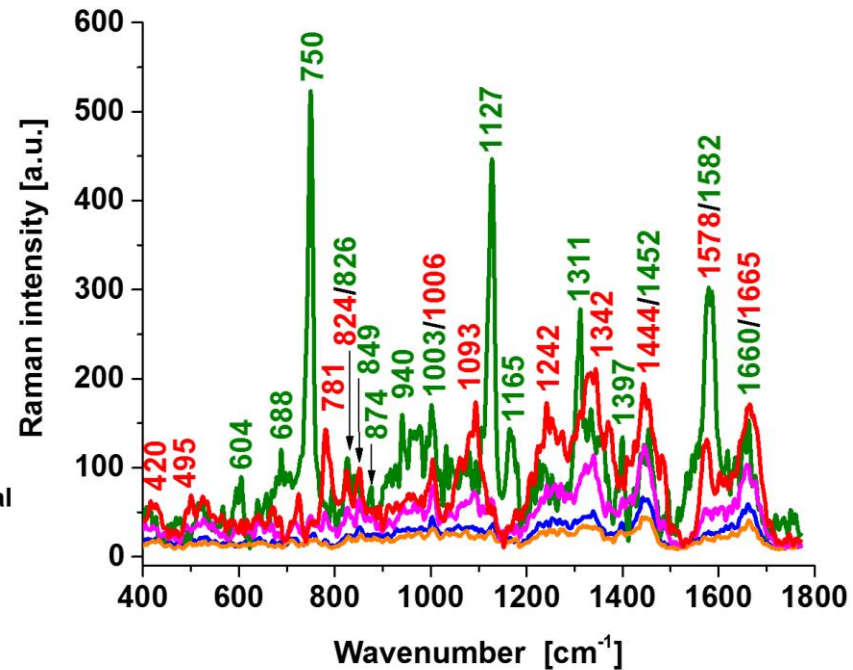
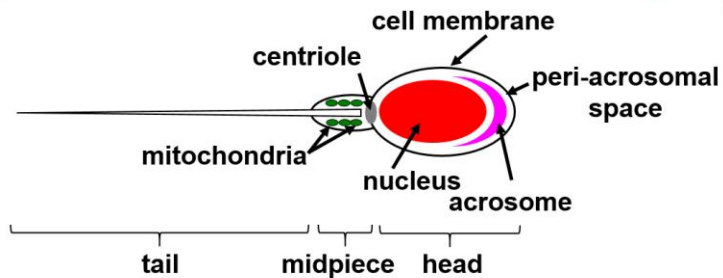
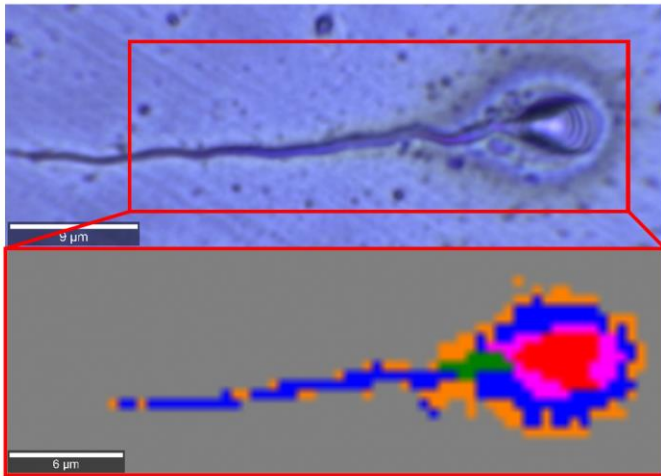


spermatozoid



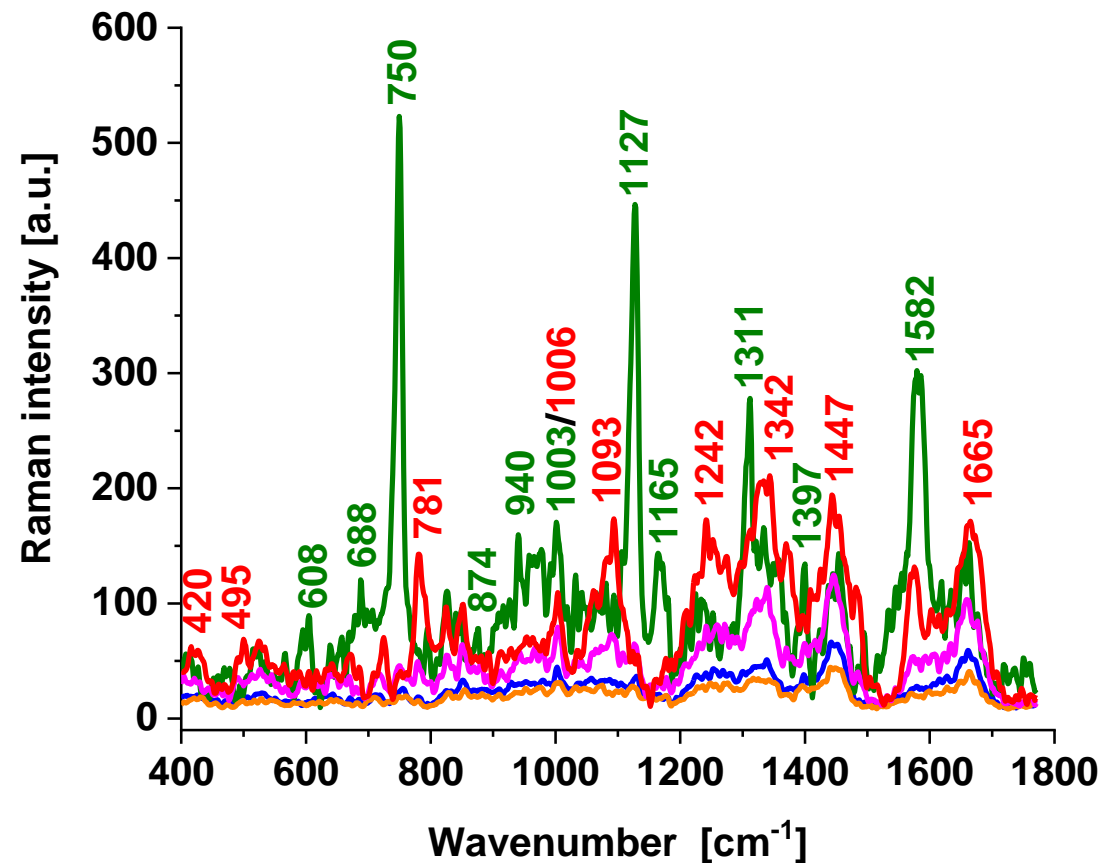
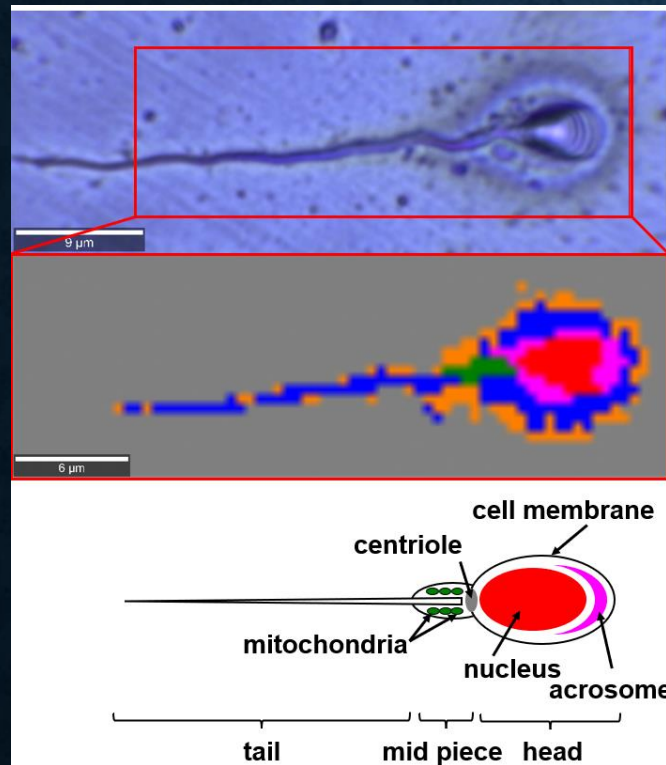
Life and death decisions are made not by cytochrome *c* itself but rather by whatever causes its release from the mitochondria.

spermatozoid



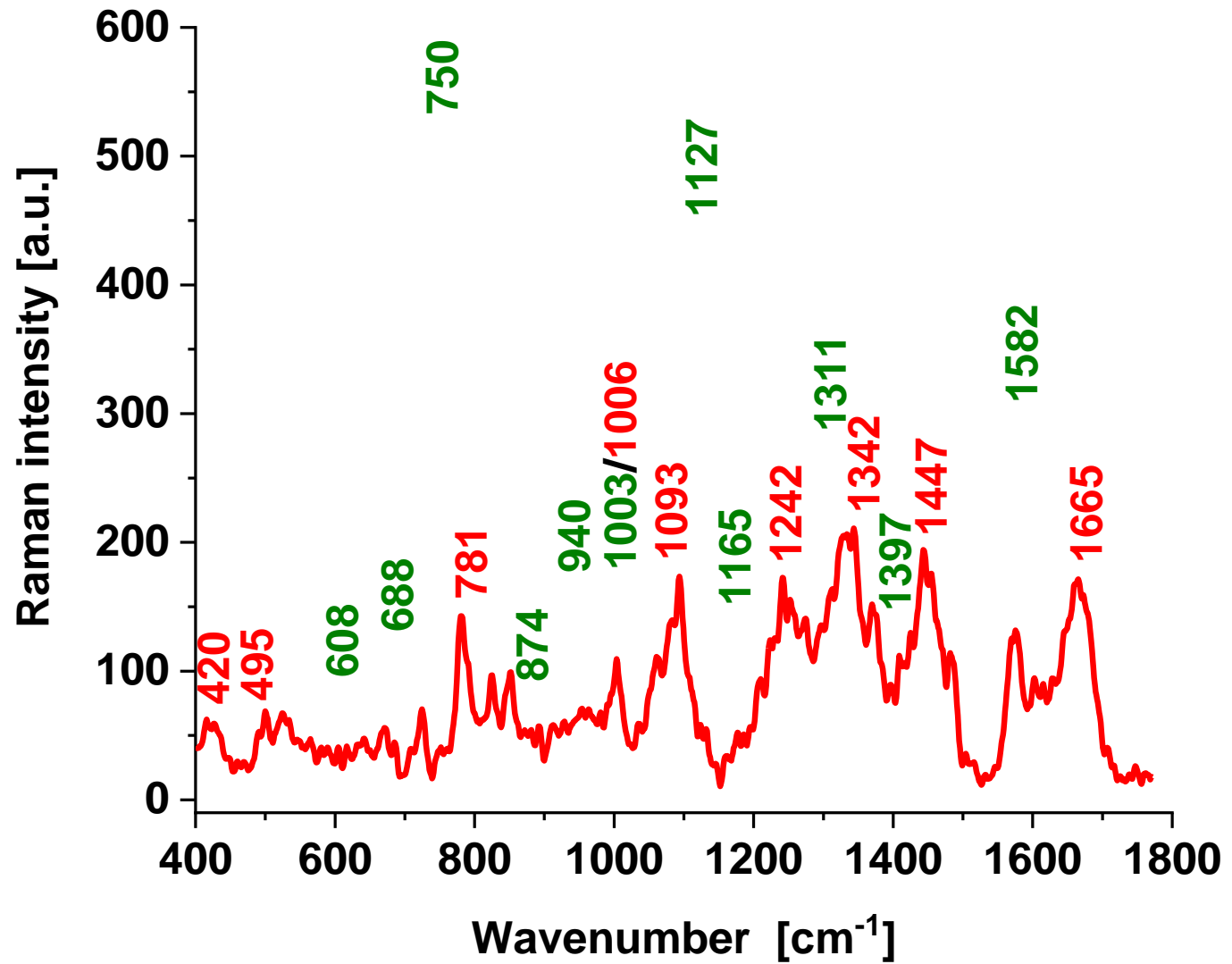
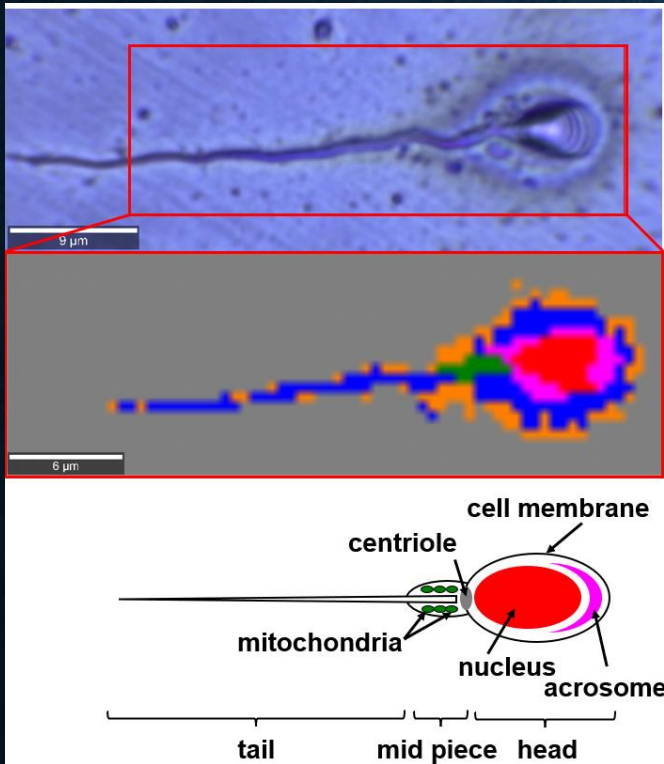
We studied the biochemical composition of specific organelles in sperm cells by Raman imaging. The structures of the head consisting of the nucleus and acrosome, the midpiece representing mitochondria, and the tail characterized by the sperm axoneme surrounded by outer dense fiber and covered by the membrane were measured.

spermatozoid

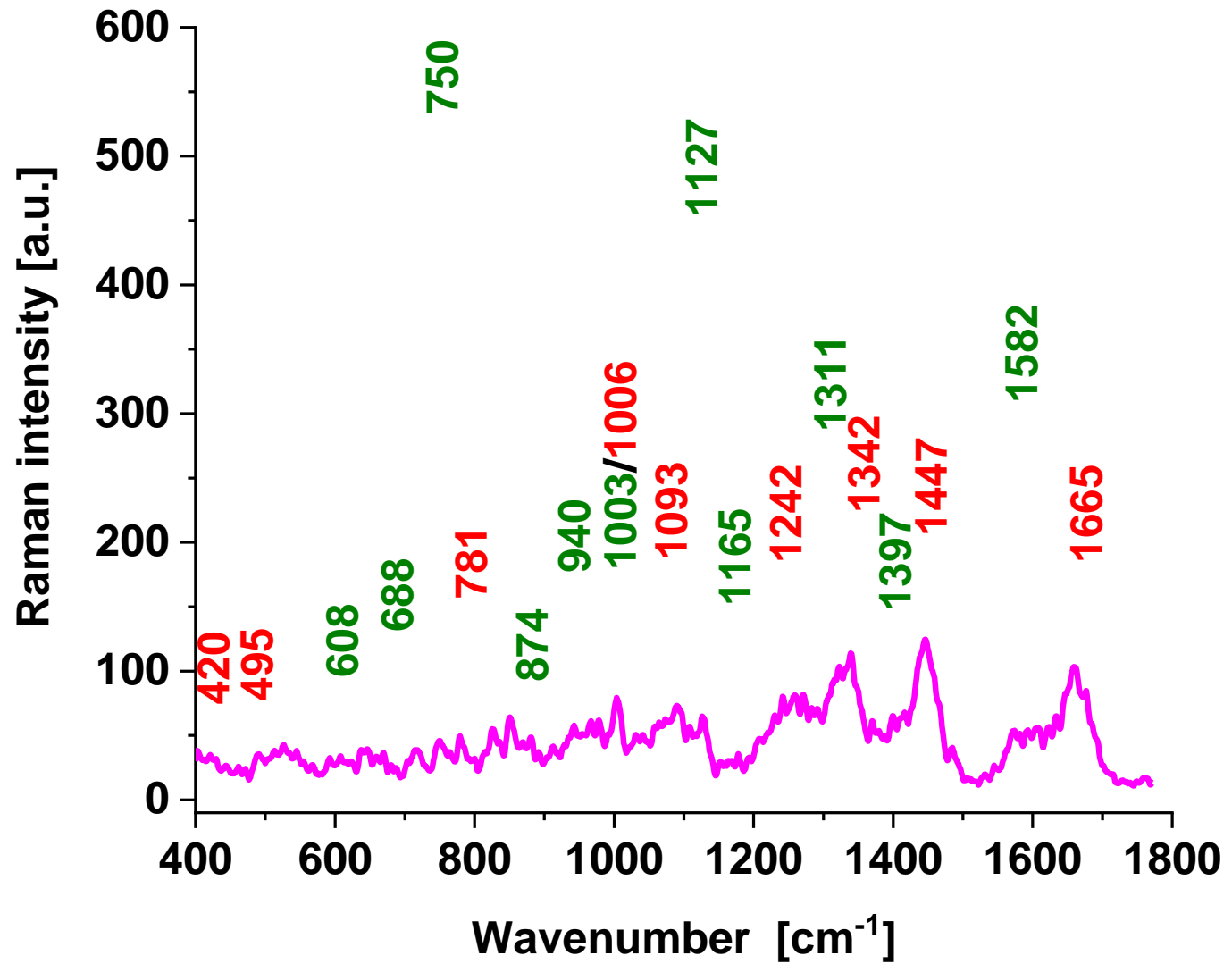
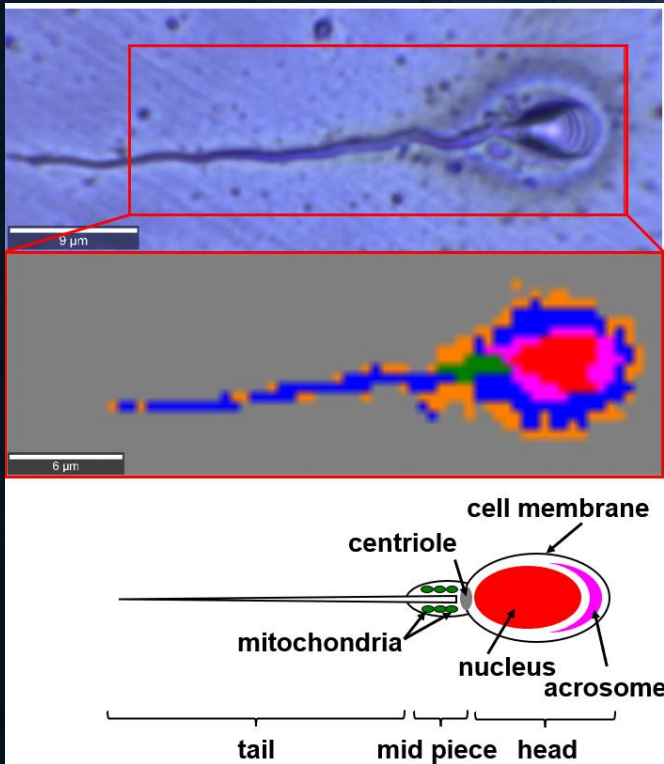


We studied the biochemical composition of specific organelles in sperm cells by Raman imaging. The structures of the head consisting of the nucleus and acrosome, the midpiece representing mitochondria, and the tail characterized by the sperm axoneme surrounded by outer dense fiber and covered by the membrane were measured.

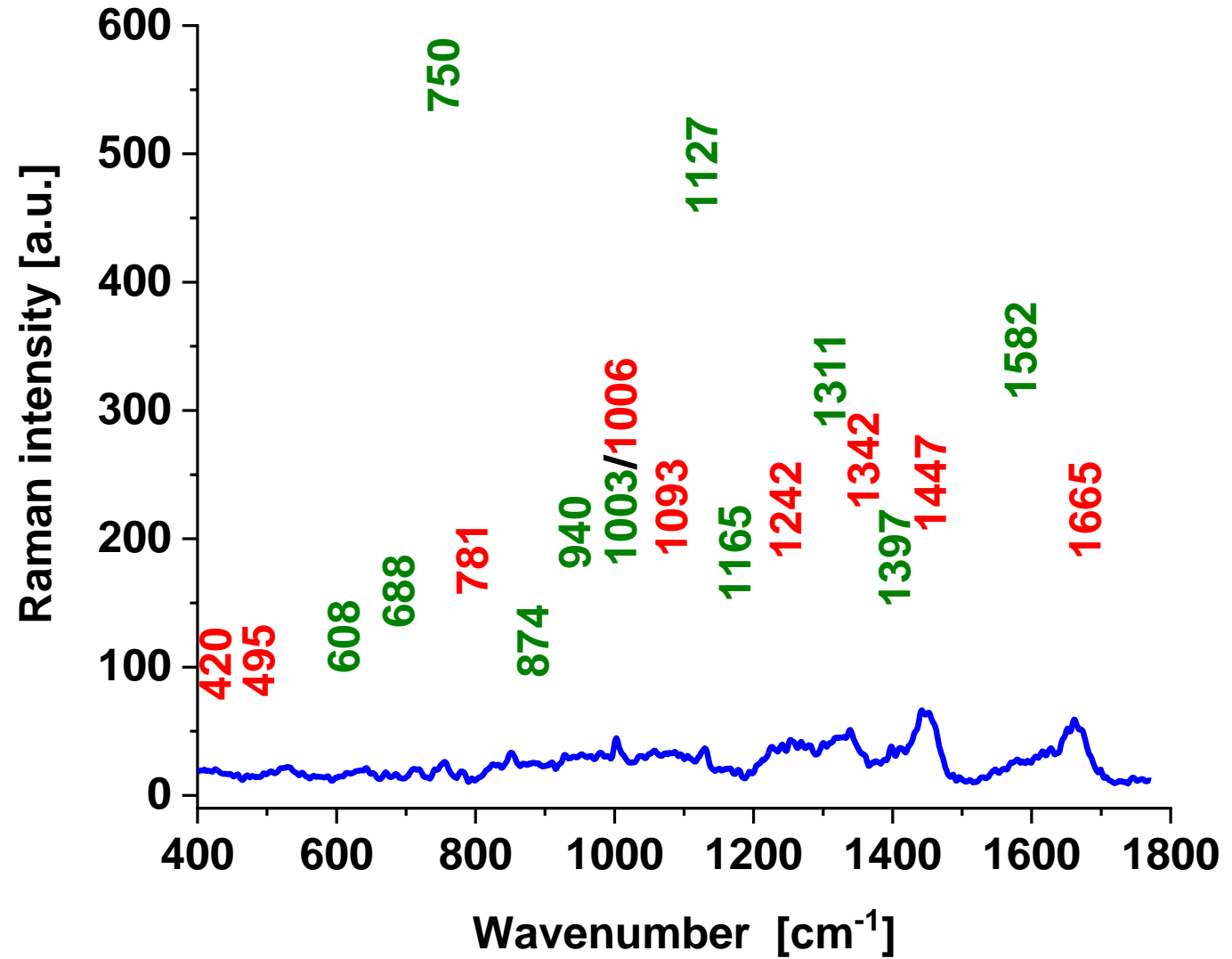
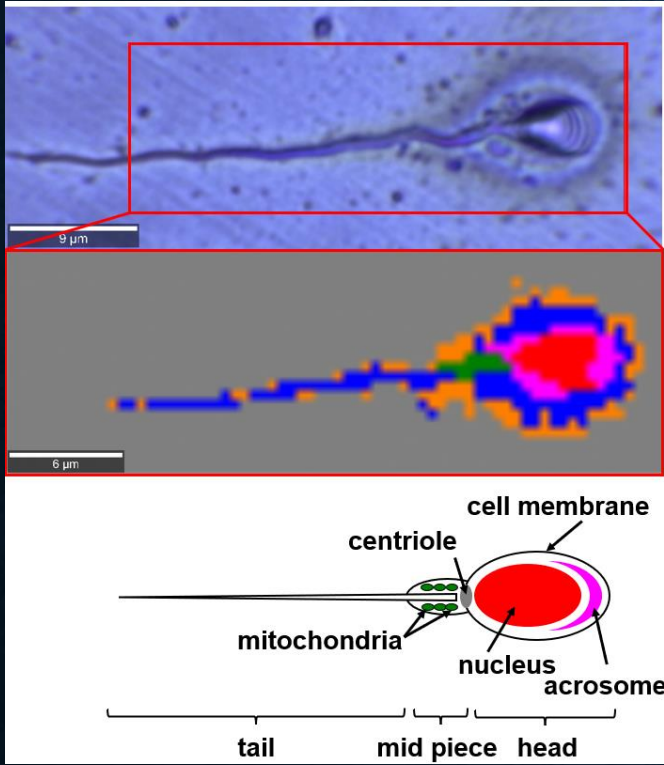
Spermatozoid nucleus



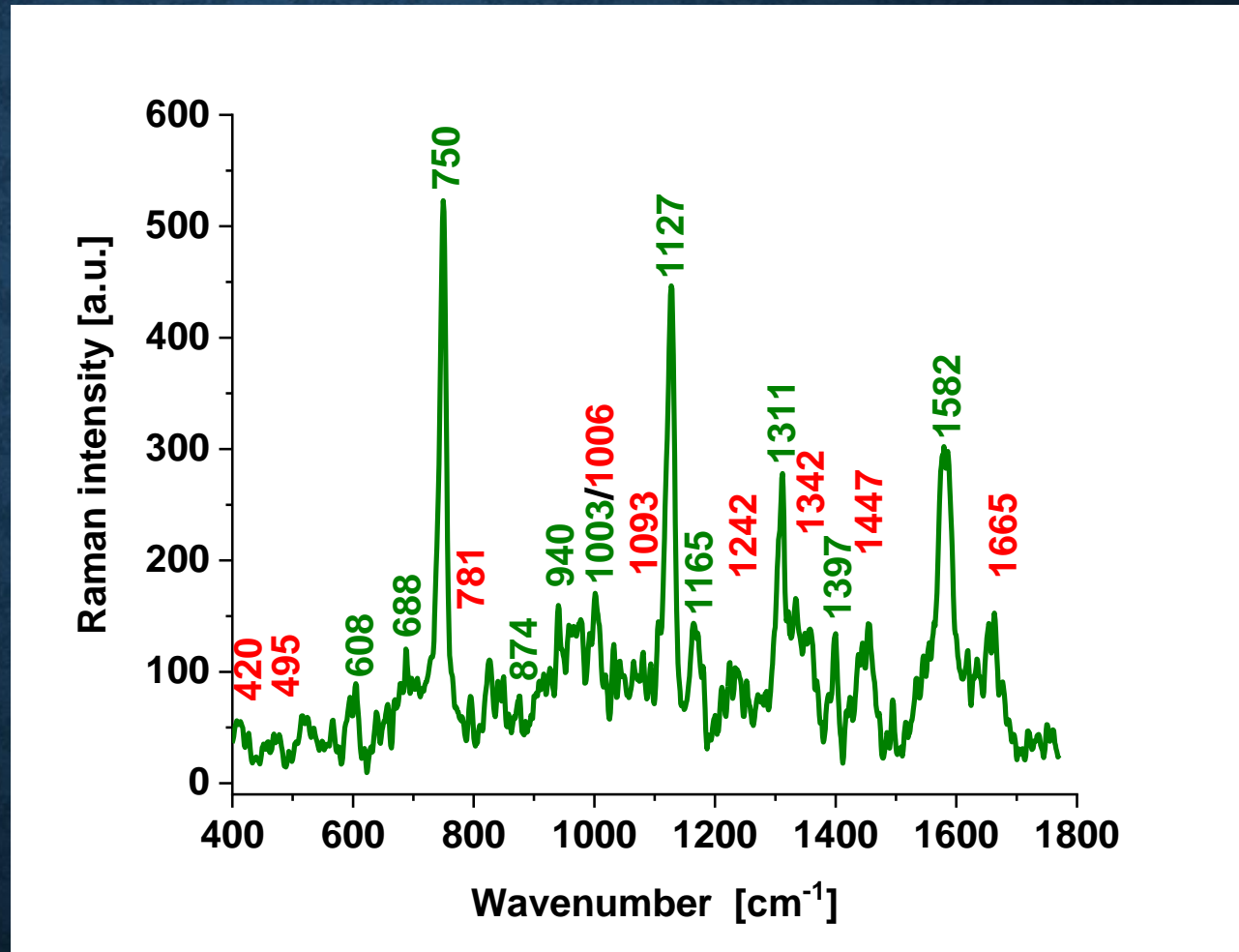
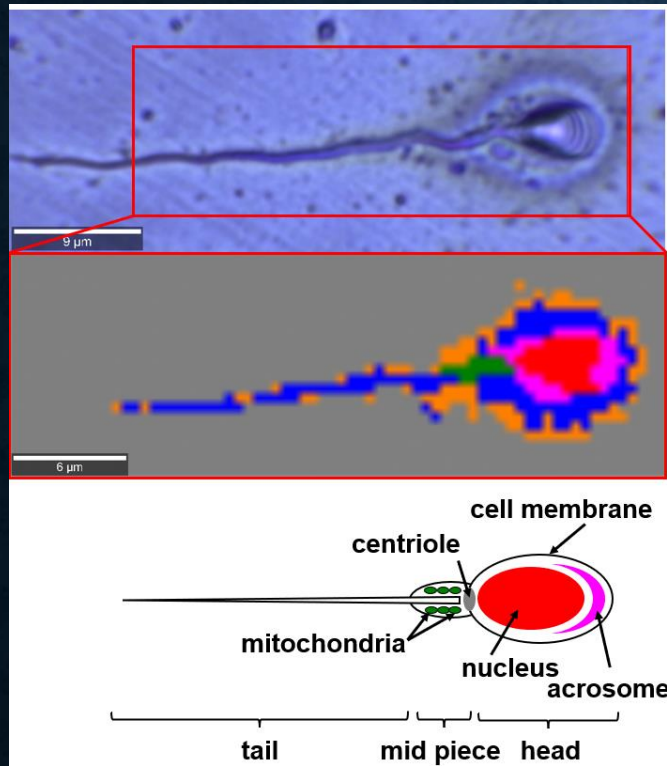
spermatozoid acrosome



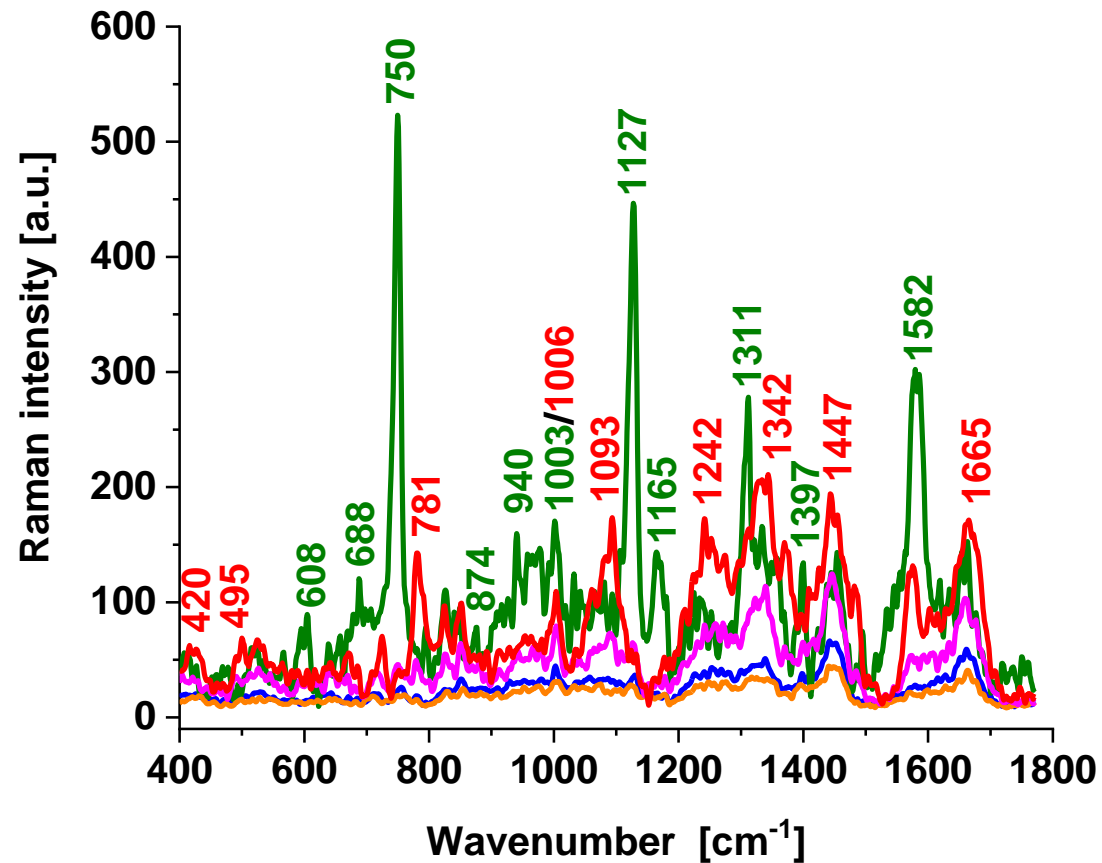
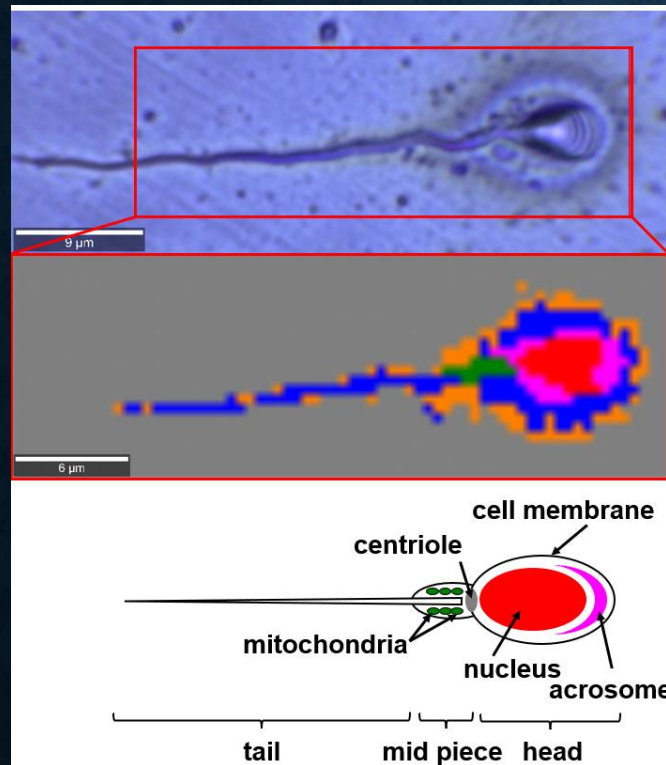
Spermatozoid periacrosomal space and membrane



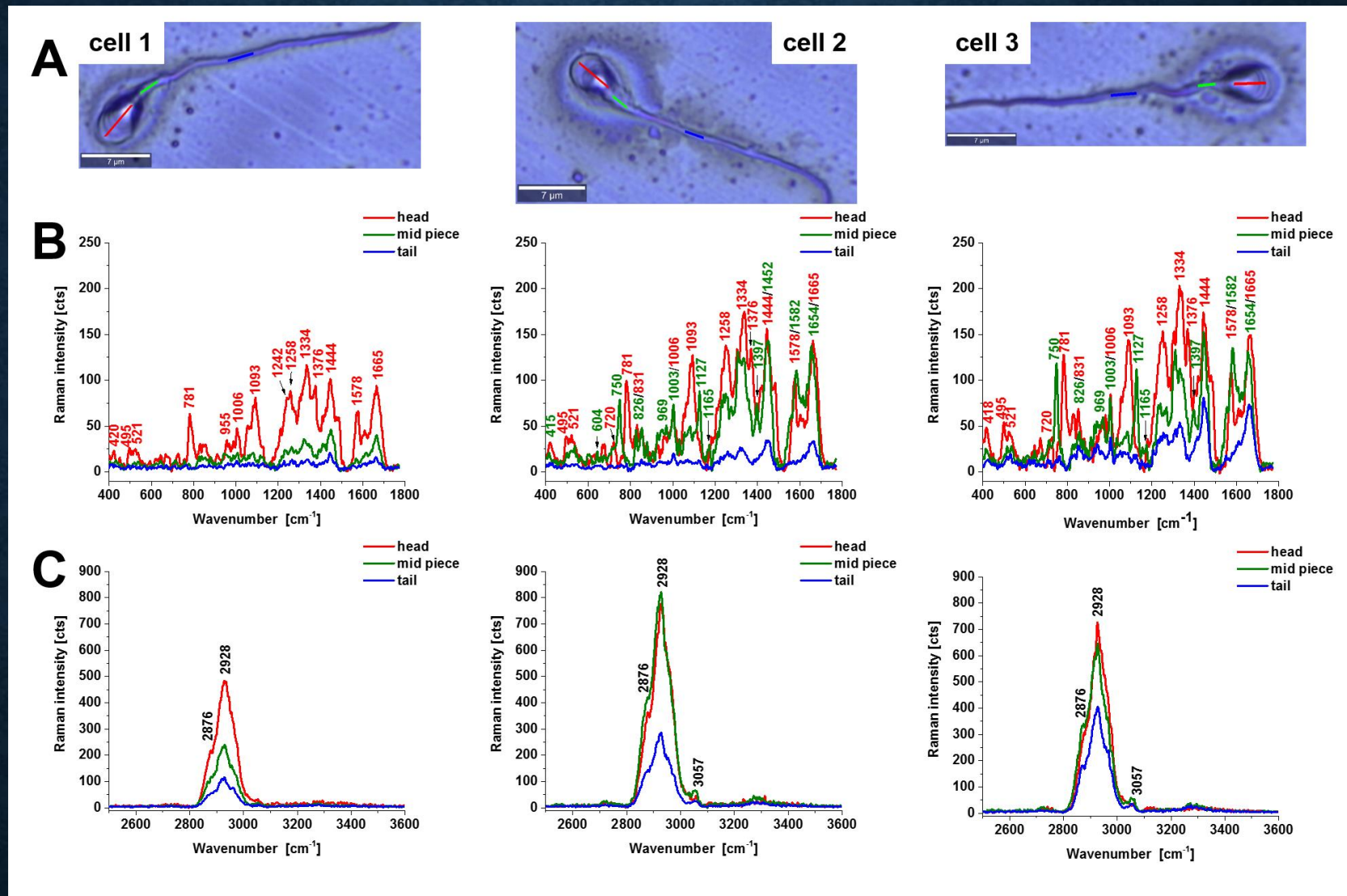
Spermatozoid - mitochondria cytochrome c



spermatozoid

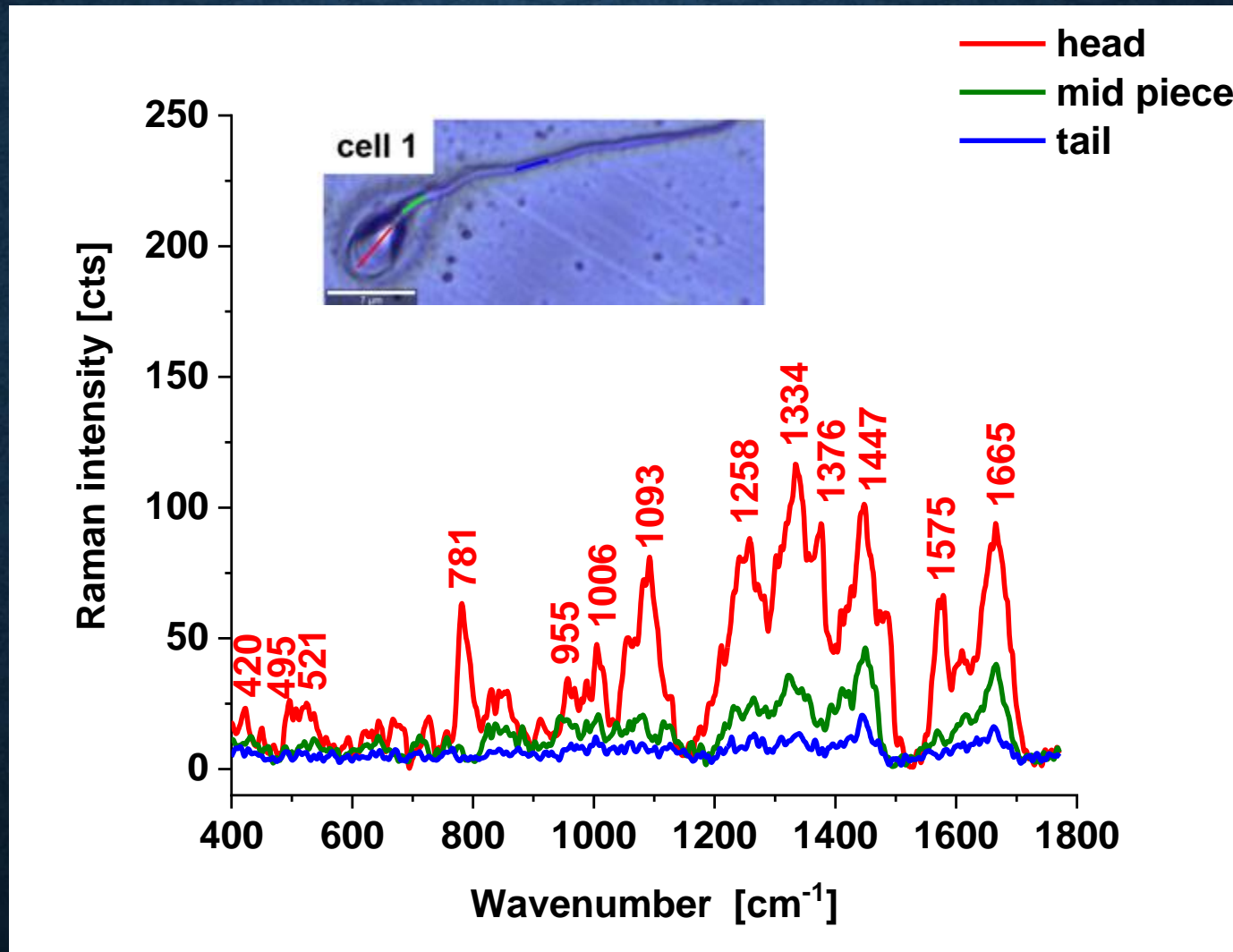


Our results show that cytochrome c is a key protein in sperm mitochondria that is needed to maintain life (respiration via oxidative phosphorylation) and cell death (apoptosis).



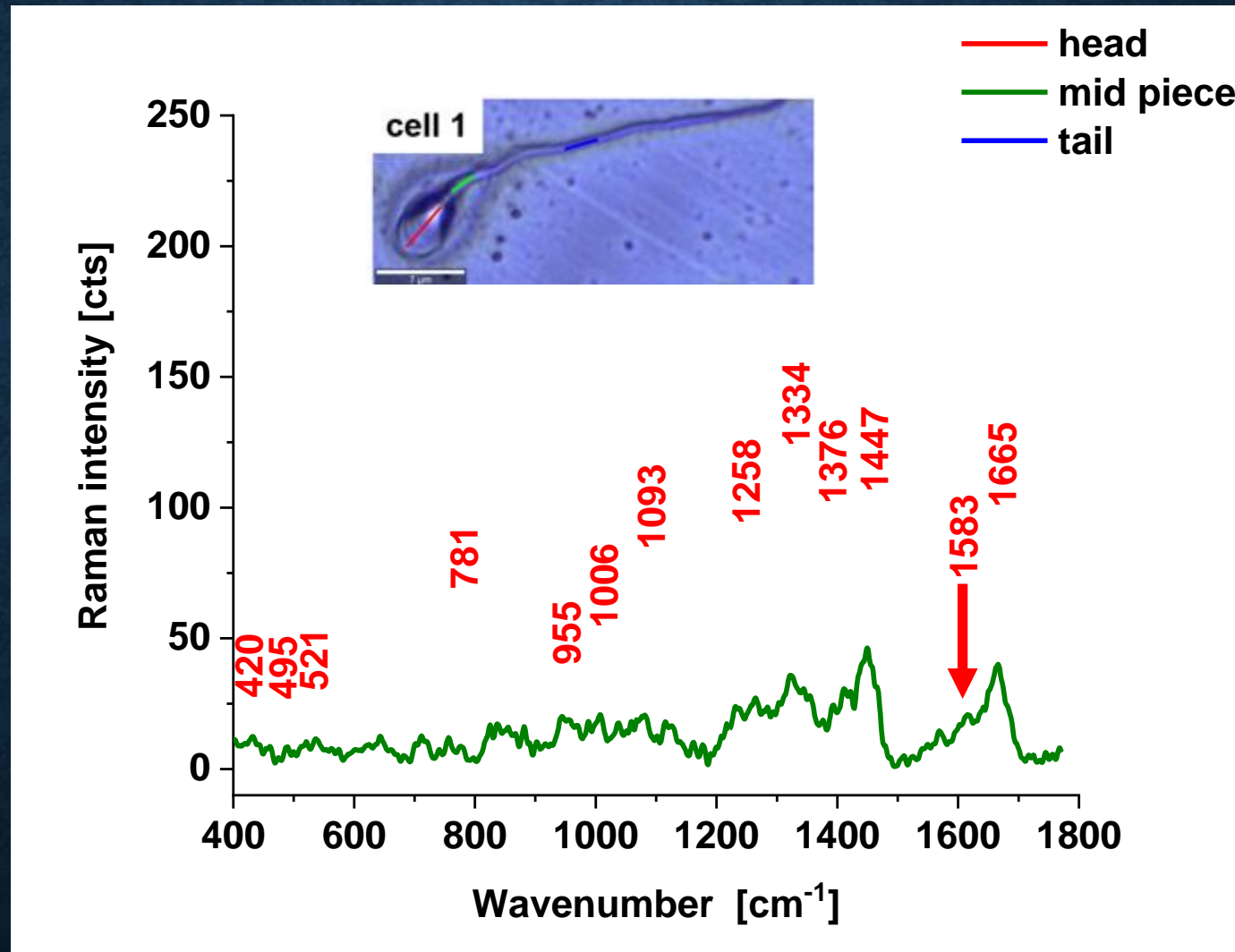
The normal functioning of sperm cells requires cytochrome *c* in the redox balanced forms: reduced and oxidized. The oxidized form of cytochrome *c* is localized in the mitochondrial intermembrane space and is a part of the electron transport chain. This ensures that electron shuttling between the complex III, cytochrome *c*, and complex IV can occur leading to controlled effective oxidative phosphorylation (respiration) and ATP production needed for most steps in spermatozoal maturation, motility, hyperactivation and fertilization.

spermatozoid



This ensures that electron shuttling between the complex III, cytochrome c, and complex IV can occur leading to controlled effective oxidative phosphorylation (respiration) and ATP production needed for most steps in spermatozoal maturation, motility, hyperactivation and fertilization.

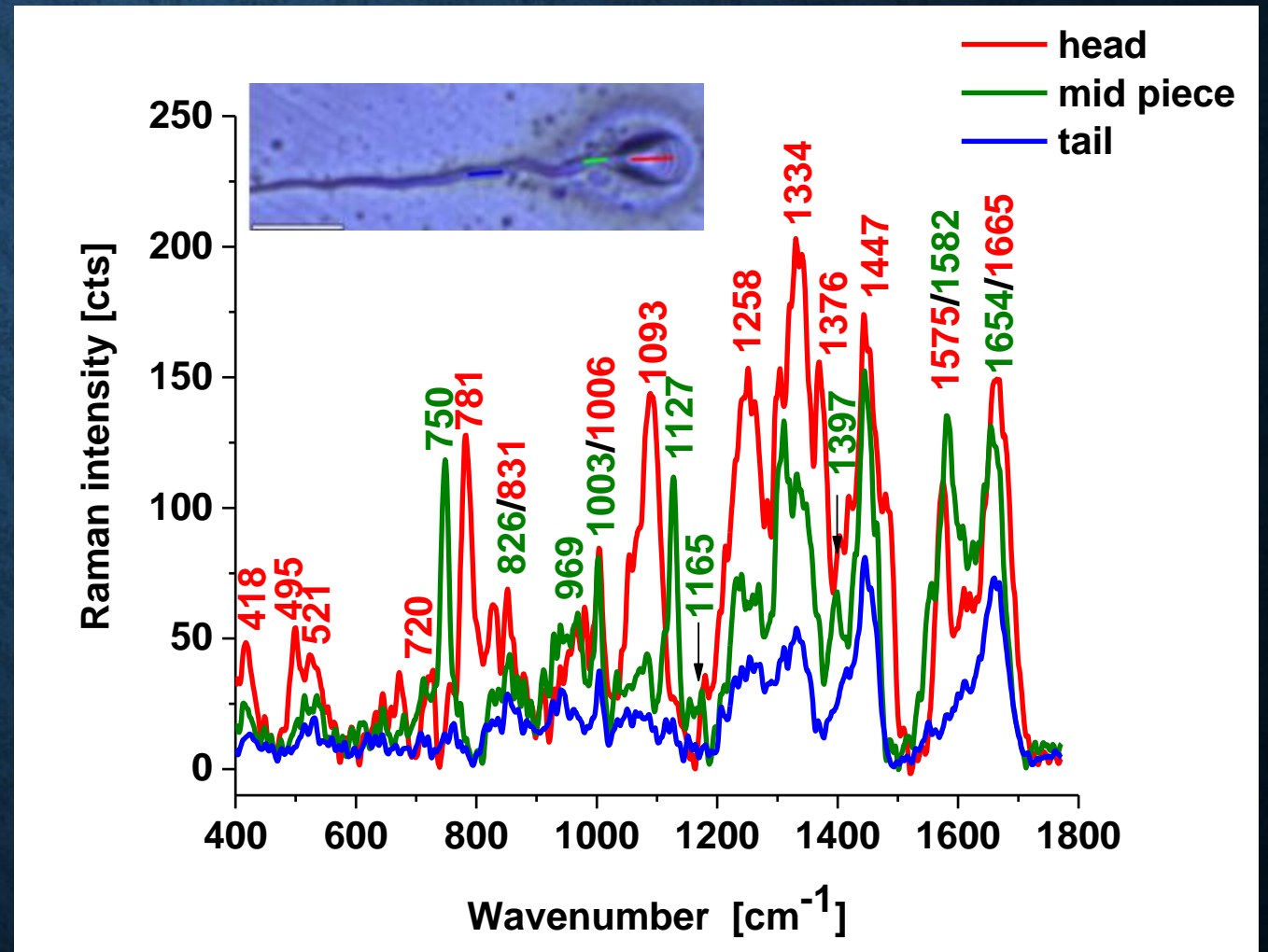
Spermatozoid cytochrome c in oxidized state



This ensures that electron shuttling between the complex III, cytochrome c, and complex IV can occur leading to controlled effective oxidative phosphorylation (respiration) and ATP production needed for most steps in spermatozoal maturation, motility, hyperactivation and fertilization.

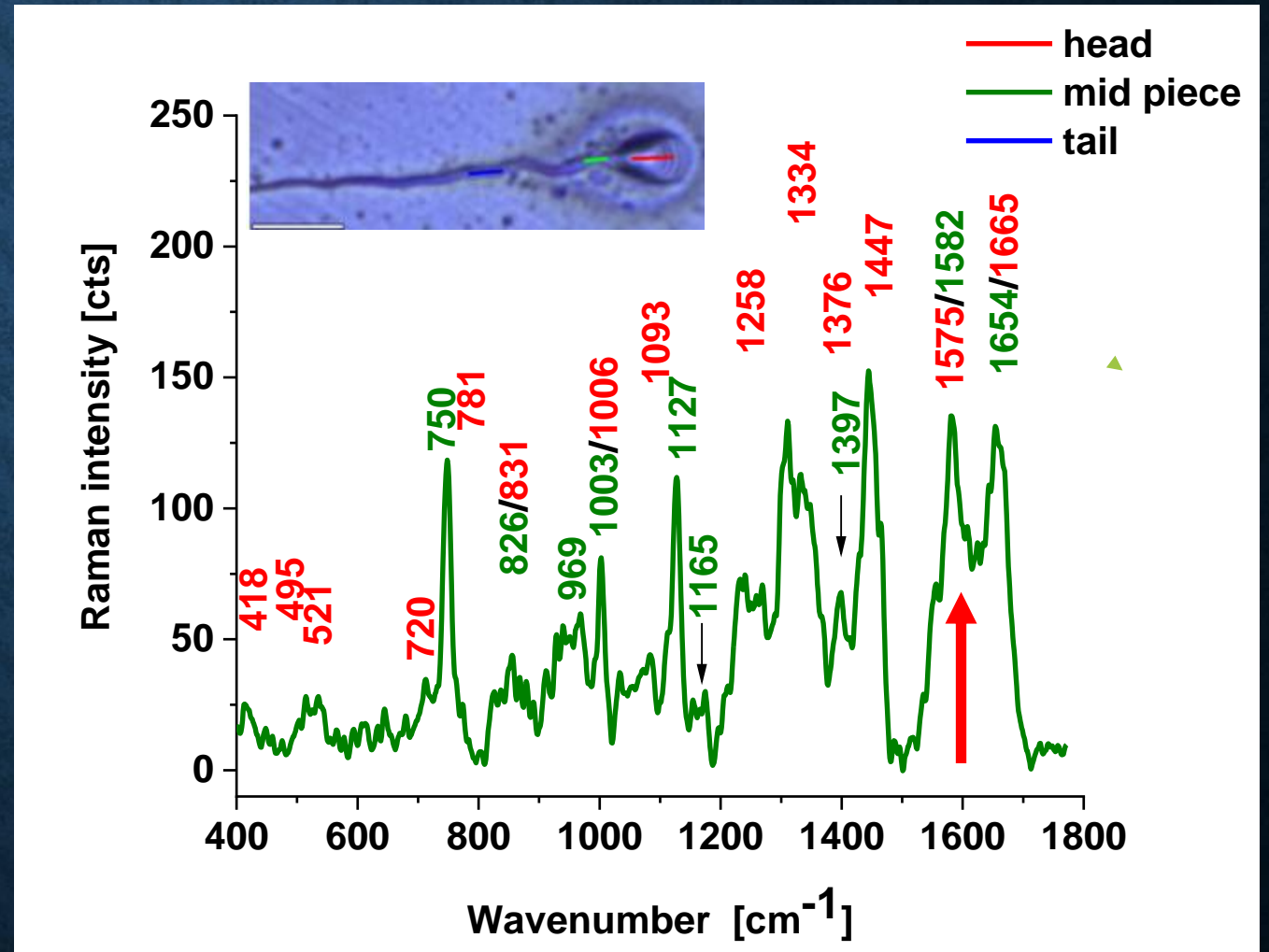
Spermatoid cytochrome c in reduced state state

This indicate that electron shuttling between the complex III, cytochrome c, and complex IV cannot occur leading to limited effectiveness of oxidative phosphorylation (respiration) and ATP production needed for most steps in spermatozoal maturation, motility, hyperactivation and fertilization.

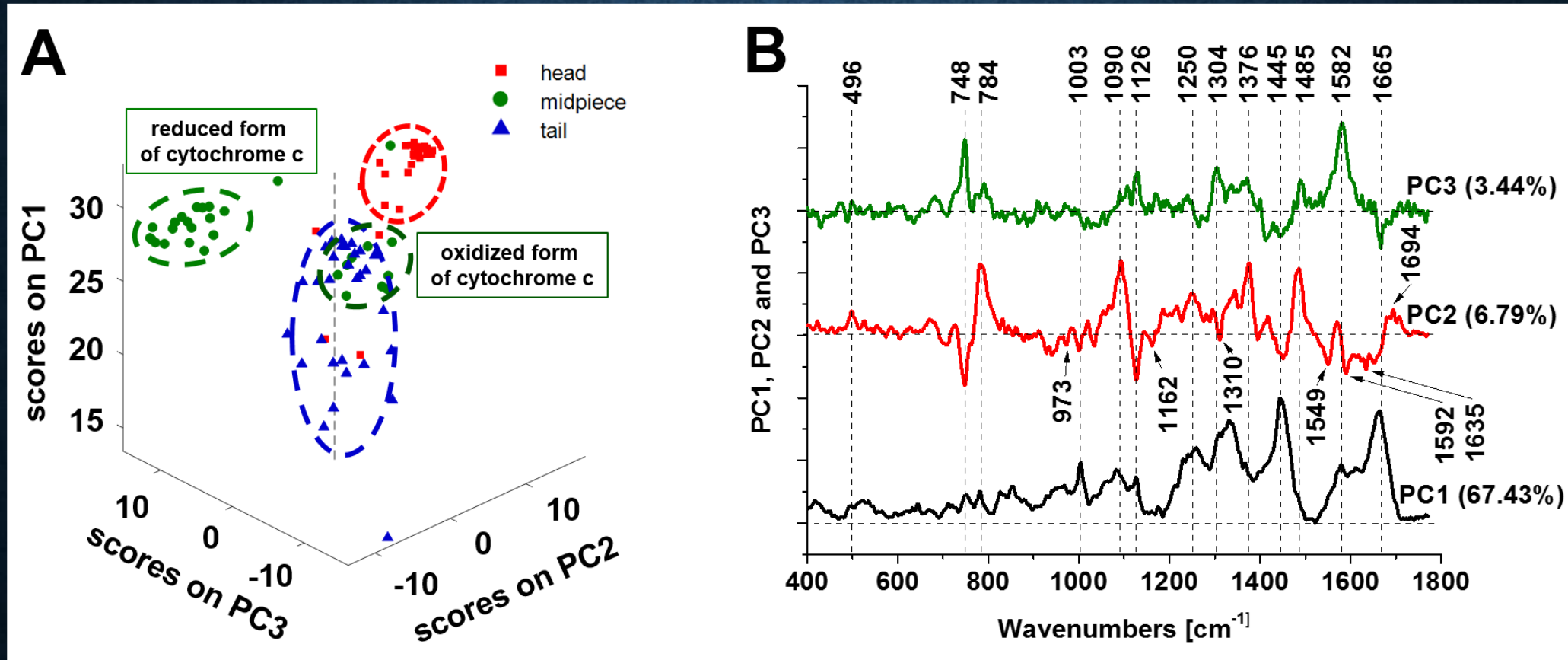


Spermatoid cytochrome c in reduced state state

This indicate that electron shuttling between the complex III, cytochrome c, and complex IV cannot occur leading to limited effectiveness of oxidative phosphorylation (respiration) and ATP production needed for most steps in spermatozoal maturation, motility, hyperactivation and fertilization.



Metabolic biochemical analysis of mitochondria, head and tail of sperm cells, and seminal plasma by using Raman imaging

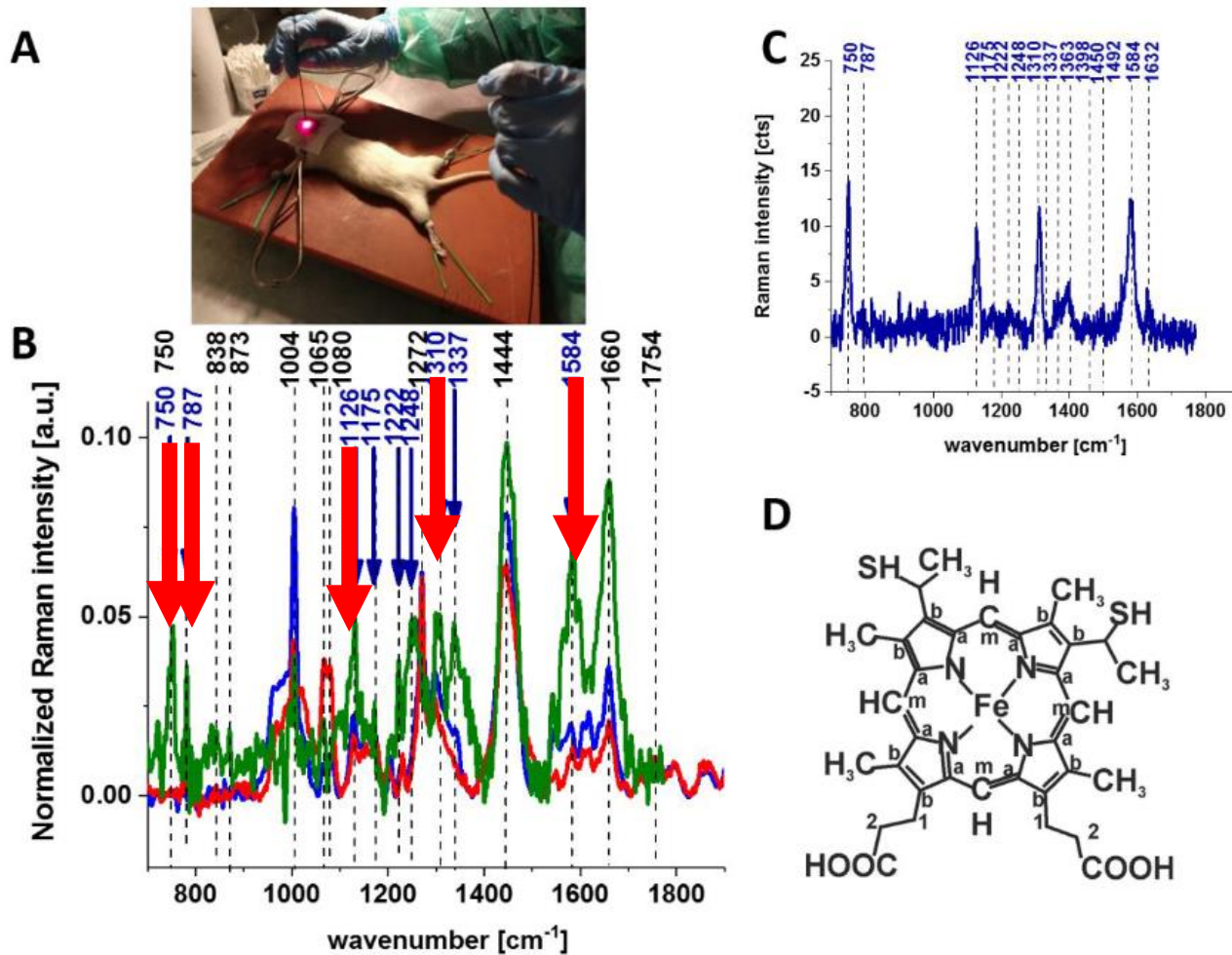


Metabolic biochemical analysis of mitochondria, head and tail of sperm cells, and seminal plasma by using Raman imaging combined with chemometric classification method of Cluster Analysis has been obtained

RAMAN SPECTROSCOPY GUIDES IN VIVO BRAIN OPTICAL BIOPSIES



Cytochrome activity in animal brain

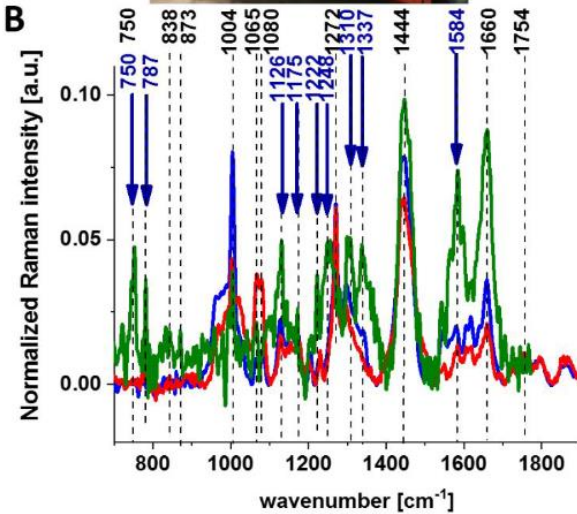


Raman- guided in vivo animal (rat) brain analysis (A), the average (n=6) Raman spectrum of the in vivo brain of animal model (rat) at the excitation 785 nm — and of the ex-vivo brain of animal model (rat) at the excitation 532 nm — and 785 nm — (B), Raman spectrum of cytochrome c — (dark blue) (C), structural formula of heme c in cytochrome c (D)

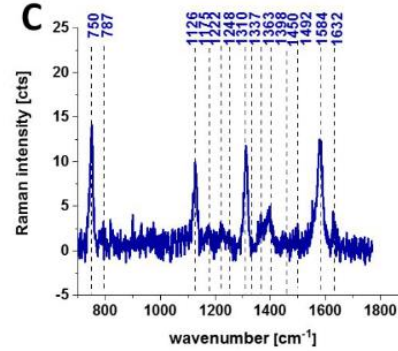
A



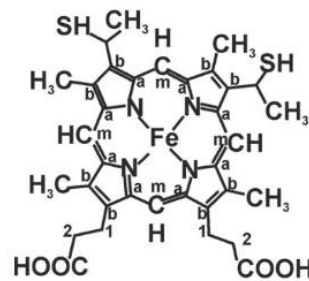
B



C



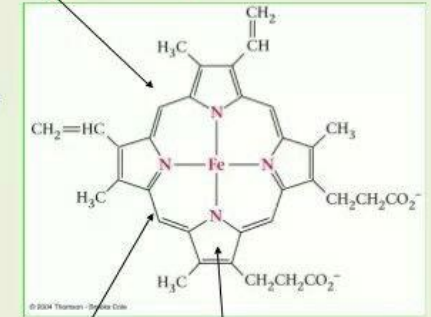
D



Heme structure Heme is a metaloporphyrine (cyclic tetrapyrrole)

•Heme contains:

- conjugated system of double bonds → **red colour**
- 4 nitrogen (N) atoms
- 1 iron cation (Fe^{2+})
→ bound in the middle of tetrapyrrole skelet by **coordination covalent bonds**



methine bridge ring

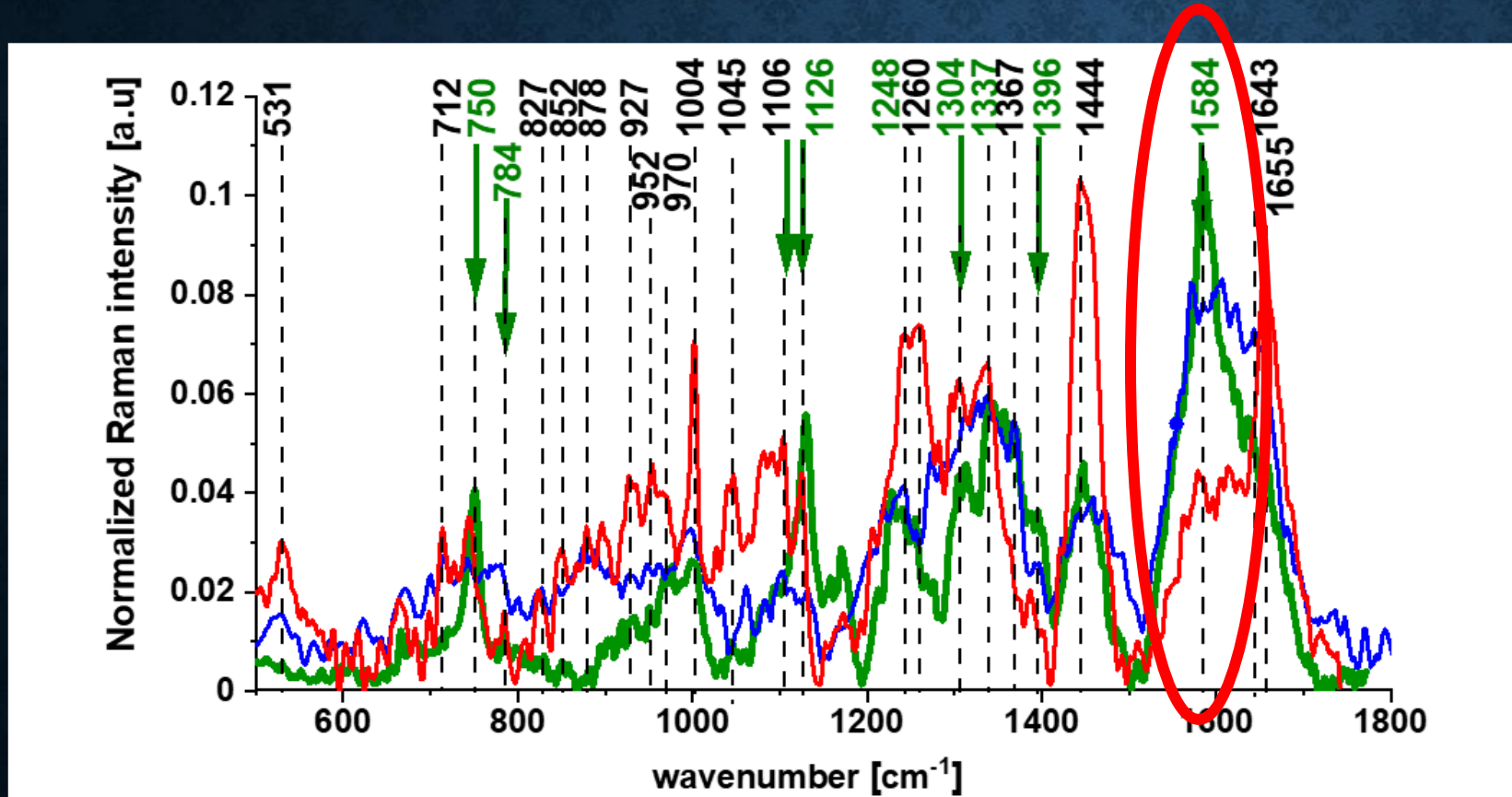
Marisa Costa, Hematologia

The vibrations of cytochrome c that are enhanced in the brain tissue are presented in Fig.1B (blue color arrows). We observe five intensive peaks: 750 (symmetric vibrations of pyrrole rings), 1126 (vibrations of C_b-CH_3 side radicals), 1310 (vibrations of all heme bonds), 1363 (mode (v_4)) and 1584 cm^{-1} (v_{19} mode, vibrations of methine bridges ($C_{\alpha}C_{\mu}$, $C_{\alpha}C_mH$ bonds) and the $C_{\alpha}C_{\beta}$ bond). There are also a number of other peaks with lower intensities 1248, 1352, 1632 cm^{-1} (methine bridges (bonds $C_{\alpha}C_m$, $C_{\alpha}C_mH$)). The Raman bands of the reduced form have

Cytochrome activity in human brain

In the view of the results for animal brain it would be extremely valuable to control cytochrome activity in humans. To help address these challenges we studied Raman enhancement of cytochromes for ex vivo human brain tissue of highly aggressive medulloblastoma

EXCITATION-WAVELENGTH RAMAN SPECTRA FOR HUMAN BRAIN CANCER TISSUE



Especially striking is the v19 mode (1584cm⁻¹), which produces one of the most prominent bands in the Raman spectrum. The band at 1584 cm⁻¹ represents the reduced form of cytochrome c which is much weaker in the oxidized form. Some of the peaks of the oxidized form of Cyt c (around 750, 1130, 1172, 1314, 1374, 1570-1573 and 1639 cm⁻¹) have the same positions as the reduced form, but their intensities are significantly lower.

Figure 1. The average Raman spectra for the human brain tissue of medulloblastoma (grade of malignancy WHO G4) at different excitations (number of patients n = 6, for each patient thousands of Raman spectra obtained from cluster analysis) of the ex vivo tumor human brain tissue of medulloblastoma at the excitations 355 nm — (blue), 532 nm — (green) and 785 nm — (red) for the same area of the samples.

Note that exactly the same as for animal brain Raman enhancement is observed for the human brain at 532 nm. The most significant resonance Raman enhancement at 532 nm is observed for the reduced forms of Cyt c at 1584 cm⁻¹.

**REDOX IMBALANCE AND BIOCHEMICAL CHANGES IN CANCER
BY
PROBING REDOX-SENSITIVE MITOCHONDRIAL CYTOCHROMES
IN
LABEL-FREE VISIBLE RESONANCE RAMAN IMAGING**



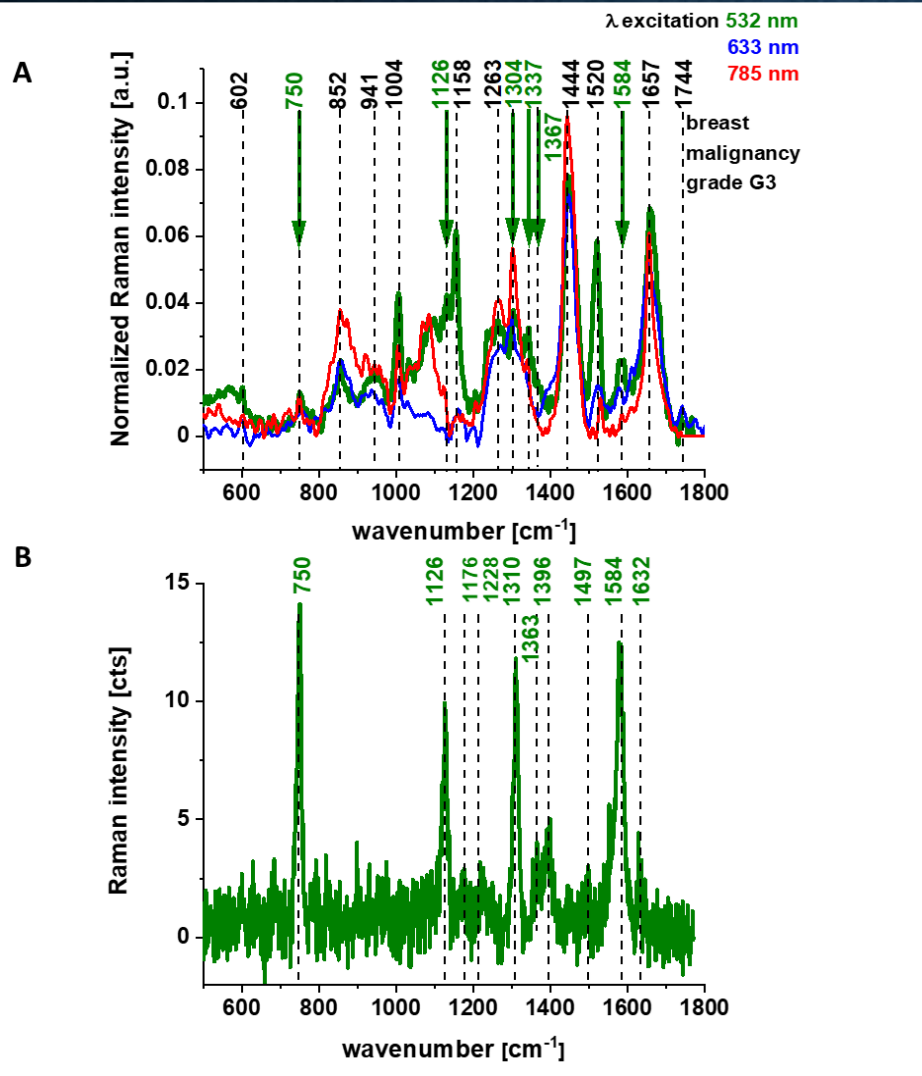
Article

**Redox Imbalance and Biochemical Changes in Cancer by
Probing Redox-Sensitive Mitochondrial Cytochromes in
Label-Free Visible Resonance Raman Imaging**

Halina Abramczyk ^{1,*}, Beata Brozek-Pluska ¹, Monika Kopec ¹, Jakub Surmacki ¹, Maciej Błaszczak ² and
Maciej Radek ²

Cancers **2021**, *13*, 960.
<https://doi.org/10.3390/cancers13050960>

EXCITATION-WAVELENGTH RAMAN SPECTRA FOR HUMAN BREAST TISSUE



The average Raman spectra of the ex vivo human breast cancer tissue surgically resected specimens, ductal cancer, grade of malignancy WHO G3 at the excitations 633 nm — (blue), 532 nm — (green) and 785 nm — (red) (number of patients $n = 5$, for each patient thousands of Raman spectra obtained from cluster analysis) (A), Raman spectrum of the pure cytochrome *c* at 532 nm excitation (B).

THE SORET AND Q-RESONANT RAMAN SPECTRA OF CYTOCHROME C

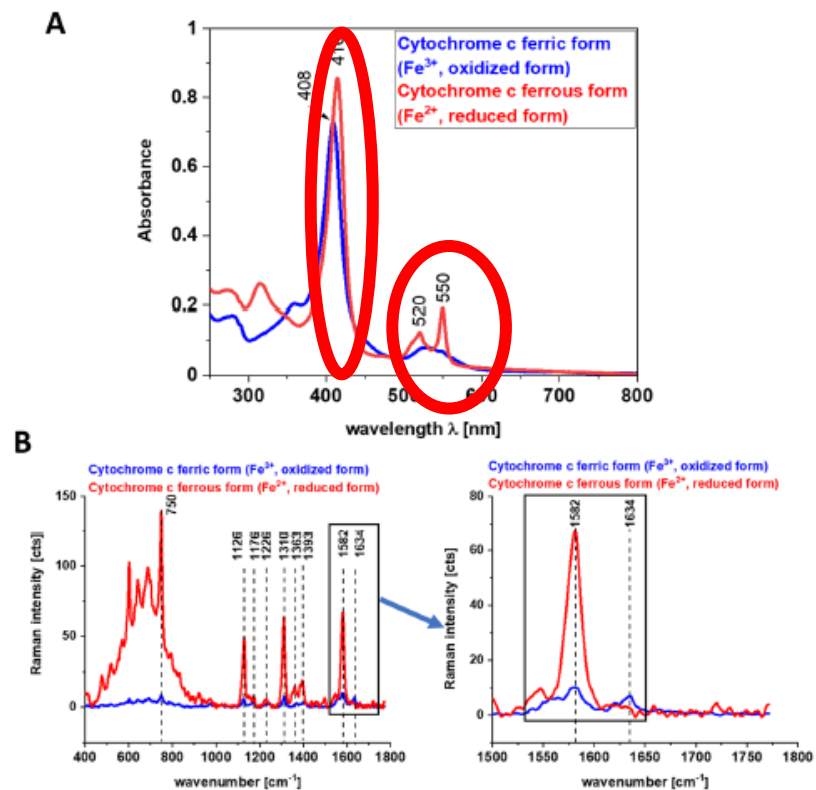
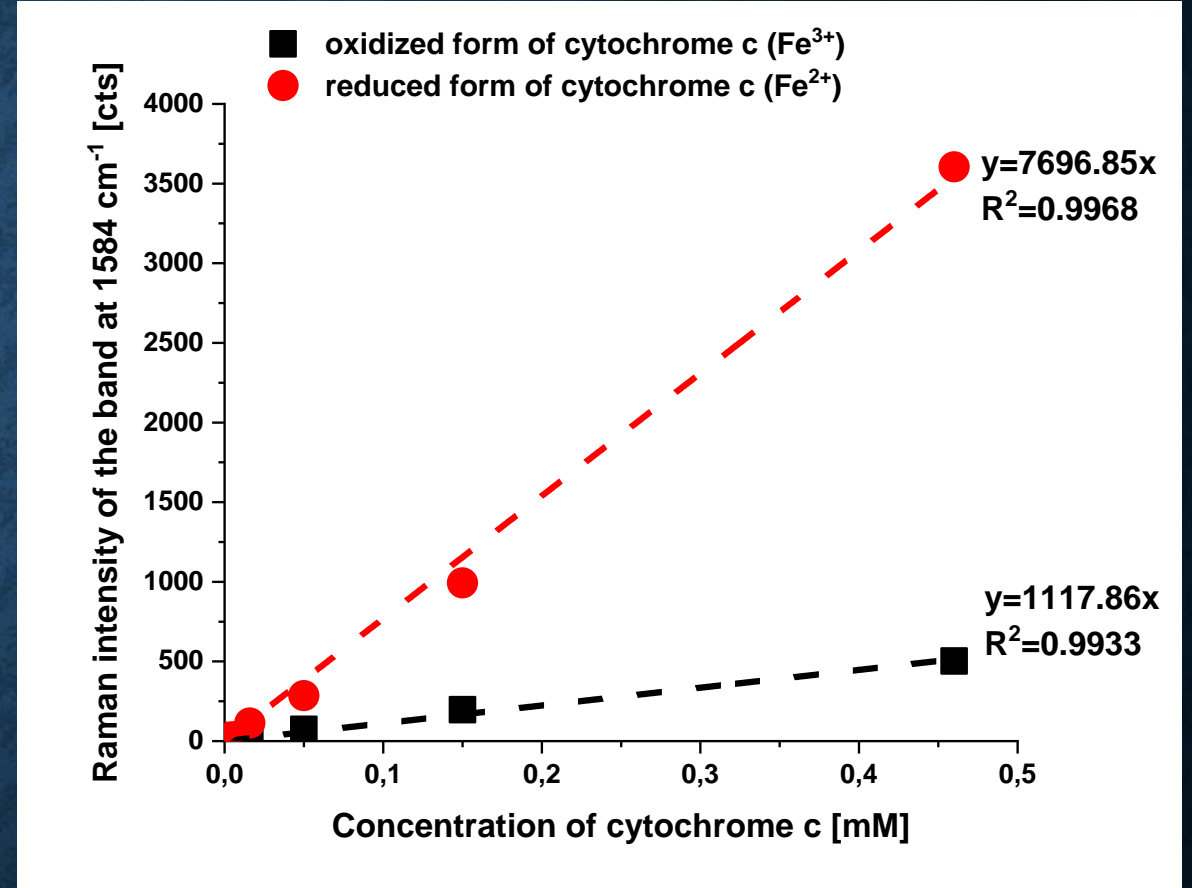
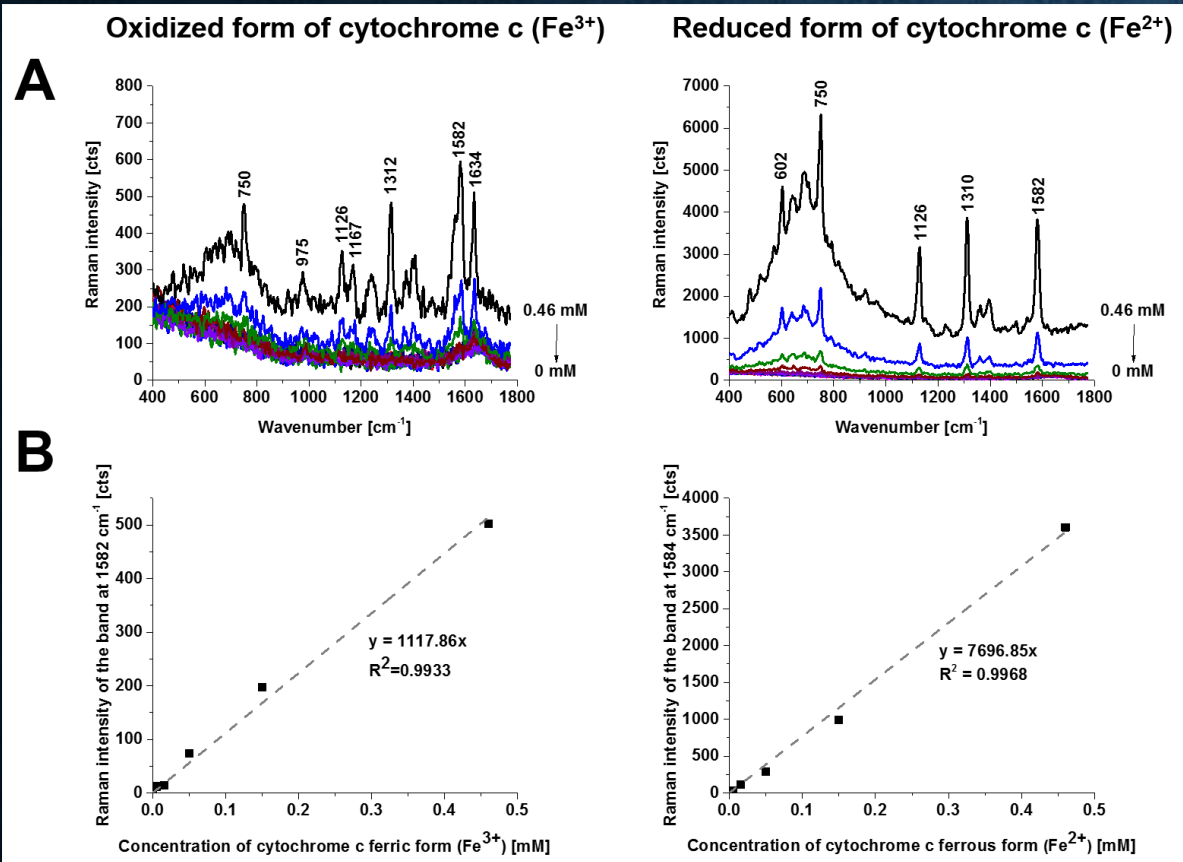


Figure 5. Electronic absorption spectra (A) and Raman spectra (B) of cytochrome *c* in ferric (oxidized, Fe³⁺) and ferrous (reduced, Fe²⁺) states in phosphate buffer pH = 7.3, cuvette optical path 1 cm. Ferric cytochrome *c* was prepared by adding 10-fold excess NaBH₄ (as a reductor).

Symmetric vibrational modes of the porphyrin ligand in Cyt *c* are enhanced to a greater degree using excitation wavelengths within the Soret absorption peaks at 408nm (ferric Fe³⁺), 416nm (ferrous Fe²⁺) states, whereas asymmetric modes are enhanced to a greater degree using excitation wavelengths within the Q absorption peak at 500-550 nm.

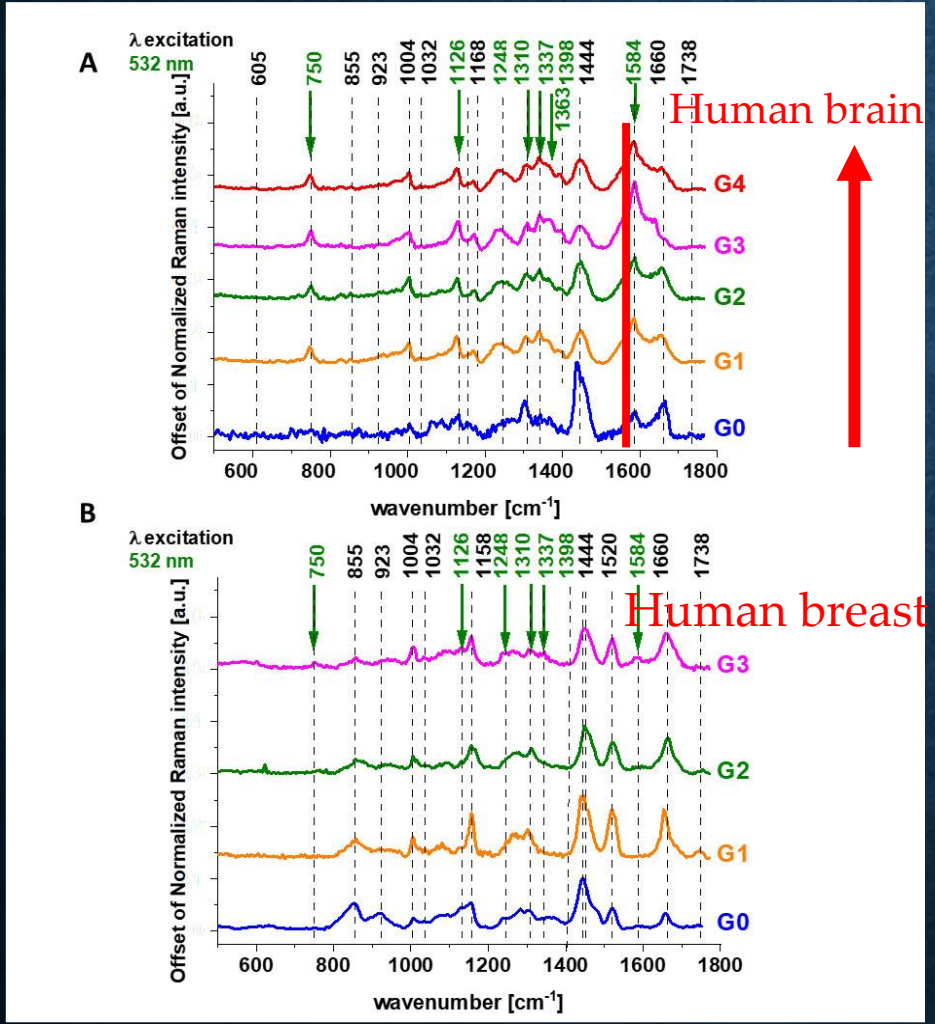
The Raman bands of the reduced form have higher intensities.

The Raman bands of the reduced form have higher intensities



• Raman spectra of oxidized (ferric form, Fe^{3+}) and reduced (ferrous form, Fe^{2+}) forms of cytochrome c as a function of concentration (PBS solutions (0-0.46 mM) (A), Raman band intensity at 1582 cm^{-1} as a function of cytochrome c concentration (B). Experimental conditions: excitation 532 nm, laser power 10 mW, integration time 0.5 s, 10 accumulations. Reduction agent NaBH_4 in tenfold excess.

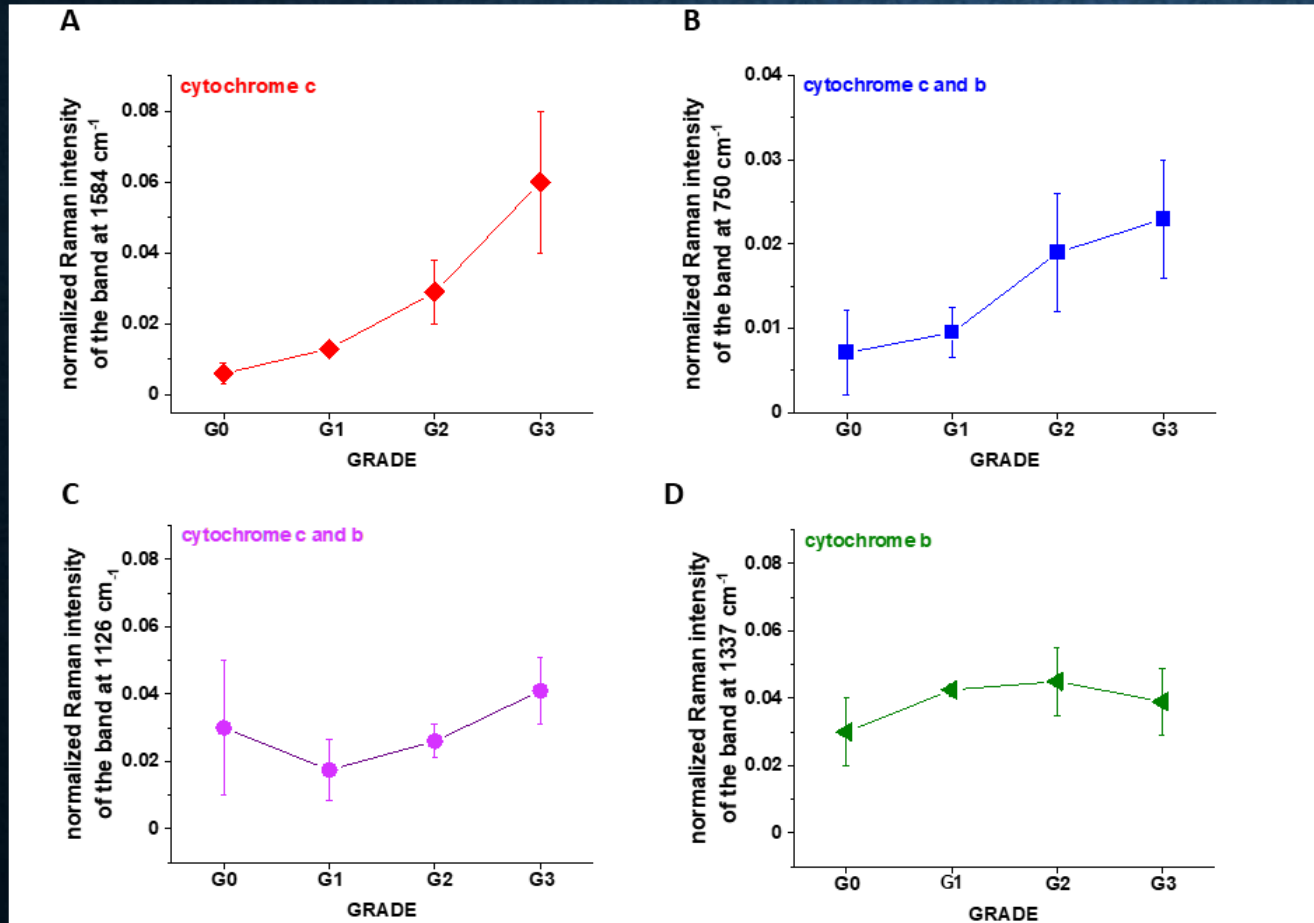
TO CHECK WHETHER THE REDOX STATE OF CYT C IS RELATED TO THE CANCER AGGRESSIVENESS WE USED THE RAMAN REDOX STATE BIOMARKER REPRESENTED BY THE RAMAN INTENSITY OF 1584 CM-1 AND OTHER CYTOCHROME RAMAN BANDS



The average Raman spectra of ex vivo human normal (grade of malignancy G0) and tumor G1, G2, G3, G4 brain tissue (n = 44) (A) and ex vivo human normal (grade of malignancy G0) and G1, G2, G3 breast tissue (n = 39) (B), surgically resected specimens at 532 nm.

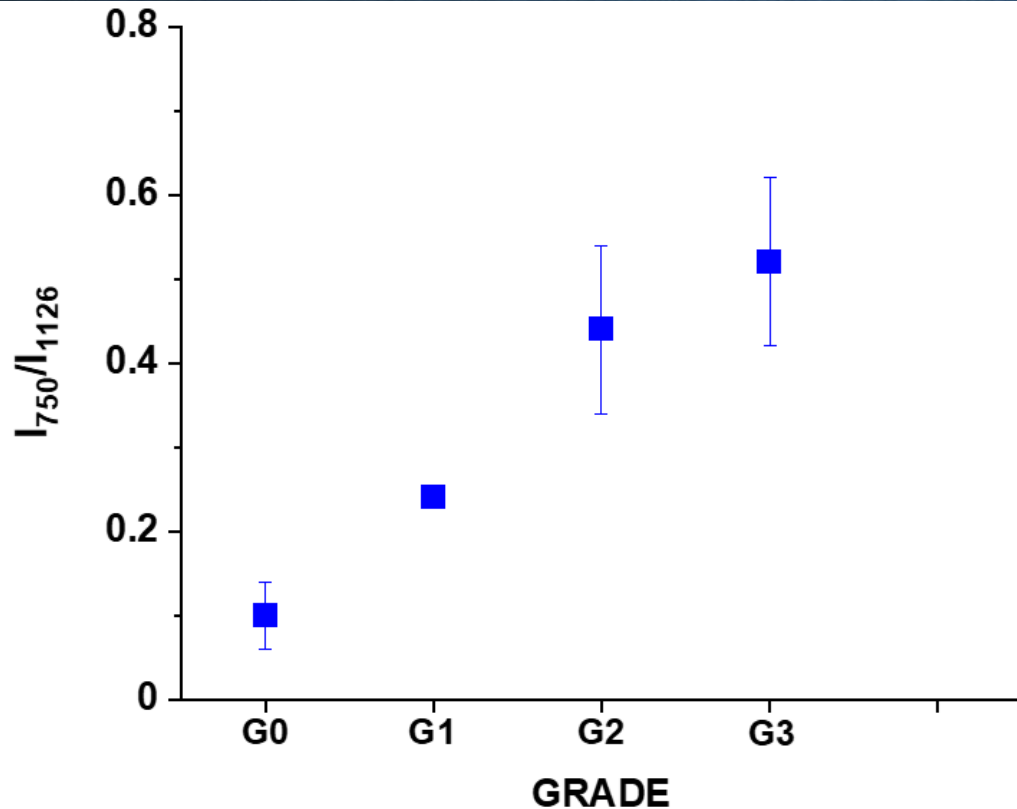
TO CHECK WHETHER THE REDOX STATE OF CYT C IS RELATED TO THE CANCER AGGRESSIVENESS WE USED THE RAMAN REDOX STATE BIOMARKER REPRESENTED BY THE RAMAN INTENSITY OF 1584 CM-1 AND OTHER CYTOCHROME RAMAN BANDS

human breast tissue for $n = 39$



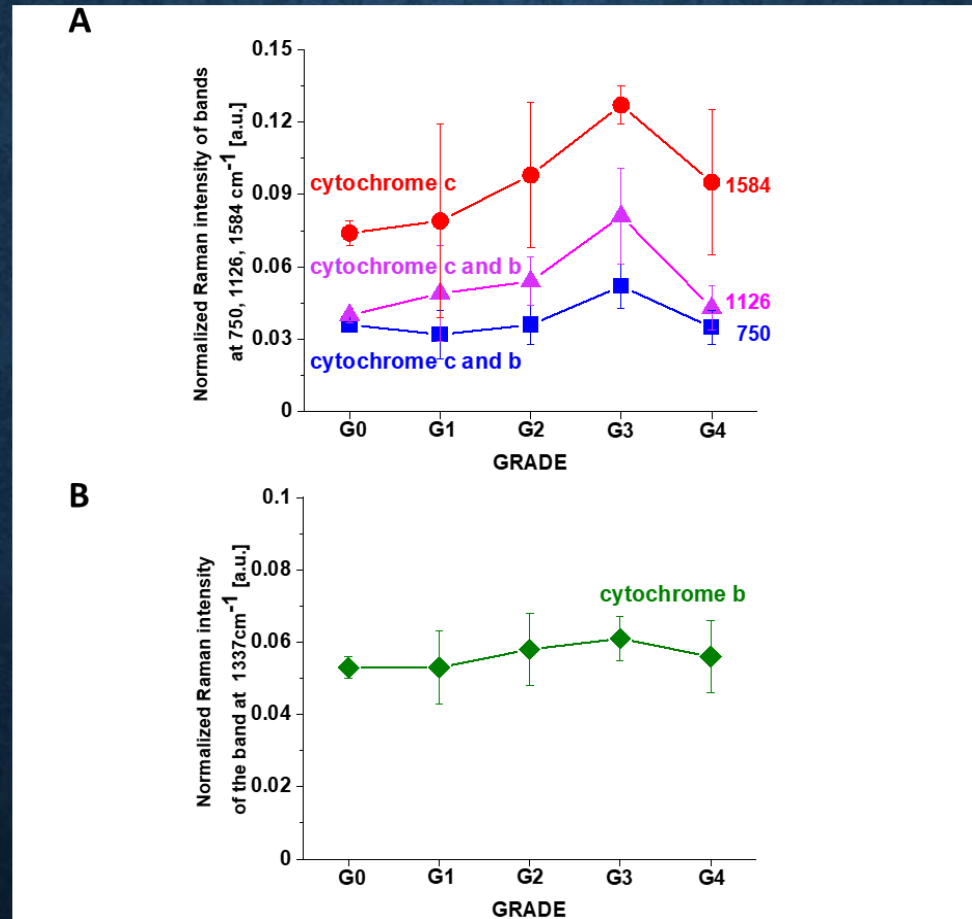
The Raman intensities of cytochrome *c* and cytochrome *b* in human breast tissue for $n = 39$: I1584 (A), I750 (B), I1126 (C), I1337 (D) as a function of breast cancer grade malignancy G0-G3 at excitation 532 nm (A). The results are presented as the mean \pm SD. Raman bands intensity were taken from normalized by vector norm spectra.

CONCENTRATION OF CYTOCHROME C IS RELATED TO THE CANCER AGGRESSIVENESS IN BREAST (G0-G3)



The Raman intensity ratio of the peaks at 750 cm^{-1} and 1126 cm^{-1} I_{750}/I_{1126} in human breast tissue as a function of breast cancer grade malignancy G0-G3 at excitation 532 nm. The results are presented as the mean \pm SD. Raman bands intensity were taken from normalized by vector norm spectra.

CONCENTRATION OF CYTOCHROME C IS RELATED TO THE CANCER AGGRESSIVENESS IN BRAIN (G0-G4)



human brain tissue for n = 42

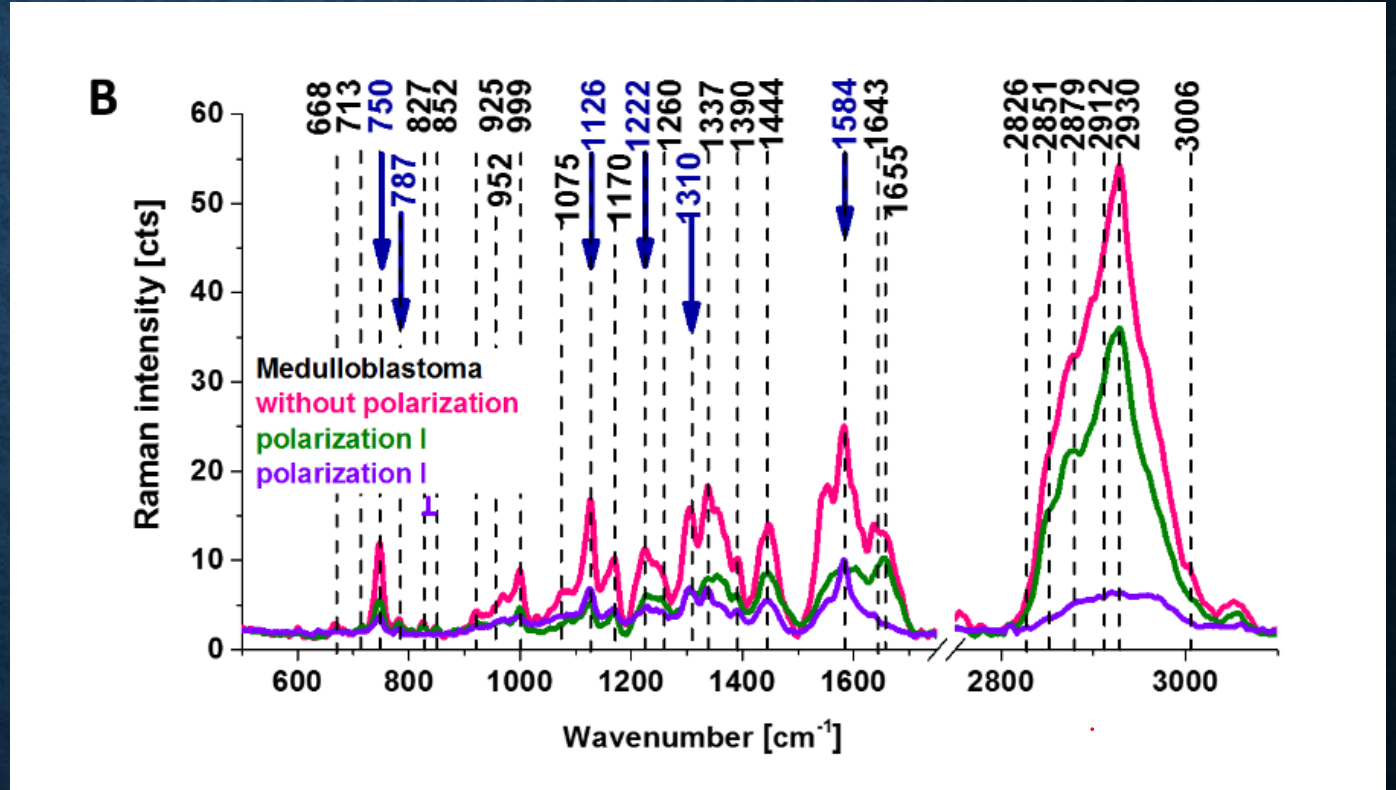
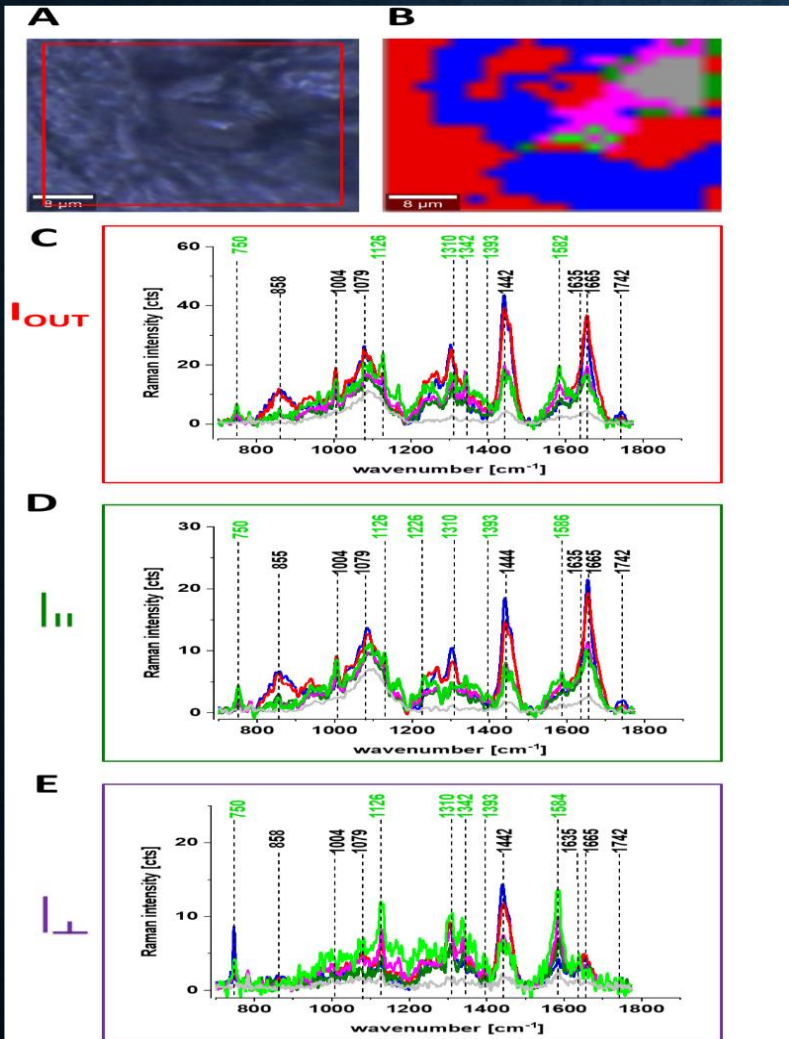
One can see that that for human brain tissue the Raman intensity of cytochrome c first increases with cancer aggressiveness while for the most aggressive grade IV decreases again. The level of cytochrome b does not change

Figure 10. The Raman intensities of cytochrome c and cytochrome b in human brain tissue: 1750, 1126, 1584 (A) and 1337 (B) as a function of brain tumor grade malignancy G0-G4 at excitation 532 nm. The results are presented as the mean \pm SD. Raman bands intensity were taken from normalized by vector norm spectra.

ANOMALOUSLY POLARIZED BANDS APPEAR IN THE Q-RESONANT RAMAN SPECTRA

human BREAST tissue

human BRAIN tissue



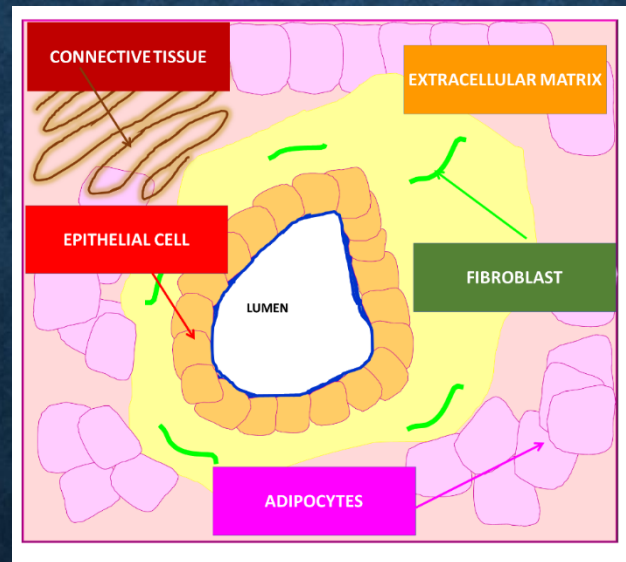
the Raman spectra for the human brain tissue of medulloblastoma at 532 nm at different experimental geometries for Raman scattering: without polarization analyzer — (magenta), at parallel — (green) and perpendicular— (violet) polarizations of the incident and Raman scattered beams.

RAMAN IMAGING CAN MONITOR THE AMOUNT OF CYTOCHROME IN SPECIFIC ORGANELLES SUCH AS MITOCHONDRIA, CYTOPLASM, OR EXTRACELLULAR MATRIX.

Circulating in blood Cyt c level is suggested to be a novel *in vivo* marker of mitochondrial injury after resuscitation from heart failure and chemotherapy.¹⁸ Various existing techniques such as enzyme-linked immunosorbent assays (ELISA), Western blot, high performance liquid chromatography (HPLC), spectrophotometry and flow cytometry have been used to estimate Cyt c concentration. However, the implementation of these techniques at POC (point of care) application is limited due to longer analysis time, expensive instruments and expertise needed for operation.¹⁸ Moreover, none of the methods used to control Cyt c concentration can provide direct evidence about the role of cytochrome c in apoptosis and oxidative phosphorylation, because they are not able to monitor the amount of cytochrome in specific organelles such as mitochondria, cytoplasm, or extracellular matrix.

Until now, no technology has proven effective for detecting Cyt c concentration in specific cell organelles. Therefore, existing analytical technologies cannot detect the full extent of Cyt c localization inside and outside specific organelles. **In Raman imaging we do not need to disrupt cells to break open the cells and release the cellular structures to learn about their biochemical composition.**

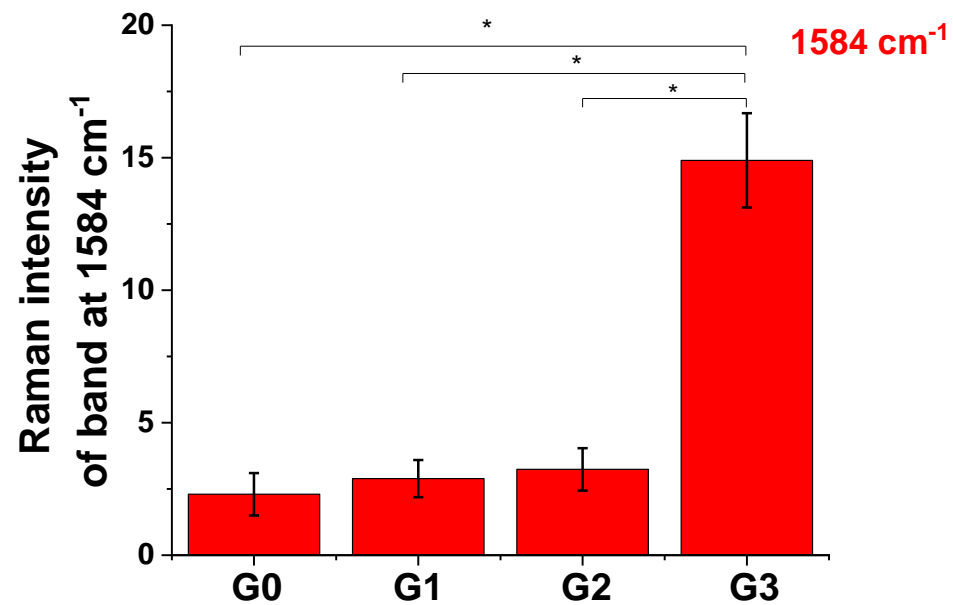
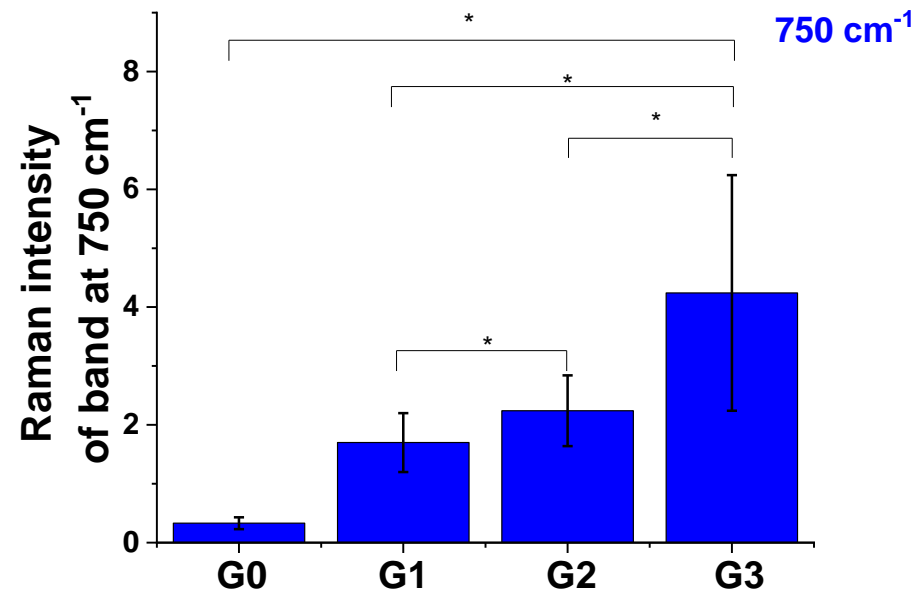
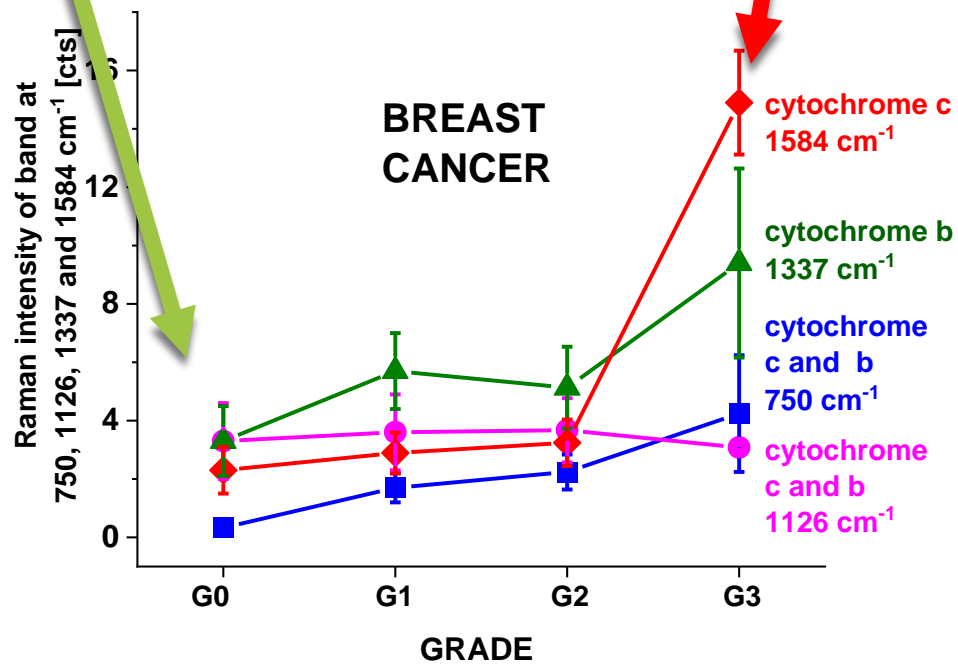
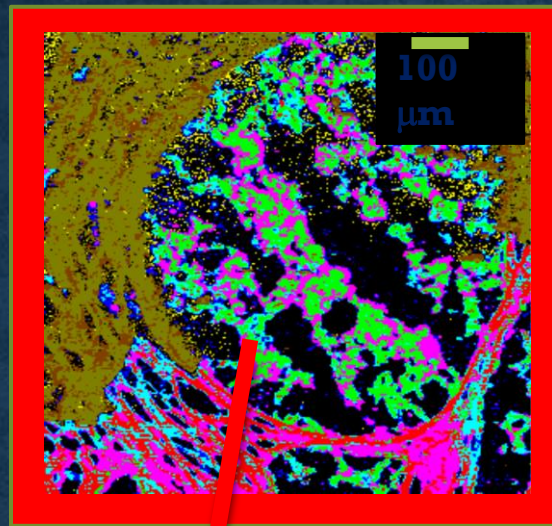
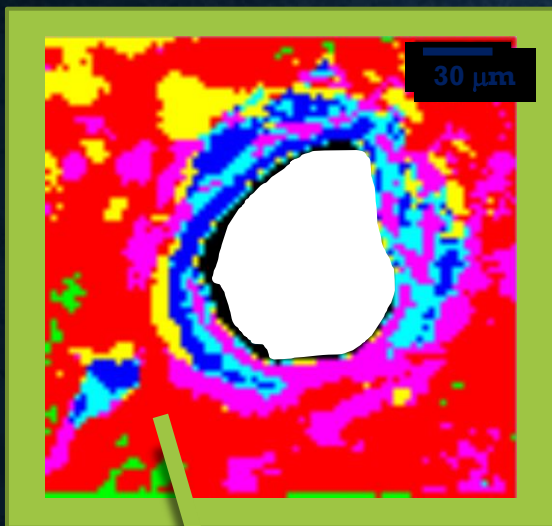
NEW LOOK INTO THE ROLE OF CYTOCHROME C IN HUMAN BREAST DUCTS WITH RAMAN IMAGING



Schematic representation of the structure of human normal duct.

Our results demonstrate how Cyt c is likely to function in cancer development.

NORMAL HUMAN DUCT **CANCEROUS HUMAN DUCT**



human normal breast duct

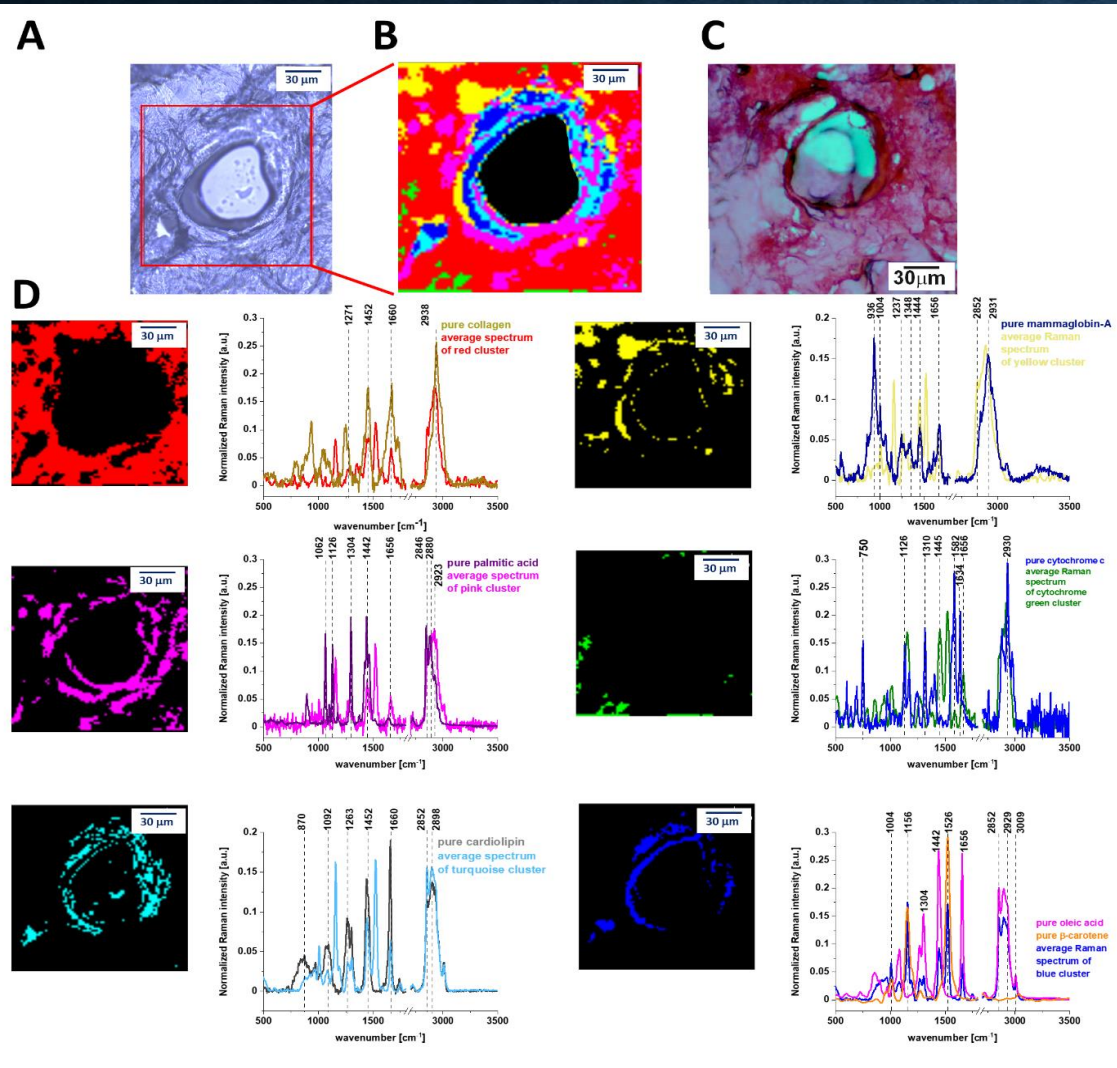


Figure S1. (A) Microscopy image of human normal breast duct, (B) the Raman image of human normal breast duct obtained by Cluster Analysis, (C) the histopathological image of human normal breast duct and (D) the comparison of average Raman spectra obtained by Cluster Analysis Method and the Raman spectra characteristic for pure chemical components: oleic acid, β -carotene, palmitic acid, mammaglobin-A, collagen, cytochrome c, cardiolipin.

human cancerous breast duct

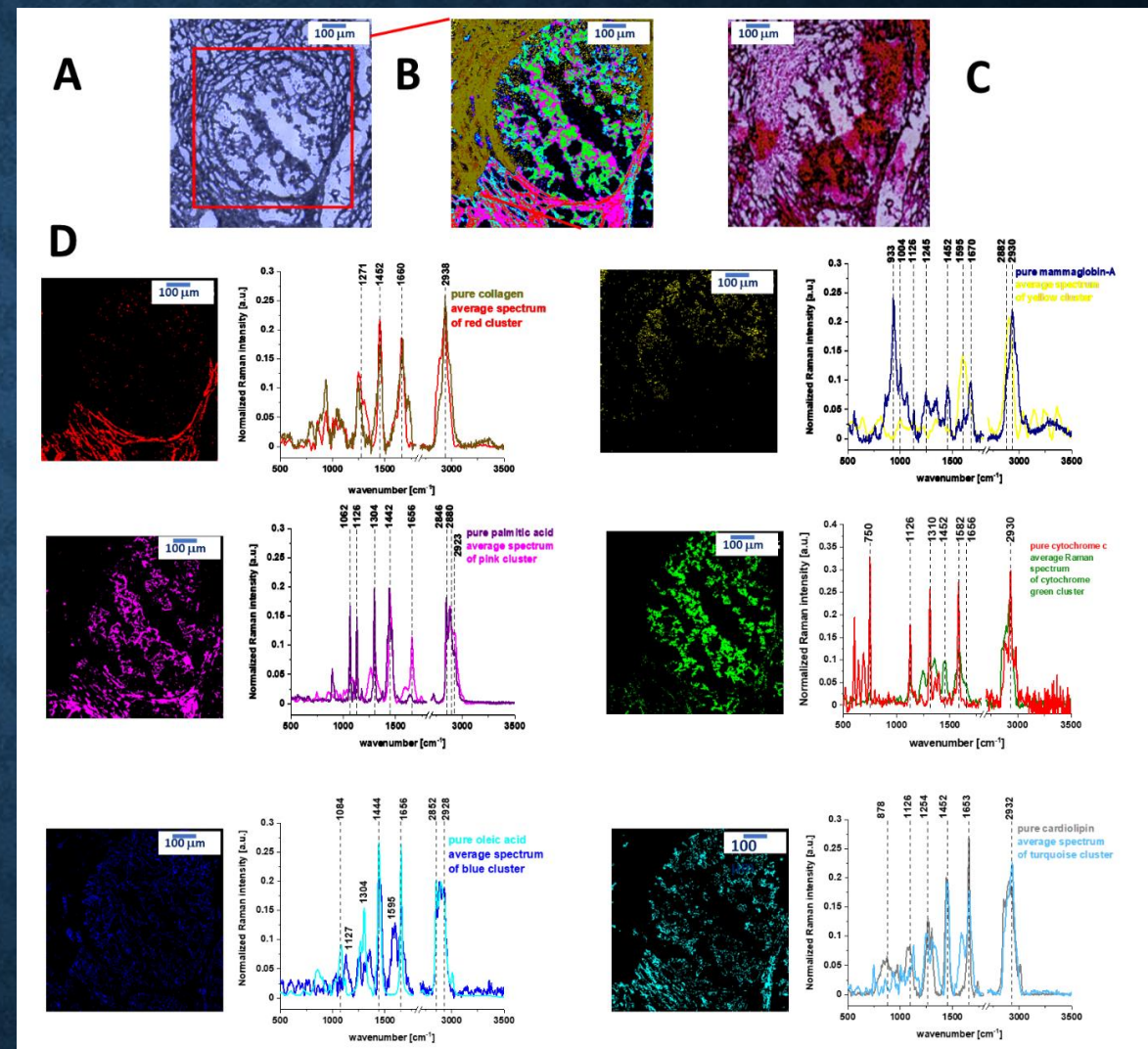


Figure S2. (A) Microscopy image of human cancerous breast duct, (B) the Raman image of human cancerous breast duct obtained by Cluster Analysis, (C) the histopathological image of human cancerous breast duct and (D) the comparison of average Raman spectra obtained by Cluster Analysis Method and the Raman spectra characteristic for pure chemical components: oleic acid, β -carotene, palmitic acid, mammaglobin-A, collagen, cytochrome c, cardiolipin.

human normal breast duct

human cancerous breast duct

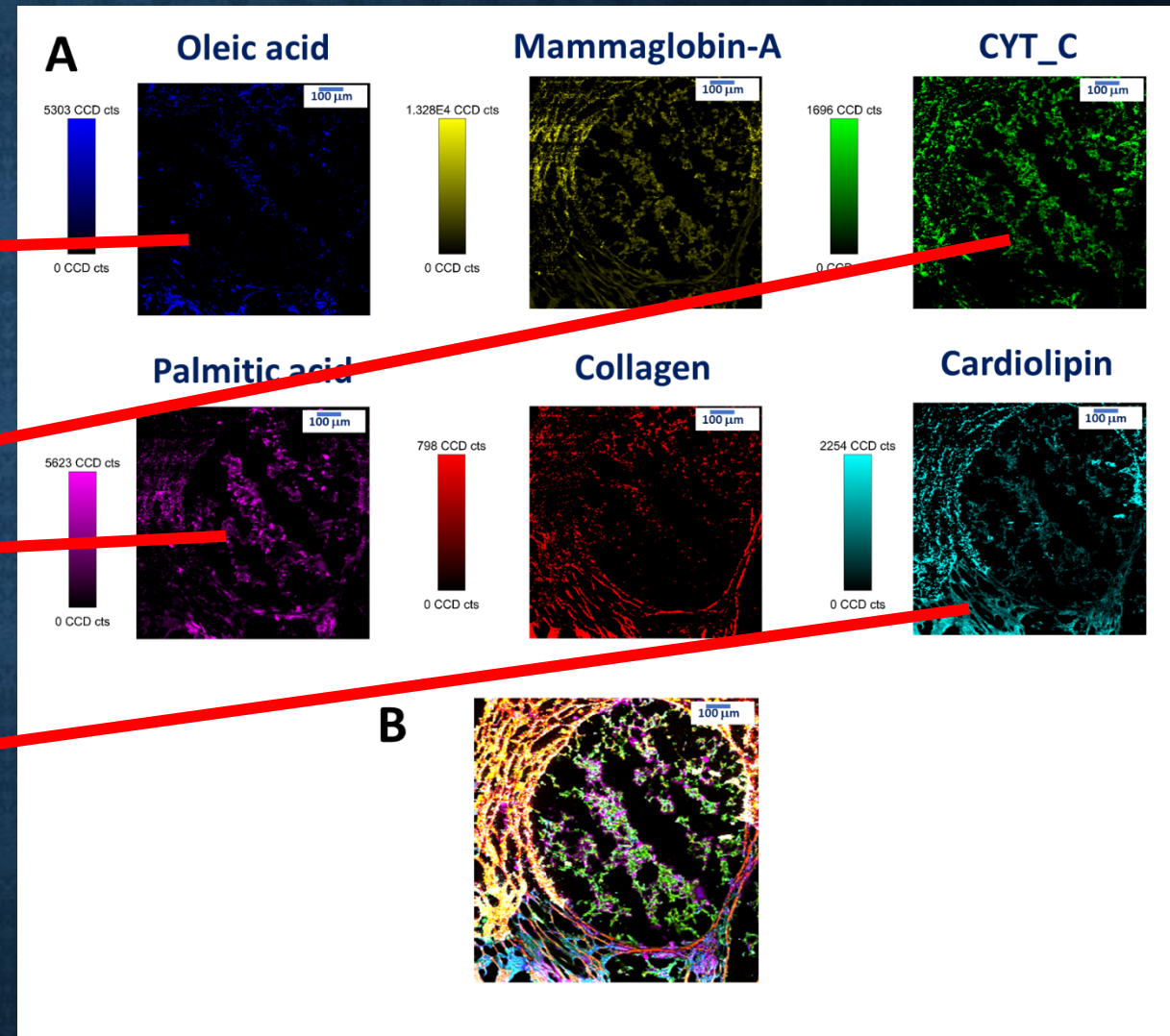
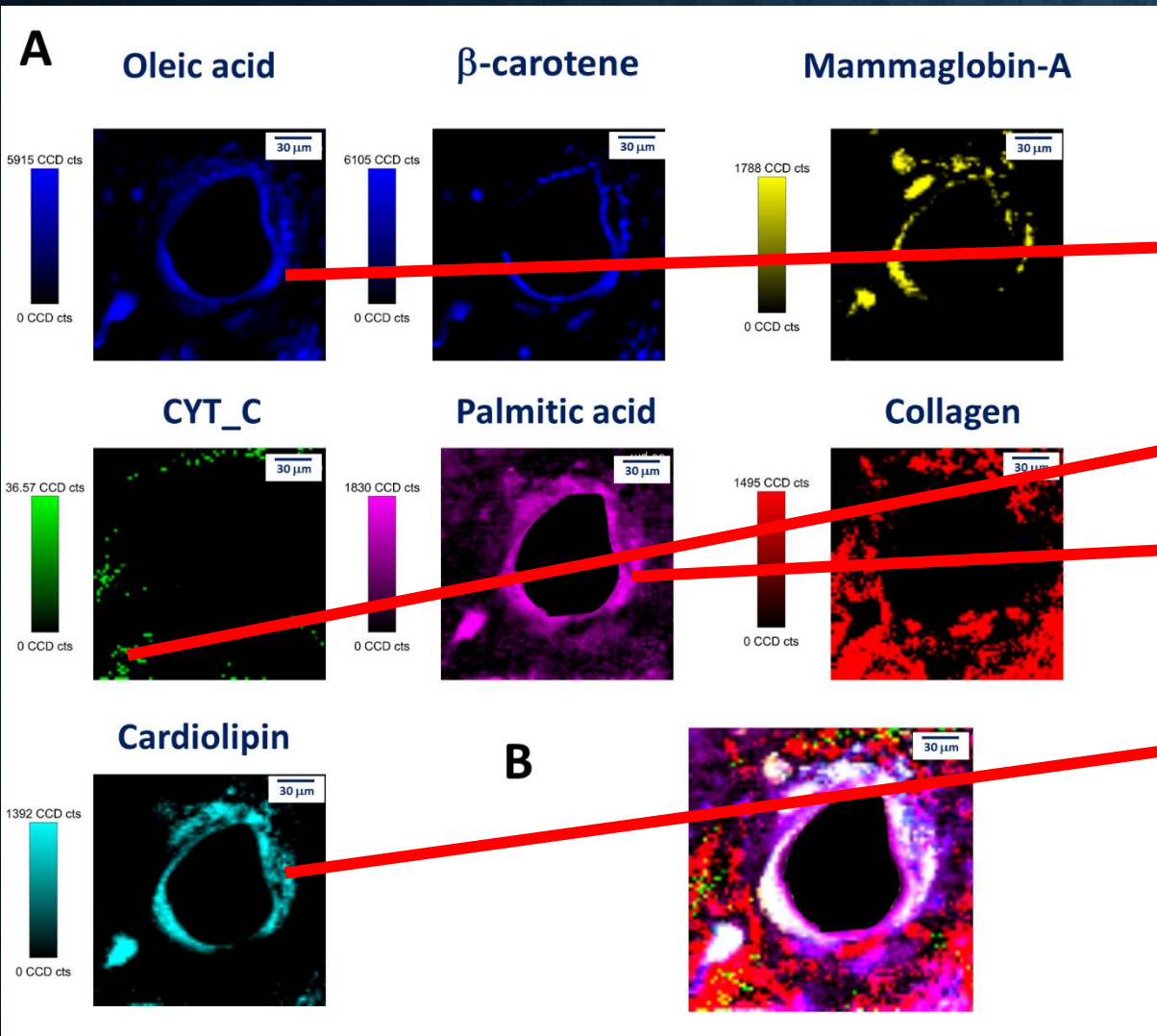
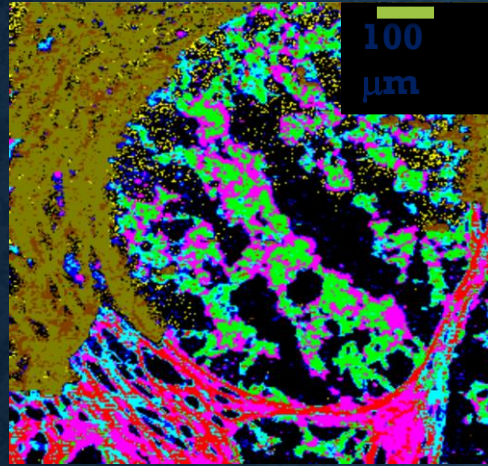


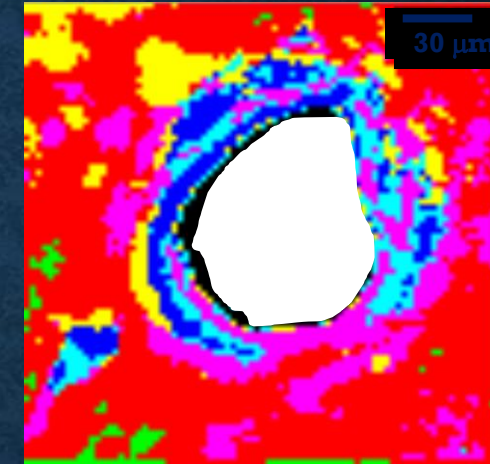
Figure S3. (A) Basis analysis performed for normal human breast duct based on the Raman spectra of pure: oleic acid, β -carotene, palmitic acid, mammaglobin-A, collagen, cytochrome c, cardiolipin; the images obtained for single chemical components and (B) the combination of images obtained for single chemical components shown on panel (A).

Figure S4. (A) Basis analysis performed for cancerous human breast duct based on the Raman spectra of pure: oleic acid, palmitic acid, mammaglobin-A, collagen, cytochrome c, cardiolipin; the images obtained for single chemical components and (B) the combination of images obtained for single chemical components shown on panel (A).

human cancerous breast duct



human normal breast duct

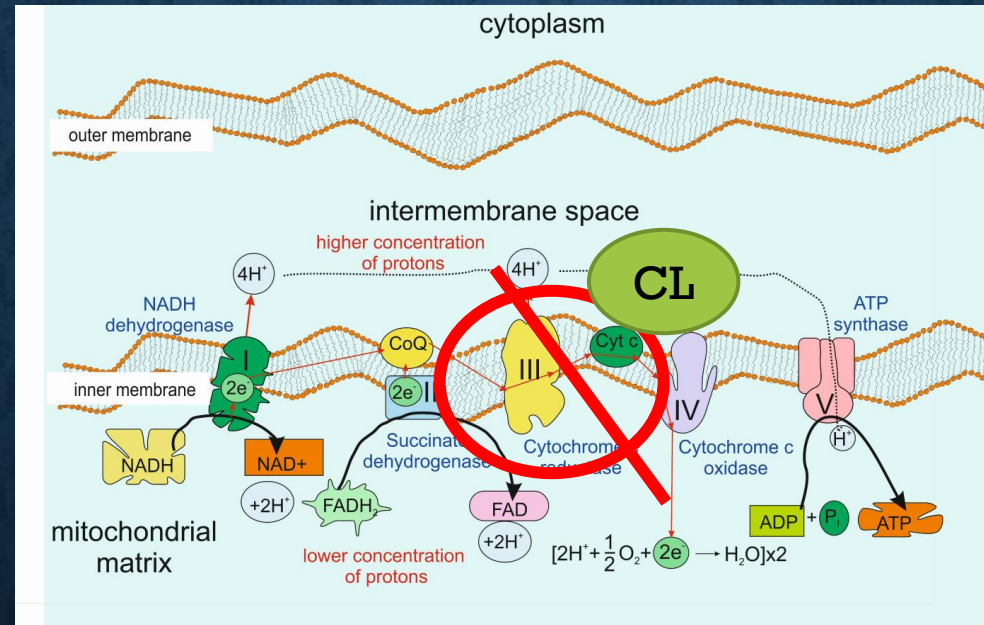


In breast cancer duct that Cyt c, cardiolipin, and palmitic acid are the main components inside the lumen of cancerous duct *in situ*. The presented results show direct evidence that Cyt c is released to the lumen from the epithelial cells in cancerous duct

In contrast the lumen in normal duct is empty and free of Cyt c.

CYTOCHROME C/CARDIOLIPIN RELATIONS IN MITOCHONDRIA: A KISS OF DEATH

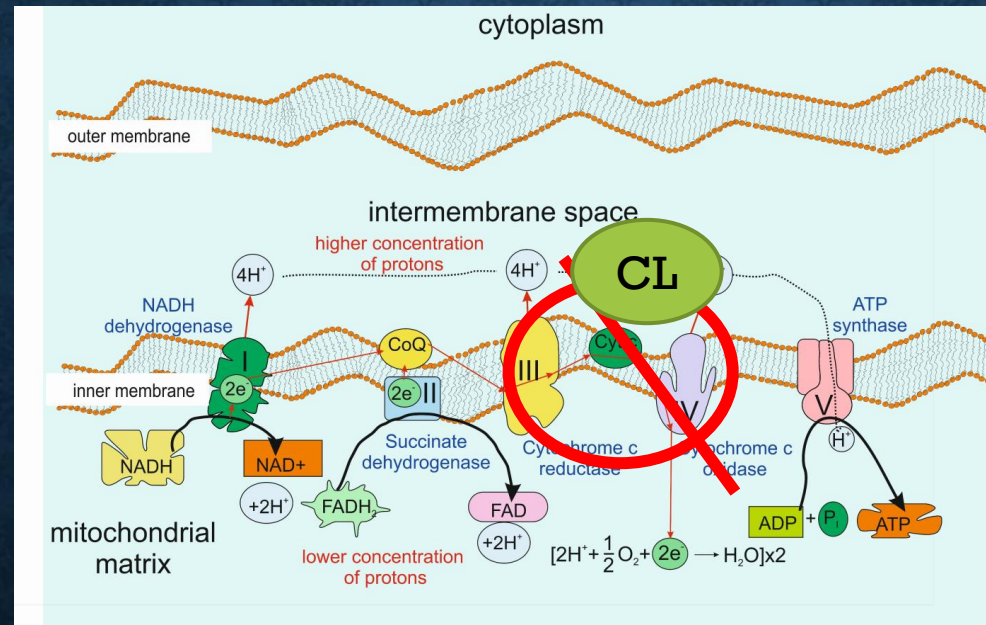
Cyt c accepts electrons from Complex III at a redox potential of about +250 mV vs SHE while it donates electrons to CuA site in Complex IV



Both redox properties and functions of *cyt c* change upon interaction with CL in the mitochondrial membrane, diminishing *cyt c*'s electron donor/acceptor role and stimulating its peroxidase activity

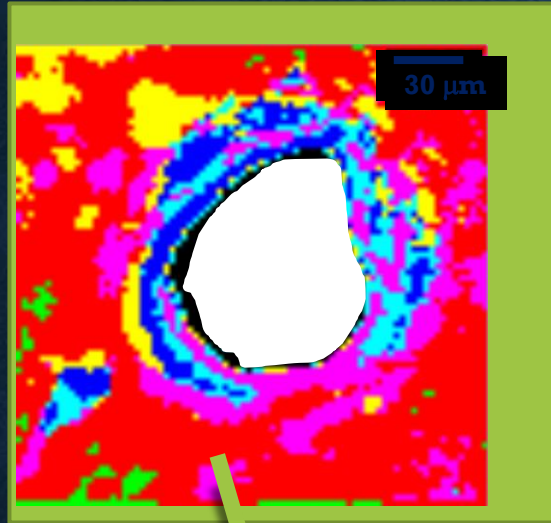
Upon cytochrome *c* interaction with cardiolipine there is a marked negative shift of *cyt c*'s redox potential (by 350–400 mV upon binding to CL-containing membranes) which precludes its operation as an electron acceptor from mitochondrial complex III. Consequently, functions of *cyt c* as an electron transporter and *cyt c* reduction by Complex III are strongly inhibited. Further, CL/*cyt c* complexes are not effective in scavenging superoxide anions

CYTOCHROME C/CARDIOLIPIN RELATIONS IN MITOCHONDRIA: A KISS OF DEATH



- Cardiolipin-bound Cyt c, probably does not participate in electron shuttling of the respiratory chain. It indicates that the process of oxidative phosphorylation (respiration) and ATP production become less effective in cancer cells.
- The reduced form of cytochrome c (Fe²⁺) cannot induce caspase activation and the process of apoptosis in cancerous cells becomes less efficient.

NORMAL HUMAN DUCT



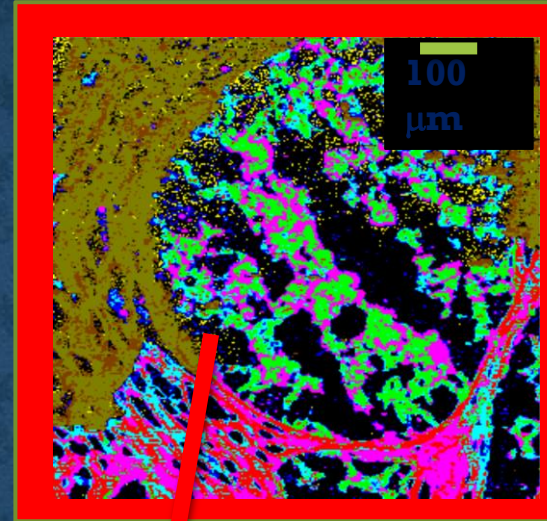
Low Raman signal of
Cytochrome c
(oxidized)

Cytochrome c unbound
to cardiolipine

Effective apoptosis
at the physiological
level

Effective respiration
(oxidative
phosphorylation)

CANCEROUS HUMAN DUCT



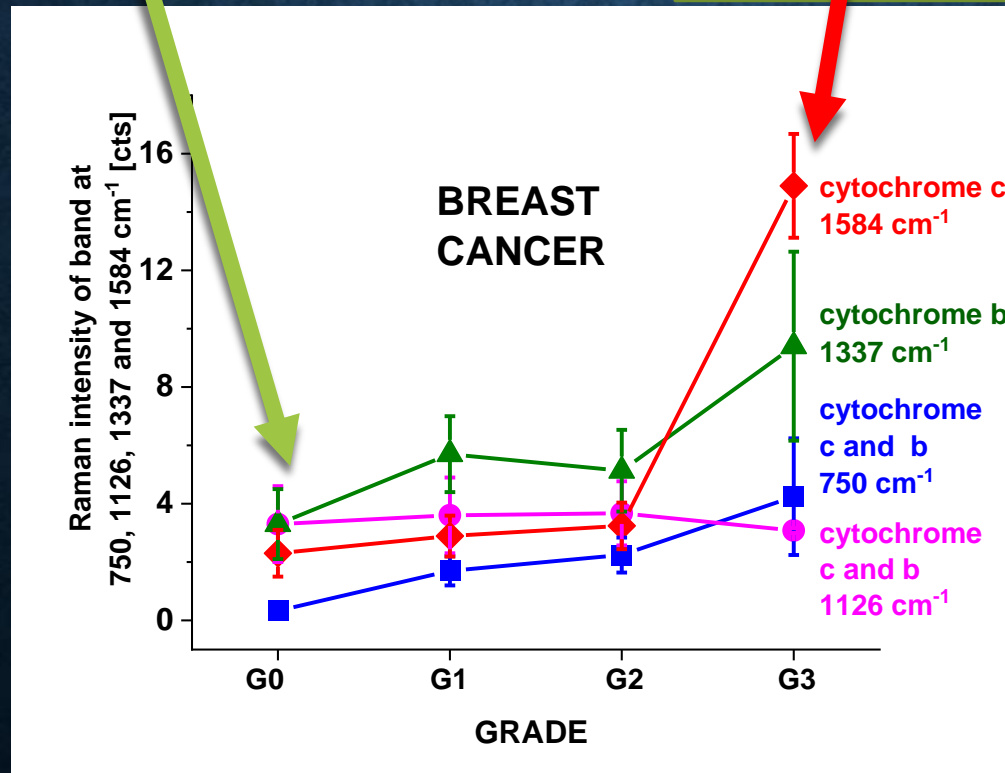
high Raman signal of
Cytochrome c (reduced)

Cytochrome c
bound to
cardiolipine

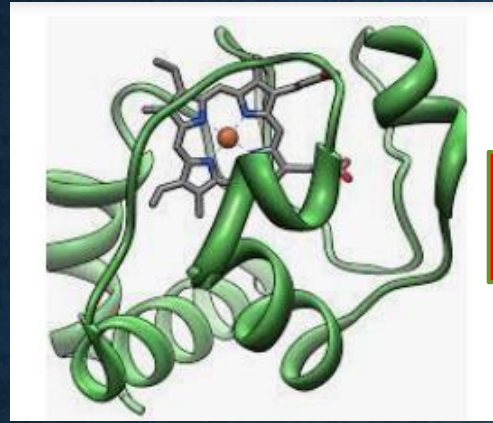
reduced apoptosis

The cancer cells can continue to grow,
divide and spread throughout the body

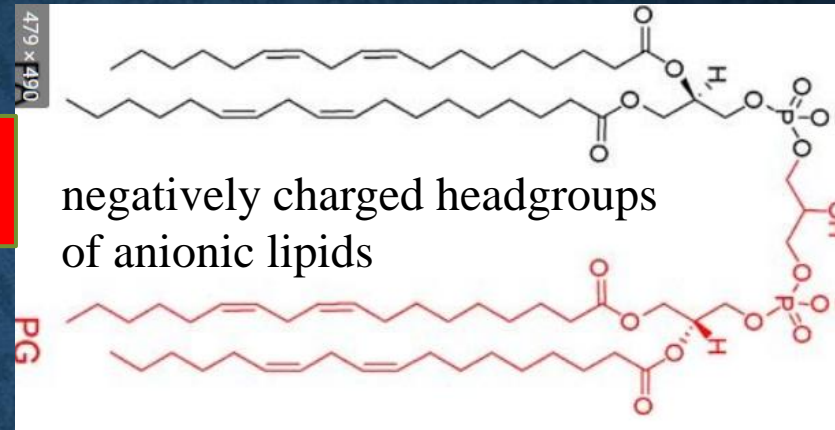
Reduced respiration
(oxidative
phosphorylation)



Positively charged *cyt c*



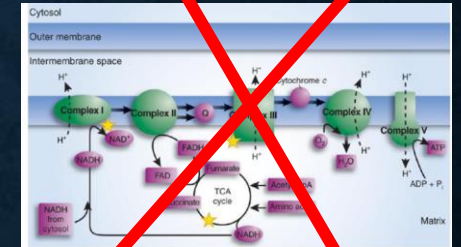
cytochrome c



negatively charged headgroups of anionic lipids

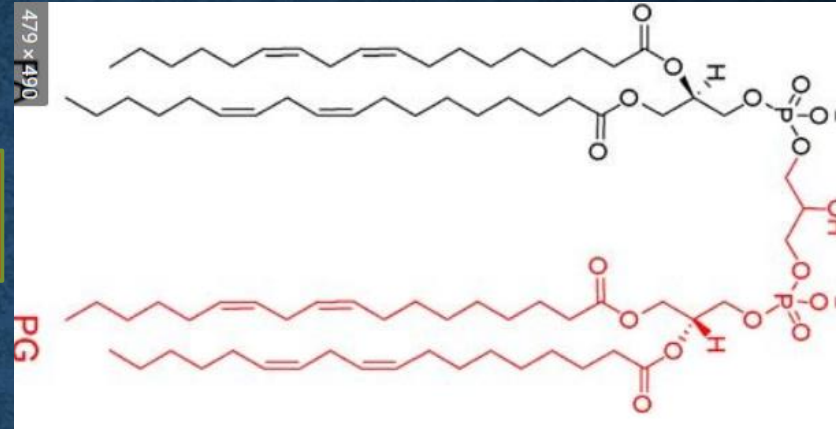
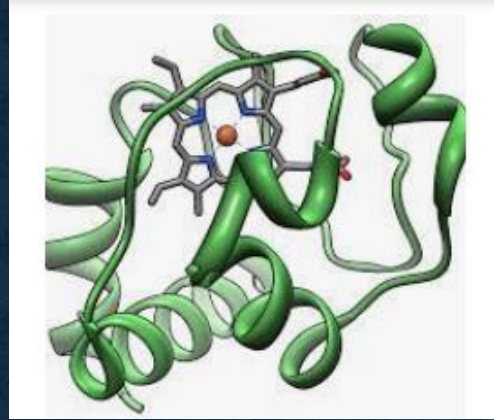
cardiolipin

Electrostatic forces are one of the major factors that govern *cyt c*-lipid interactions. Positively charged *cyt c* molecules (isoelectric point is near pH 10, net charge is +8e at neutral pH) are strongly attracted to the negatively charged headgroups of anionic lipids



Cyt c is mostly protonated meaning that most *Cyt c* binds via electrostatic bonds to acidic phospholipids, particularly cardiolipin. Cardiolipin-bound *Cyt c*, probably does not participate in electron shuttling of the respiratory chain. It indicates that the process of oxidative phosphorylation (respiration) becomes less effective in cancer cells.

On the other hand, the reduced form of cytochrome c (Fe^{2+}) cannot induce caspase activation and the process of apoptosis in cancerous cells becomes less efficient.



Because high affinity binding of cardiolipine (CL) with *cyt c* – accompanied by unfolding of the protein – is realized largely through an electrostatic interface between negatively charged phosphates on CL and positively charged lysines on *cyt c*, as well as through hydrophobic interactions of CL's acyl groups with a hydrophobic domain of the protein, other negatively charged phospholipids may also bind and unfold *cyt c* via analogous mechanisms.

Interaction of *cyt c* with negatively charged lipid membranes induces considerable disruption of the native compact structure of the protein and induces intermediate conformations between the native and fully unfolded states, called a “molten globule”. This state, an “alternative folding”, is defined as a compact conformation with a secondary structure comparable to that of the native state and fluctuating tertiary conformation due to a high enhancement of intramolecular motion [13,27,35,36].

CYTOCHROME C AS POTENT PEROXIDASE

The organization of native *cyt c* favors its most common function as an electron shuttle between complexes III and IV of mitochondria.

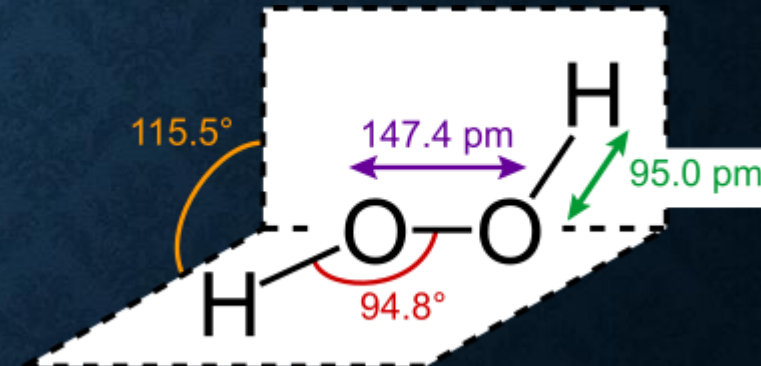
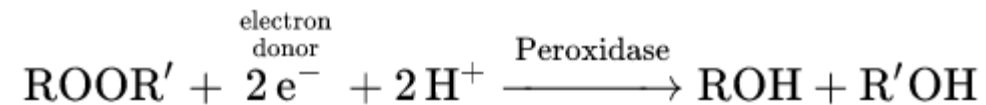
However, the binding of *cyt c* to anionic phospholipids unfolds the protein and converts it from an electron shuttle into a potent peroxidase. In mitochondria, this peroxidase activity displays remarkable specificity towards cardiolipin, causing oxidation as well as hydrolysis of CL-OOH

Peroxidase function of *cyt c* requires its direct physical interaction with cardiolipine

PEROXIDASES

Peroxidases or **peroxide reductases** are a large group of enzymes which play a role in various biological processes. They are named after the fact that they commonly break up peroxides. For many of these enzymes the optimal substrate is hydrogen peroxide, but others are more active with organic hydroperoxides such as lipid peroxides.

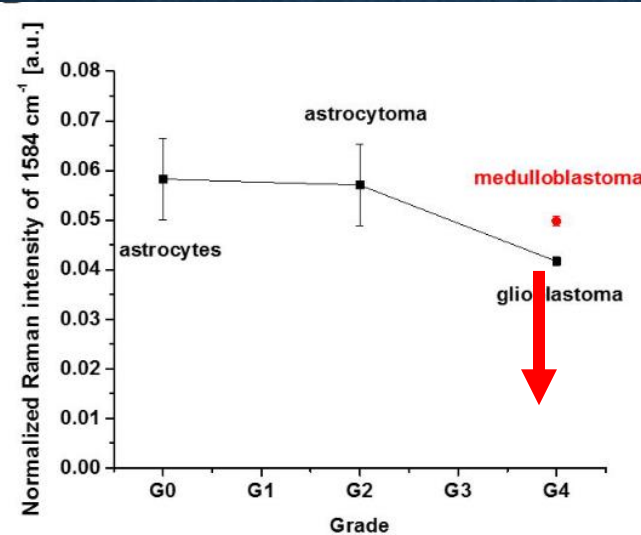
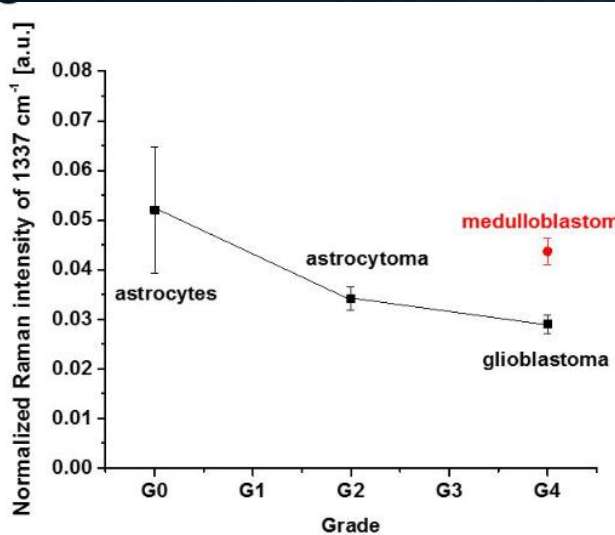
Peroxidases typically catalyze a reaction of the form:



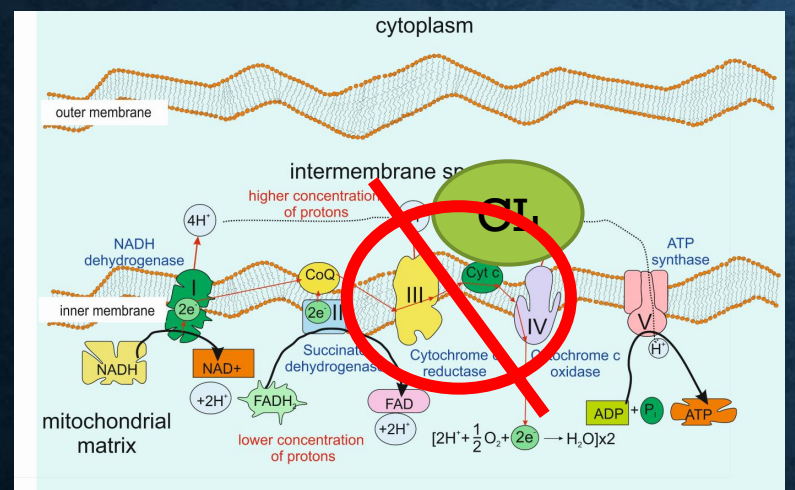
Peroxidases can contain a heme cofactor in their active sites,!!!!!!!!!!!!!!!!!!!!!!

Cyt *c* contains several potentially oxidizable amino acid residues: four tyrosines, some of which (Tyr67, Tyr48) are within 5.0 Å of the heme porphyrin ring, and one tryptophan residue [90]. The radical intermediates from these residues can be detected by low temperature EPR spectroscopy [85]

Cytochrome c/cardiolipin relations in mitochondria: a kiss of death U87 Glial cells of glioblastoma

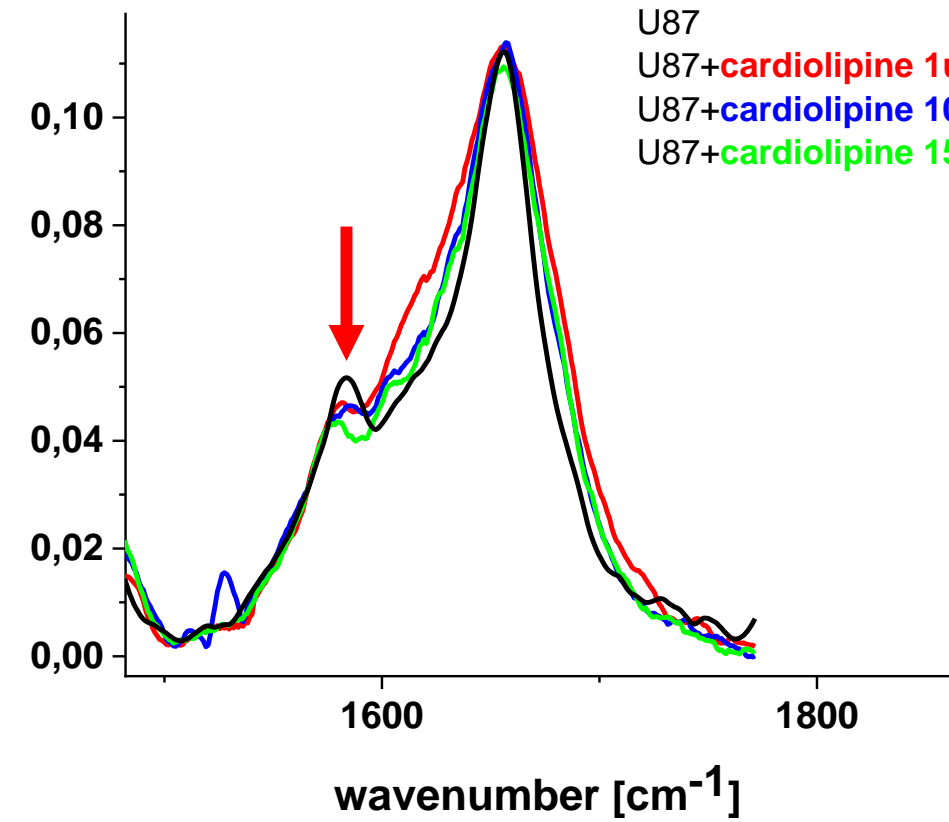


U87
 U87+cardiolipine 1uM
 U87+cardiolipine 10 uM
 U87+cardiolipine 15 um



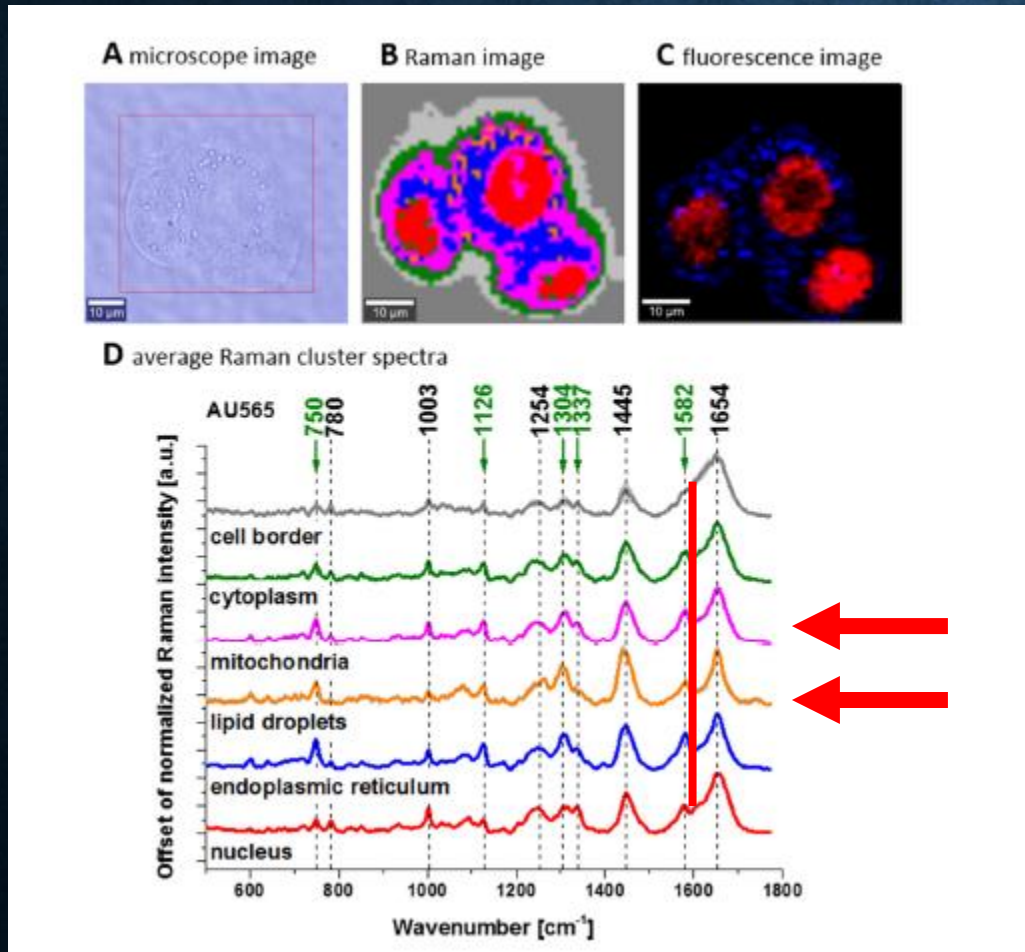
Cardiolipin-bound Cyt c, probably does not participate in electron shuttling of the respiratory chain. It indicates that the process of oxidative phosphorylation (respiration) becomes less effective in cancer cells

Normalized Raman intensity [a.u.]



U87
 U87+cardiolipine 1uM
 U87+cardiolipine 10 uM
 U87+cardiolipine 15 um

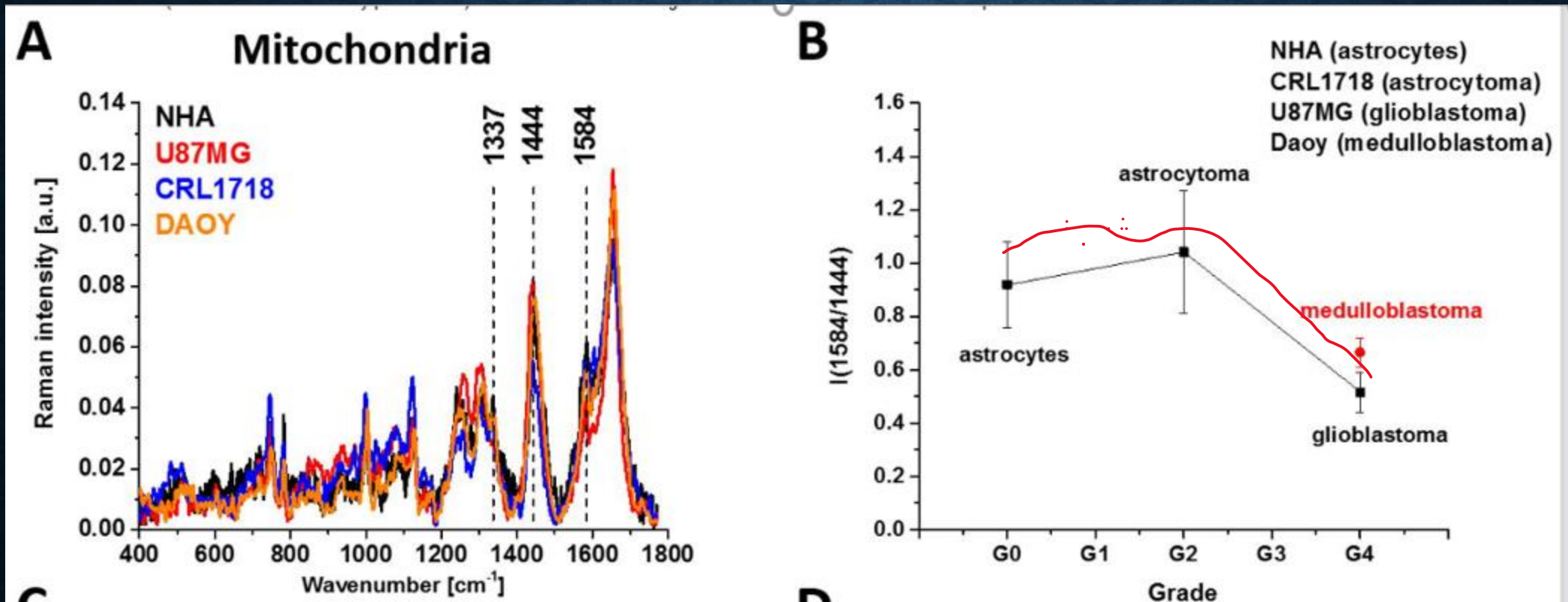
TO CHECK IF VIBRATIONS OF CYTOCHROME C CAN BE USED ALSO FOR PATHOLOGY ASSESSMENT IN LIVING CELLS WE ANALYSED RAMAN SPECTRA OF BRAIN AND BREAST CANCER CELLS LINES AT IN VITRO INCUBATION.



Confocal Raman spectroscopy analysis of the human adenocarcinoma cell line (invasive ductal cancer (AU565)) at the 532 nm wavelength excitation. (A) Microscopy image, (B) Raman image from the cluster analysis (nucleus (red), endoplasmic reticulum (blue), lipid droplets (orange) cytoplasm (green), mitochondria (magenta), cell border (light grey), area out of the cell (dark grey), image size: 55 μm x 50 μm, resolution of 1 μm, laser excitation 532 nm, power 10 mW, integration time 0.3 sec), (C) fluorescence image of lipids (blue, Oil Red O staining) and nucleus (red, Hoechst 33342 staining). (D) Average Raman cluster spectra for the number of cells, n = 20 (8639 spectra were recorded (n(nucleus) = 2142, n(endoplasmic reticulum) = 1530, n(lipid droplets) = 121, n(cytoplasm) = 1464, n(mitochondria) = 1689, n(cell border) = 1693).

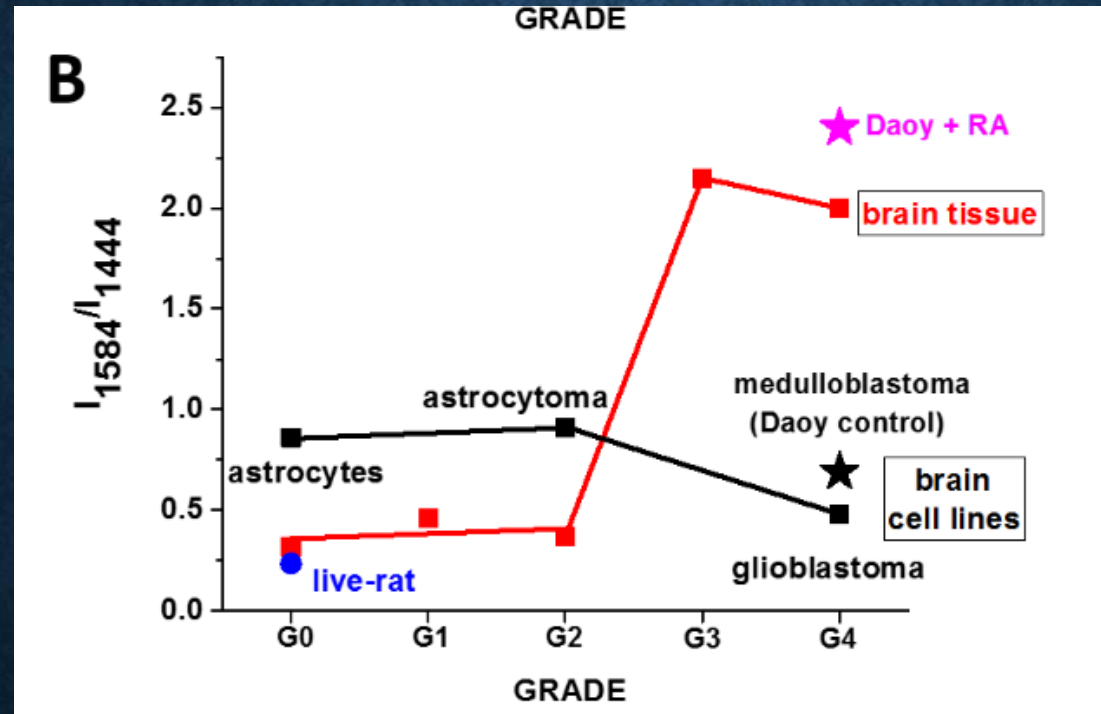
One can see that cytochrome c can be easily detected in vitro cells. The concentration of cytochrome c is different in different organelles. The highest level is in mitochondria and lipid droplets

Cytochrome c activity in glial brain in vitro cells



Lower concentration of oxidized cytochrome c in in vitro conditions indicates higher aggressiveness of brain tumor

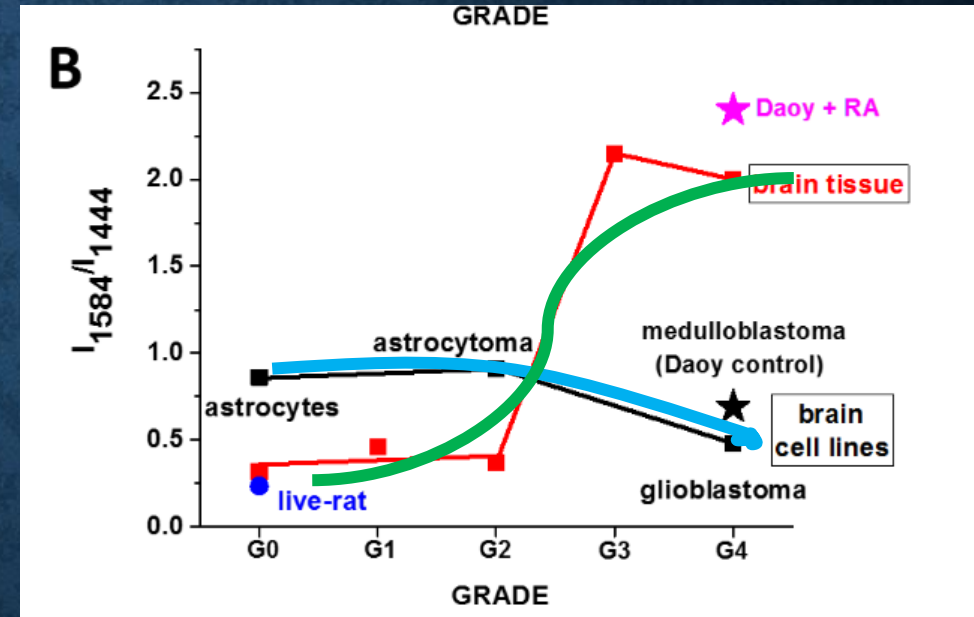
Cytochrome c plays a crucial role in the development and progression of cancer



Here one can see the dependence of the Raman biomarker $I(1584)/I(1444)$ of the Cyt c vs cancer malignancy has a threshold character. The optimal concentration of cytochrome c in the mitochondrium cells that are needed to maintain cellular homeostasis corresponds to the ratio 0.05 for the breast tissues and 0.37 for brain. The concentrations of the Cyt c below the threshold modulate protective, signaling-response pathways, resulting in positive effects on life-history traits. The reduced Cyt c levels above the threshold trigger a toxic runaway process and aggressive cancer development (0.42 for breast and 2.15 for brain).

The second important finding presented in Figure is the striking trend for in vitro cells, which is evidently opposite to that observed in the tissues. The Raman signal $I(1584/1444)$ increases in the brain tissues, whereas it decreases with brain tumour aggressiveness in in vitro cells. This finding demonstrates evidence that the tumour environment plays a crucial role in cancer development. During the last decade this conclusion has been solidified and demonstrated that cancer cells must encompass the tumor microenvironment, revealing that the biology of tumors can no longer be understood simply by studying isolated cells in in vitro cultures. **Our results from Fig. confirm the importance of tumor microenvironment, which comprises prominent components of cancer progression within the immediate vicinity of tumor cells such as fibroblasts, immune cells and the extracellular matrix.** The results demonstrate that there must exist intracellular reductants in tissue other than the reduced nicotinamide adenine dinucleotide (NADH) (present in the growing medium in cell culturing) that contribute to Cyt c activity.

The important finding presented in Figure is the striking trend for in vitro cells, which is evidently opposite to that observed in the tissues.



EFFECT OF EXTRACELLULAR MATRIX

- To answer this issue we compared the correlation between the concentration of cytochrome c vs cancer agresiveness for human tissues and in vitro cell cultures

The important finding presented is the striking trend for in vitro cells, which is evidently opposite to that observed in the tissues

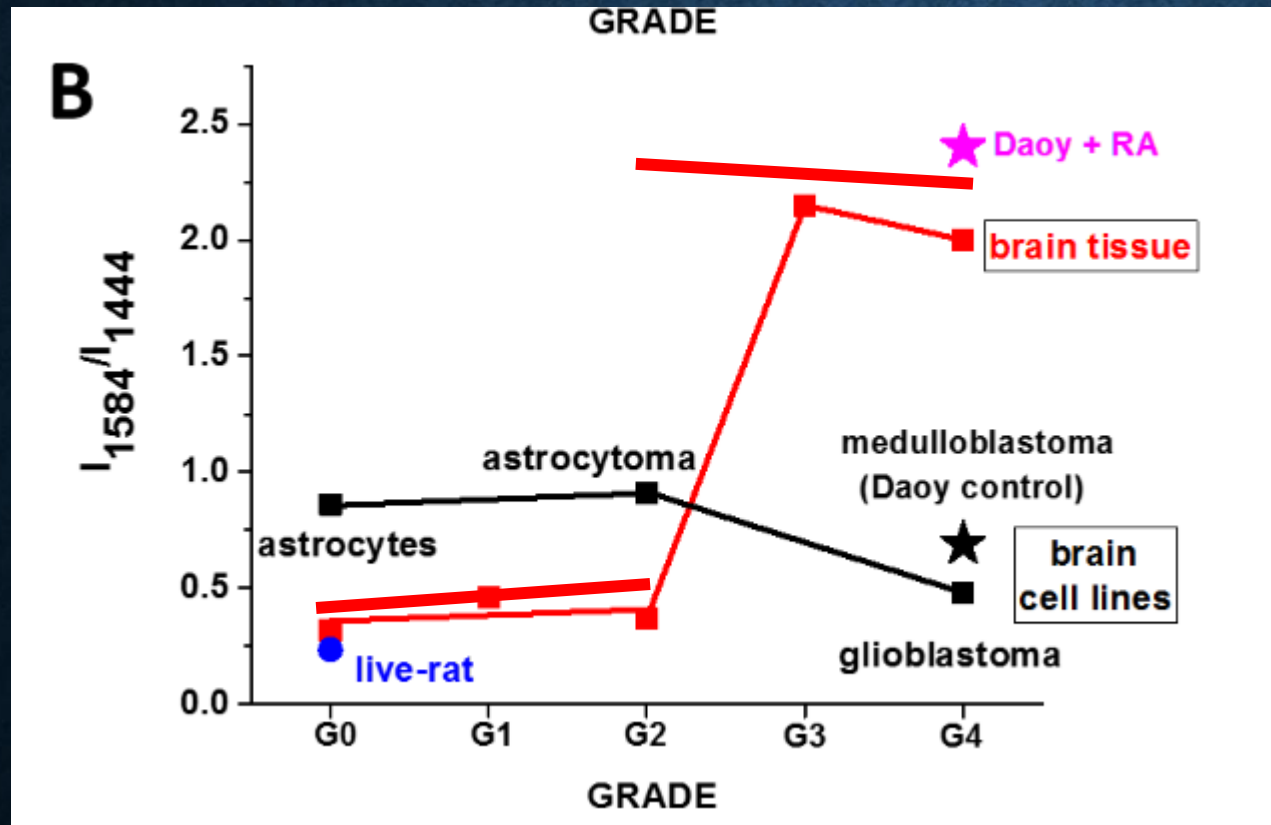


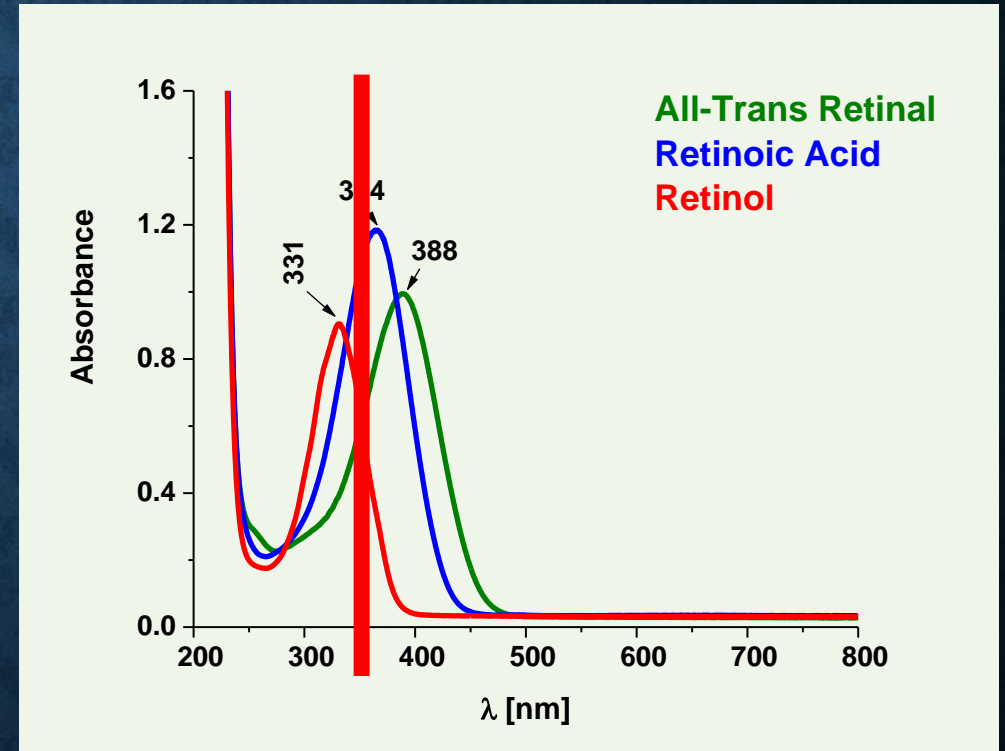
Figure shows the Raman biomarker $I(1586/1444)$ as a function of brain tumor grade malignancy G0-G4 for the human tissues and for in vitro human brain cells of normal astrocytes (NHA), astrocytoma (CRL-1718), glioblastoma (U87-MG) and medulloblastoma (Daoy),

The plots provide an important cell-physiologic response, normally the Cyt c operates at low, basal level in normal cells, but it is strongly induced to very high levels in pathological cancer states by certain cellular stress, the most obvious of which is Reactive Oxygen Species - ROS stress or certain nutrients deficiency.

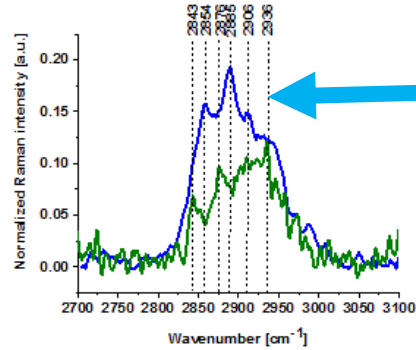
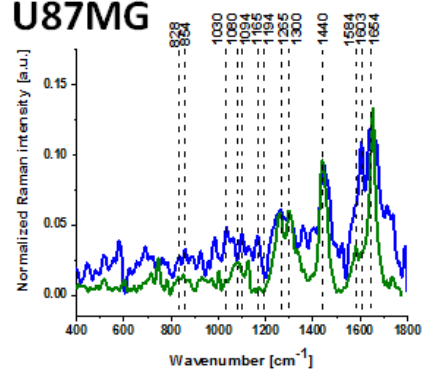
What intracellular reductants are not present in in vitro cultures?

Some hints on the essential components from the microenvironment that are important for the activity of Cyt c in the tissues can be provided by detailed analysis of Raman spectra. **For this purpose we compared the Raman spectra of the brain tumor cells using different laser excitation wavelengths.** This approach might generate Raman resonance enhancement for some tissue components that cannot be visible for non-resonance conditions. Raman spectra of lipid droplets in glioblastoma U87MG and in normal astrocytes NHA cells in the high frequency region recorded at 355, 532, 785 nm excitations show spectacular differences in Raman spectra due to the various excitation wavelengths. Our results demonstrates a significant Raman resonance enhancement at 355 nm where the family of retinoids have the absorption

355 nm



A U87MG

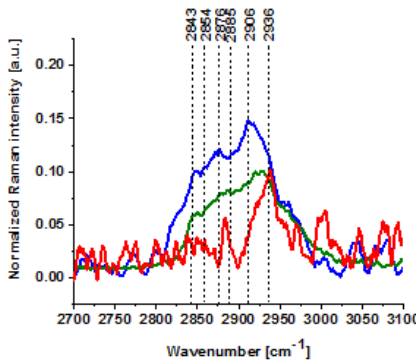
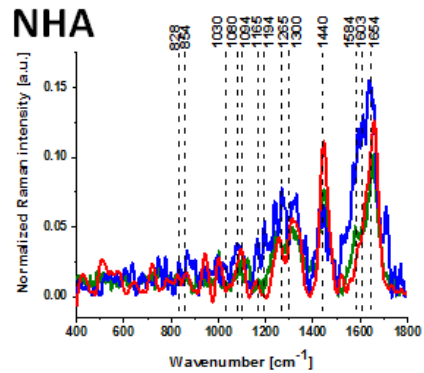


355 nm

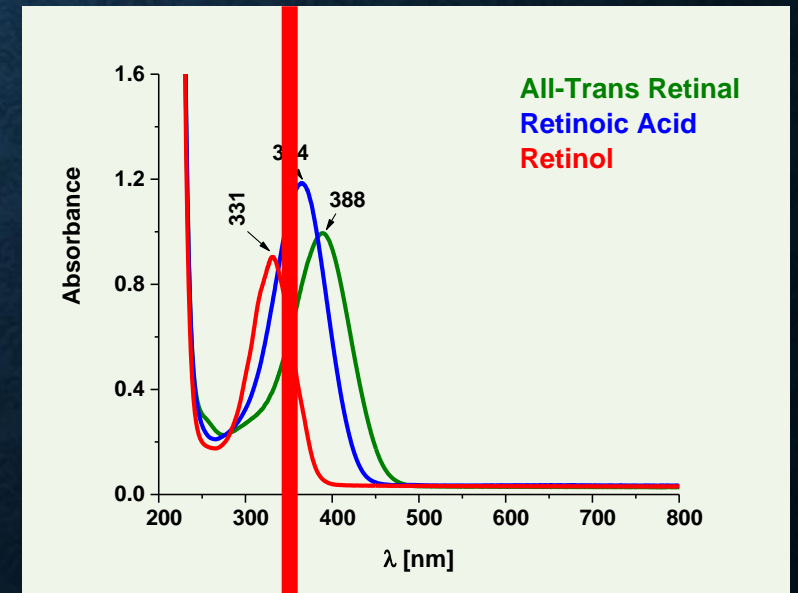
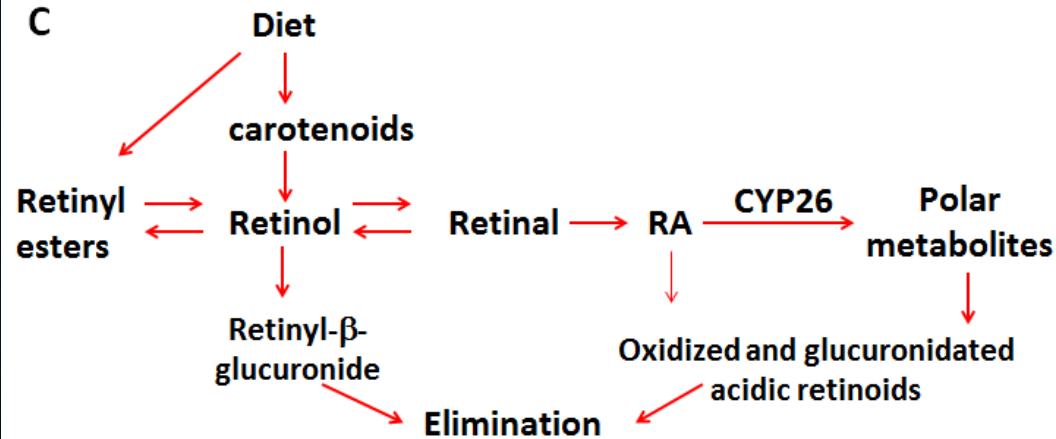
Figure S4. Raman spectra of lipid droplets in glioblastoma U87MG (A) and in normal astrocytes NHA cells (B), — 355 nm (blue), — 532 nm (green), — 780 nm (red), metabolism of vitamin A (C).

Figure demonstrates a significant Raman resonance enhancement at 355 nm where the family of retinoids have the absorption

B NHA



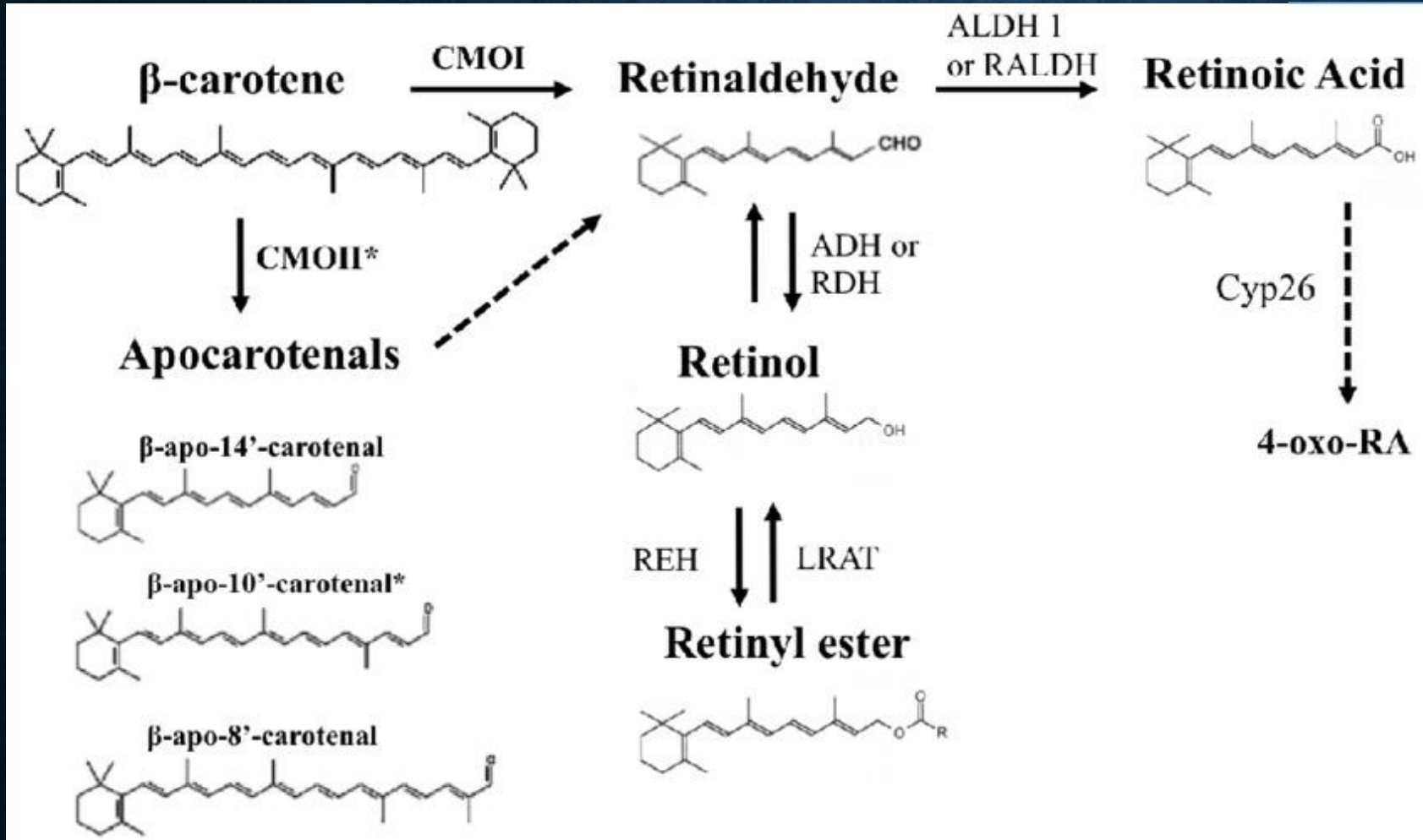
C



What intracellular reductants are not present in in vitro cultures?

retinoic acid

We recorded the Raman spectra of cells receiving redox stimuli by retinoic acid (RA) in the absence of cell to cell interactions in in vitro cultures. For these purposes, we incubated the medulloblastoma cells (Daoy) with retinoic acid (RA)

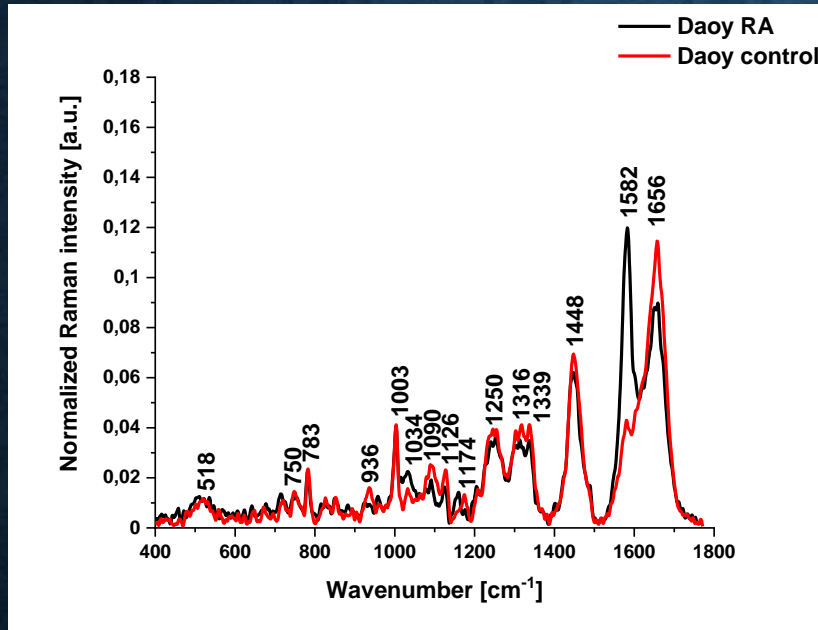


Further oxidation of retinoic acid by enzymes that belong to the cytochrome P450 (CYP) 26 family converts retinoic acid into more polar compounds, including **4-oxo retinoic acid**, which are believed to be transcriptionally inactive

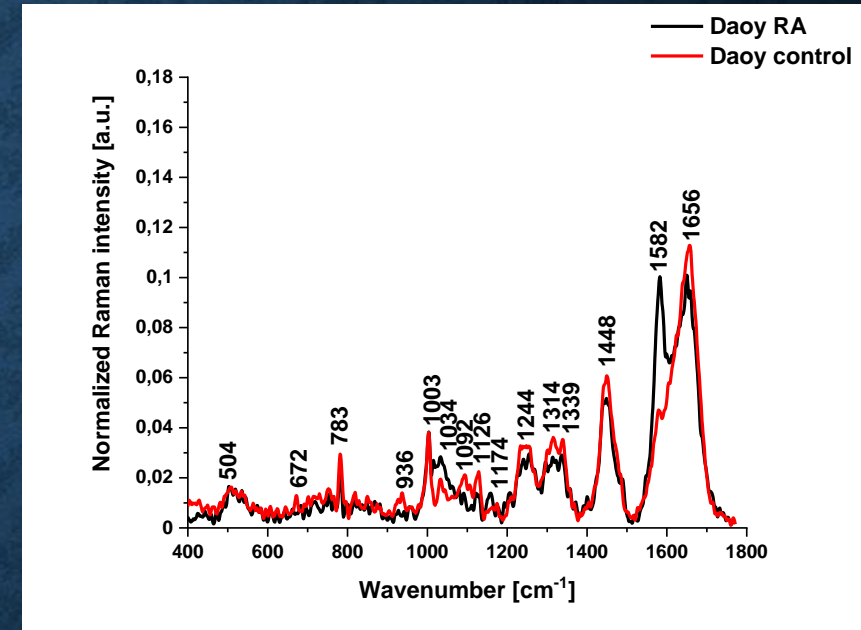
Immunity - the ability of an organism to resist a particular infection or toxin by the action of specific antibodies or sensitized white blood cells.

Medulloblastoma G4 brain tumor

Nucleus

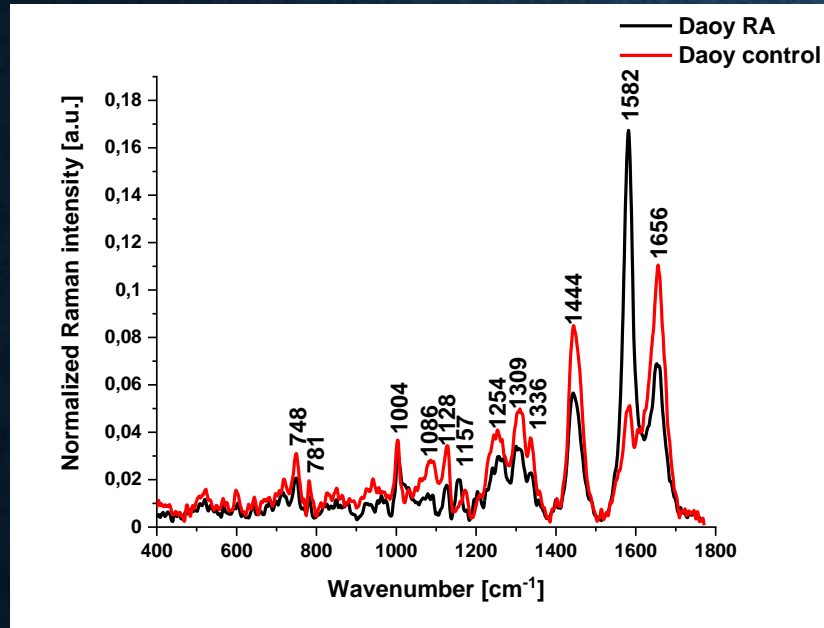


Cytoplasm

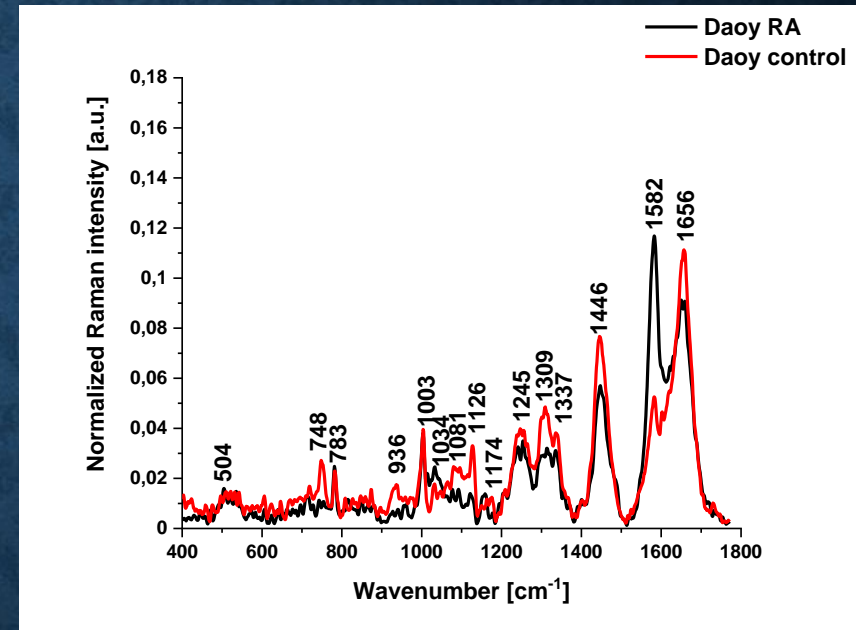


Incubation cells in vitro with retinoic acid increases the amount of reduced cytochrome c.

Lipid droplets



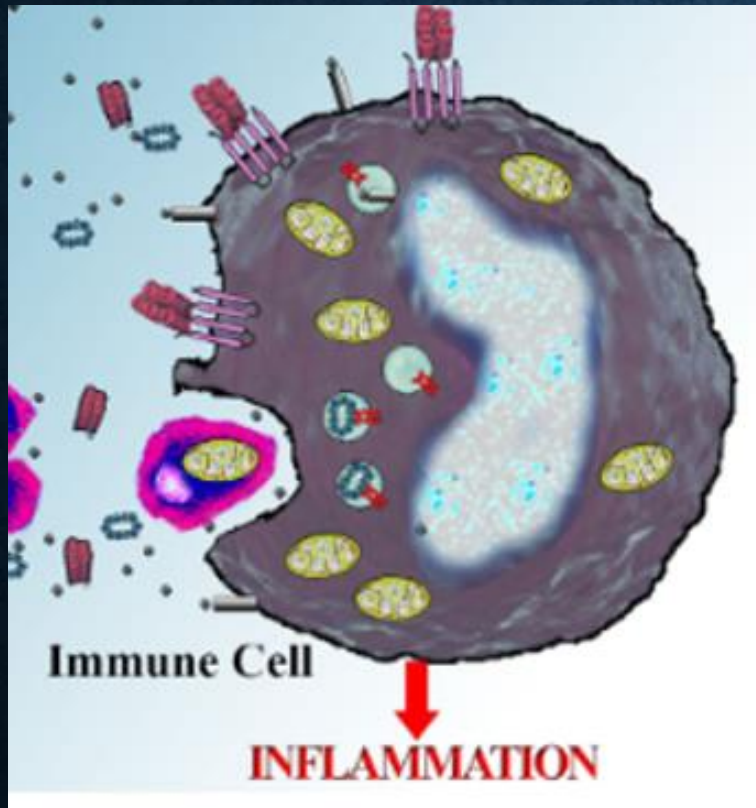
Mitochondria



Incubation in vitro with retinoic acid increases the amount of reduced cytochrome c.

Incubation in vitro with retinoic acid increases the amount of reduced cytochrome c.

THERE IS EVIDENCE THAT CYTOCHROME C WHEN IS INAPROPRIATELY LOCATED MAY BEHAVE AS A DAMP AND ELICIT AN INFLAMMATORY RESPONSE IN THE IMMUNE SYSTEM



The mRNA-based BNT162b2 vaccine from Pfizer/BioNTech was the first registered as COVID-19 vaccine and has been shown to be up to 95% effective in preventing SARS-CoV-2 infections. Little is known about the possible consequences of the new class of mRNA vaccines, especially whether they have combined effects on innate and adaptive immune responses.

CYTOCHROME C VS IMMUNE SYSTEM

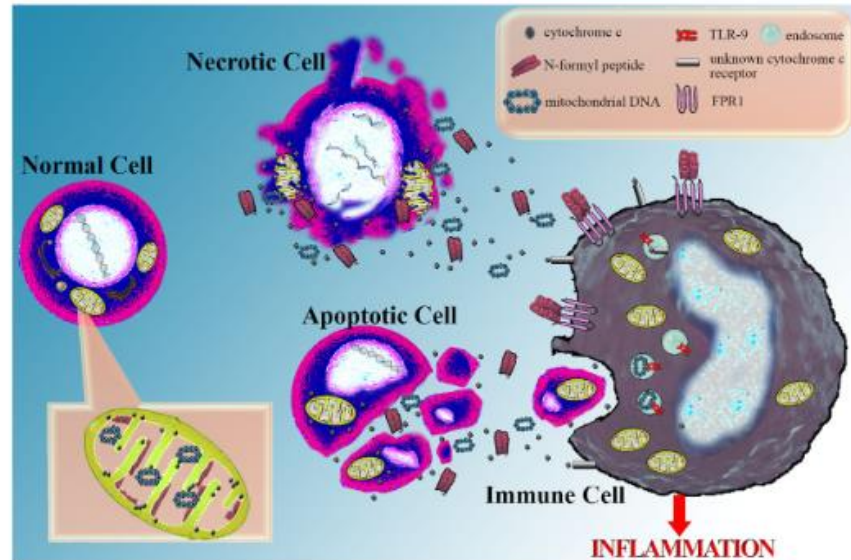
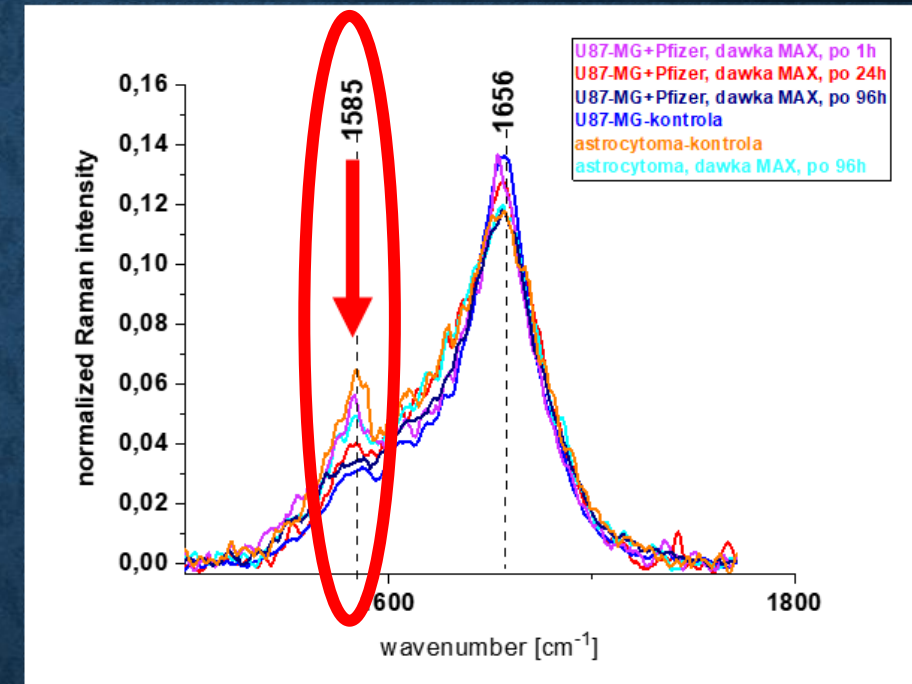
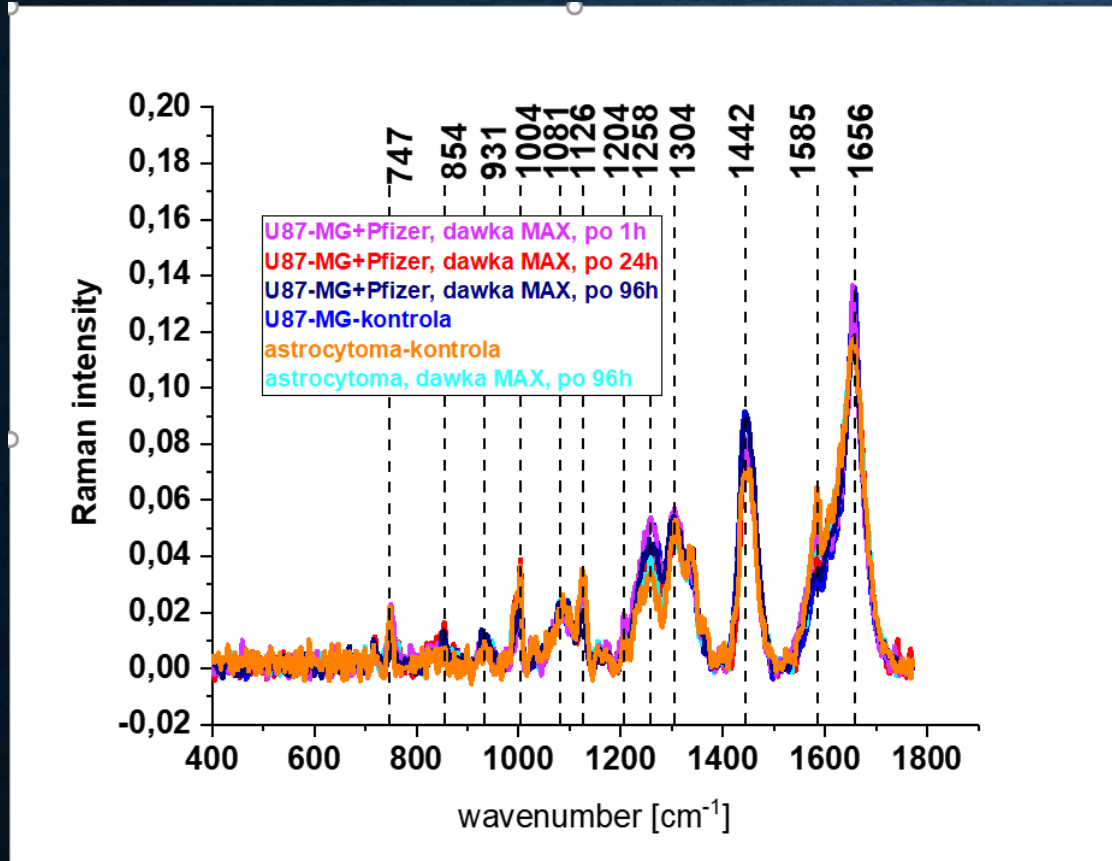


FIGURE 1 | Cytochrome c as a marker of cellular damage and its potential role as a danger-associated molecular pattern. Serious cellular damage results in cell apoptosis or necrosis. In both cases, cytochrome c is released into the extracellular space and can be easily measured in the serum serving as a marker of severe cellular damage and death. Possibly, along with cytochrome c, other mitochondrial molecules are also released into the extracellular space. Among them are annotated some well-defined danger-associated molecular patterns (DAMPs), such as mitochondrial DNA, recognized by the toll-like receptor 9 (TLR9) into the endosomes of immune cells and *N*-formyl peptides, sensitized by the formyl peptide receptor 1 (FPR1) on the cell membrane of immune cells. Besides the above DAMPs, which resemble bacterial structures, there is evidence that cytochrome c, a universal self-molecule, when is inappropriately located into the extracellular space may behave as a DAMP and elicit an inflammatory response. However, further studies are required for supporting this role for cytochrome c and the responsible pattern recognition receptor(s) remain to be discovered.

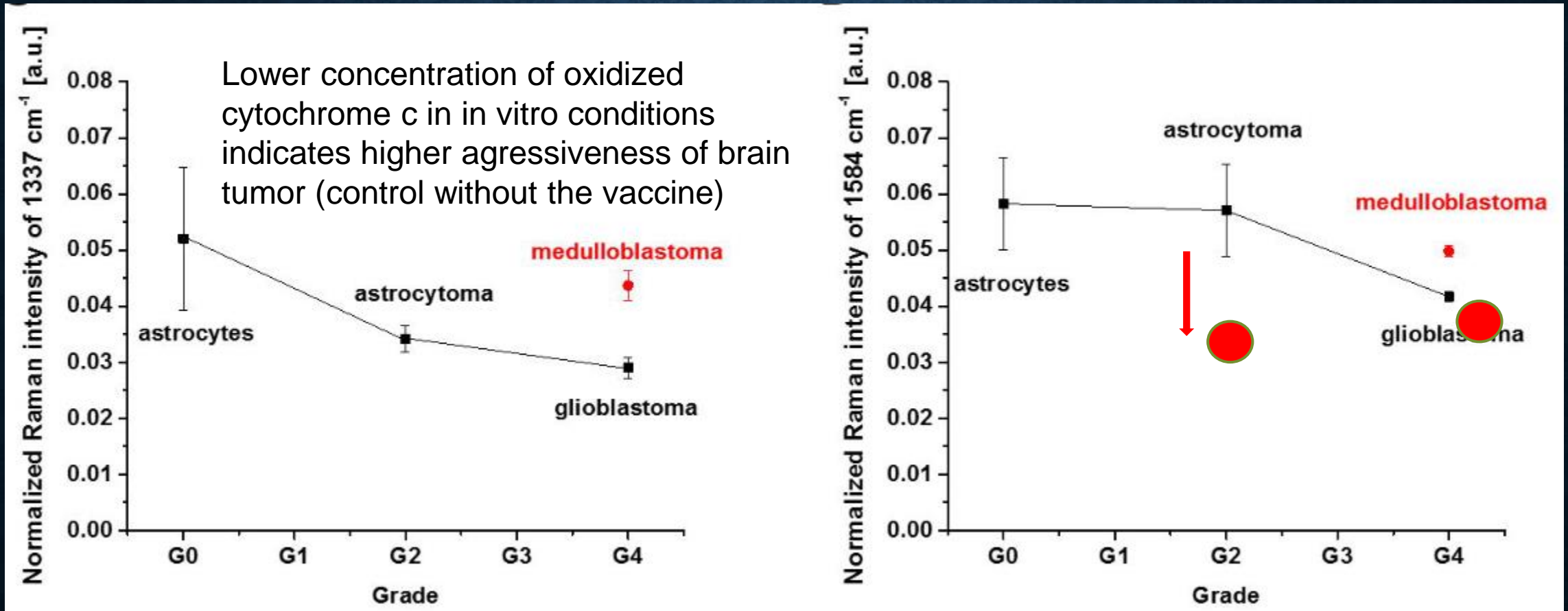
Damage-associated molecular patterns (DAMPs) are **endogenous danger molecules** that are released from damaged or dying cells and activate the innate immune system by interacting with pattern recognition receptors (PRRs). Although DAMPs contribute to the host's defense, they promote **pathological inflammatory responses**.

The effect of The mRNA-based BNT162b2 vaccine from Pfizer/BioNT on cytochrome c



Cytochrome c activity has been shown to be modified by the Pfizer/BioNT (BNT162b2 mRNA) vaccine against SARS-CoV-2. It can be used to study both adaptive and innate immune responses.

The mRNA-based BNT162b2 vaccine from Pfizer/BioNT



Here we confirmed that BNT162b2 vaccine modulate the production of inflammatory cytochrome c upon incubation with astrocytoma for 96 h. The response of tumorous cells of astrocytoma was lower upon BNT162b2 vaccination, while medulloblastoma responses did not change. Lower concentration of oxidized cytochrome c in in vitro conditions indicates higher aggressiveness of brain tumor. Upon incubation with the vaccine we also observe lower concentration of oxidized cytochrome c. It indicates that the process of oxidative phosphorylation (respiration) and ATP production become less effective in cancer cells upon incubation with the vaccine.

CONCLUSIONS

- Our findings in the field of cancer cell metabolism suggest that change in the cellular redox status of cytochrome *c* is important cancer driver, controlling various aspects of malignant progression.
- The biochemical results obtained by Raman imaging showed that human tissue demonstrate a redox imbalance by upregulation of cytochrome *c* in cancers.
- The results demonstrate the critical role of extracellular matrix in mechanisms of oxidative phosphorylation and apoptosis. We showed that the concentration of reduced cytochrome *c* (monitored at 1584 cm^{-1}) is lower in cancer single cells where the effect of microenvironment is eliminated. In contrast, the redox balance shows a reverted trend in breast cancer and brain tumor tissues when there are interactions with the environment. The concentration of reduced cytochrome *c* (monitored at 1584 cm^{-1}) is significantly higher in cancer tissue when compared with the normal tissue.